MECHANICAL STRESS IN THE TEMPOROMANDIBULAR JOINT (TMJ)

A theoretical and experimental study

by

JEFFREY CHARLES NICKEL

A thesis submitted to the Faculty of Graduate Studies

in partial fulfillment of the requirements

for the degree of

DOCTOR OF PHILOSOPHY

Interdisciplinary Programme
Faculty of Graduate Studies
University of Manitoba

Winnipeg, Manitoba

December, 1991

ISBN 0-315-77831-8

MECHANICAL STRESS IN THE TEMPOROMANDIBULAR JOINT (TMJ)

A THEORETICAL AND EXPERIMENTAL STUDY

BY

JEFFREY CHARLES NICKEL

A Practicum submitted to the Faculty of Graduate Studies of the University of Manitoba in partial fulfillment of the requirements for the degree of

DOCTOR OF PHILOSOPHY

ABSTRACT

MECHANICAL STRESS IN THE TEMPOROMANDIBULAR JOINT (TMJ)

The control of mechanical stresses in a synovial joint is considered important for the longevity of the joint. Factors such as growth and congruence of the osseous surfaces, the minimization of joint loads, and the load distribution and lubrication properties of the TMJ disc were evaluated for their ability to limit the magnitudes of stress in the TMJ.

Using the osteological remains of individuals between the ages of birth and twenty-five years, in combination with a numerical model of minimal joint loading, theoretic stresses in the TMJ were determined for conditions of isometric biting on the molar and incisor teeth. The average stresses in the TMJ were found to be of the same magnitude as reported in the literature for limb joints. However, the lack of congruity between osseous surfaces in the TMJ resulted in theoretic local stresses which were two to three times the magnitude of the average stresses. *In vitro* experimental techniques were developed to determine the ability of TMJ discs to distribute normal loads over incongruent surfaces, and to evaluate the lubrication characteristics of the disc. The domestic pig was used as a model. During normal loading, stress concentrations of varying magnitudes were found to exist for all discs. The magnitude of peak stresses depended on disc thickness. Friction on the disc surface was affected by the duration of loading, the hydration of the disc, and the impulse energy of an impact load.

The results showed that there are conditions in which the TMJ disc and growth of the osseous surfaces do not prevent high local stresses. Overall, stress control in the TMJ appears to be unstable due to the lack of neural monitors of mechanical stress in the articular tissues.

ACKNOWLEDGEMENTS

The joy and satisfaction of the graduate experience is a reflection of the special people who support in the effort. At this time I would like to acknowledge the contributions of several individuals.

Over the last eight years, I have had the extraordinary fortune of having Ken McLachlan as mentor and friend. Ken's council has been the benchmark by which I have made my way as a graduate student. Thank you Ken for your consideration, advise, and hard work.

Fellow graduate students Laura Iwasaki, Peter Trainor, and David Tait have been reliable and astute friends. This body of work is also a product of their efforts. I am indebted to my comrades in the lab.

The fact that the experimental portion of this project used TMJ discs from pigs was made possible through the gracious services of Burns Meats Ltd (Winnipeg). Burns Meats afforded unencumbered access to gather the precious tissue specimens. Our laboratory is thankful for the wonderful support of Burns Meats.

Throughout the project a number of people have been generous with their time and talent. Mr. S. Meyerhoff, Mr. N. Piamsalee, and Mr. M. McVey, Civil Engineering Workshop, provided technical work and advise. During the early stages of this project, Mrs. J. Haines and Dr. N. Stanger, Department of Animal Science, helped with technical problems and a pilot study. Dr. C. Dowse, Department of Oral Biology, very kindly made available for our use several amplifiers and an FM tape recorder. The Dean's MRC Fund, Faculty of Dentistry, provided additional financial support for the purchase of strain gauges and biochemical reagents.

The laboratory facility used for the research portion of the interdisciplinary degree was provided by the Department of Civil Engineering. As well, the Environmental Engineering group of the Department of Civil Engineering made equipment available for the preparations of and storage of physiologic solutions.

Being a graduate student means living under the circumstances of austere home economy. Financial support through a University of Manitoba Fellowship, Manitoba Health Research Council Studentship, and Medical Research Council of Canada Fellowship has made it possible to remain a graduate student for the last 5 years. As well, the support of the Office of the Dean, Faculty of Dentistry is acknowledged. A clinical practice stipend was made available through the Office of the Dean.

The duration of my graduate studies have been encouraged by the love and support of my mother and father. My parents provided hospice for the times when I needed to renew my vigour, and were empathetic listeners during times of crisis. Thanks Mom and Dad.

TABLE OF CONTENTS

page #

CHAPTER 1

MECHANICAL STRESS AND THE TEMPOROMANDIBULAR JOINT

CHAPTER 2

THEORETICAL STRESSES IN THE GROWING TMJ

CHAPTER 3

AN ANALYSIS OF THE LOAD DISTRIBUTION PROPERTIES OF THE TMJ DISC

CHAPTER 4

Lubrication Properties of the Temporomandibular Joint Disc

CHAPTER 5

Summary and Conclusions

LIST OF FIGURES

CHAPTER 1 page #

CHAPTER 2

CHAPTER 3

CHAPTER 4

LIST OF TABLES

CHAPTER 1

MECHANICAL STRESS AND THE TEMPOROMANDIBULAR JOINT

1.1 Introduction

In the practice of dentistry, the dentist has occasion to see patients who seek help due to discomfort and dysfunction of the jaw. In some cases, it is the synovial joint of the jaw, the Temporomandibular Joint (TMJ), which is the source of the patient's distress. There is hope on behalf of both patient and dentist that treatment will be successful in alleviating pain and restoring normal function. In most cases of degenerative joint disease of the TMJ, given a period of time of one to three years, pain from the joint slowly goes away and acceptable function returns to the joint (Ogus, 1979-80). The relief of pain and resumption of function is due to the natural course of the disease (Irby and Zetz, 1983) rather than due to any particular form of therapy performed by the dentist. In some instances the pain and dysfunction is chronic, and is never resolved to the satisfaction of the patient.

The current lack of success in treating degenerative temporomandibular joint disease has helped focus research on the identification of individuals who have the potential for developing degenerative joint disease of the TMJ (Carlson _et al_., 1985). There is the hope that by earlier identification of such individuals, prevention will be a more successful form of therapy than treating degenerative joint disease of the TMJ after it occurs.

The early identification of individuals who are prone to degenerative joint disease of the TMJ is hampered, in part, by inadequate understanding of the processes which ultimately result in the disease. It is agreed that the health of synovial joints, such as the TMJ, depends in large measure on the control of mechanical stresses which occur during the function of the joint (Ogus, 1979-1980; Toller, 1973; Pullinger and Seligman, 1987). In a synovial joint, the magnitude of mechanical stress is proportional to the magnitude of the load which pushes the articulating surfaces together. The magnitude of stress is also inversely proportional to the area of the load bearing surfaces and, therefore, is a function of the relative shapes of the contacting surfaces.

Mechanical stresses are needed for the normal development of the anatomy of a synovial joint, and for the maintenance of the health of the hyaline cartilage or fibrous connective tissue lining the articular surfaces. The development of normal anatomy of the TMJ is critically dependent on the temporospatial distribution of stress, which selectively stimulates the bone forming cells to produce the osseous morphology of the mature joint (Copray et al., 1983, 1985a,b,c,d; Nickel et al., 1988b). Stress and the resulting deformation are factors in the generation of a fluid transport system which moves metabolites through the articular cartilage. The movement of fluid is needed, as well, to produce the lubrication which gives very low resistance to movement of a joint.

Although it is important to have some stress to maintain TMJ health, degenerative disease of the TMJ can be produced by stresses of long duration or high frequency, or by abnormally high stresses. Abnormally high stresses can be produced by excessively large loads, which increase the general (average) stresses in the articular linings. High stresses can also be produced, during normal loading, by incongruent joint surfaces which produce a condition of stress concentration (Figure 1.1). Local stresses due to stress concentration can be very large, but the general (average) stresses remain virtually unchanged.

Theoretically, there are two general modes of initiating cartilage failure, namely trauma and fatigue, which eventually manifest as joint disease. Stress is a common factor, but each mechanism is considered to be different due to the time required to produce the damage. With respect to trauma, the rate of application of load, and the consequent pressure gradient, will determine if damage occurs to the connective tissue of the joint. Fatigue, on the other hand, is a consequence of long term use of the joint, and is more likely to occur in a joint which is used more often, or sustains greater stresses. The complex interplay between these mechanisms of fatigue and trauma complicate the understanding of the development of degenerative joint disease. Microtrauma (Zarb and Carlsson, 1979) may damage the cartilage of the joint in a manner so as to reduce fatigue life of the cartilage. Accordingly, fatigue failure, sometimes facilitated by microtrauma, is currently considered to be the most common structural event in the early expression of degenerative joint disease of the TMJ.

The previous discussion has noted the importance of mechanical stress in both the normal development and maintenance of joint health, as well as in the degenerative processes of the joint. The long term health of the joint is dependent on mechanisms which reduce the magnitude of stress and, hence, increase the likelihood of continued good health of the articulating components. The objective of this project is to measure the effectiveness of mechanisms which reduce the magnitude of stress in the TMJ. The mechanisms that were evaluated were the growth of the loading areas of the joint surfaces, the age-related changes in joint loading, and the role of the TMJ disc in load distribution and lubrication. In chapter 2, a theoretical analysis is presented to support the hypothesis of coordination of the neuromuscular system and joint surface development in reducing TMJ stress. As described in chapter 2, data obtained from osteological remains were used with a numerical model of TMJ loading to demonstrate coordination of load control factors and developmental factors, and the subsequent age-related increases in the general stresses in the TMJ. In chapter 2, evidence of site specific joint surface incongruities is also presented. The consequences of these incongruities are that theoretical local stresses are considerably higher than general stresses.

Experiments to determine the normal load distributing properties of the TMJ disc are reported in chapter 3. A comparison is presented between the natural disc and two disc analogues. A theoretical model is also presented to help explain the potential role of the disc in the development of local perturbations to the surface anatomy of the condyle.

Chapter 4 addresses the role of the disc in reducing tensile and shear stresses across the surfaces of the joint. In chapter 4, frictional properties of the surfaces of the TMJ disc are described together with the conditions under which lubrication by the disc may be compromised.

The experimental portion of the work, as presented in chapter 3 and 4, focussed on the TMJ disc. The disc was chosen for stress analysis primarily because of lack of information describing the mechanical properties of the disc, and because the disc seems to be the first "victim" in the early stages of degenerative joint disease in the TMJ (Solberg et al., 1985). As noted by Irby and Zetz (1983), the status of the disc has a pronounced effect on the course of degenerative joint disease. Overall, chapters 2 through 4 present a discussion of the mechanisms which prevent the development of excessive stresses in the TMJ. These chapters also describe the conditions when one or more of these mechanisms fail, and stresses in the joint increase. The results of this work will be presented and discussed in support of an hypothesis that stress control in the TMJ may well be unstable. The hypothesis is that the lack of direct neural monitoring of local joint stresses produces stress instability.

1.2 <u>**TMJ Anatomy**</u>

1.2.1 <u>General anatomy of the TMJ</u>

The TMJ is a bilateral diarthrosis (Figure 1.2) between the squamous portion of the temporal bones of the skull, and the mandibular condyles. A fibrous connective tissue layer covers the osseous surfaces of the condyle and temporal bone. Interposed between the surfaces is a fibrous plate or disc. Tensile and shear stresses occur in the joint linings and disc due to loading of the condyle during biting (Figure 1.5b).

In the TMJ of an adult, the mandibular condyle can be likened to a bent cylinder (semicylindroid, Sicher and DuBrul, 1975), with the long axis being in a mediolateral direction, with a slight posterior convergence (Figure 1.2, 1.3). The long axes of the two condyles are said to intersect near the foramen magnum. The condyle is approximately 15 to 20 millimetres (mm) in the mediolateral dimension, and 8 to 10 mm anteroposteriorly (Figure 1.3). The degree of curvature of the condyle in the frontal plane can vary from slightly convex to a tentlike (Sicher and DuBrul, 1975) or gabled roof appearance (Figure 1.4). In the sagittal plane, the anterior and posterior surfaces of the condyle slope away from the height of convexity. Rees described the anterior slope as being approximately 5 mm in width, and the posterior being 12 mm in width (Figure 1.5a). In the fully developed joint, the condyle has a fibrous connective tissue articulating layer, approximately 0.4 to 0.5 mm in thickness, but varies mediolaterally (0.15 to 0.37 mm laterally, with a median of 0.26 mm; and 0.18 to 0.48 mm medially, with a median of 0.33 mm, Hansson and Nordstrom, 1977; Hansson and Oberg, 1977; Hansson et al., 1977). In the adult human, there is a thin cortical plate supporting the articulating layer.

The temporal component of the adult joint comprises a concave temporal fossa posteriorly, and a convex articular eminence and flat preglenoid plane anteriorly (Figure 1.6). In the frontal plane, the fossa is concave (Figure 1.4). The crest of the eminence is also concave, but to a lesser degree (Bhussry, 1976). The roof of the glenoid fossa is thin, which is cited as evidence that although the posterior band of the TMJ disc is contained in the fossa, it is not a stress bearing area (Figure 1.6). The posterior slope of the eminence and crest, in the adult, have thickened subchondral bone which is cited as evidence of a heavily loaded region of the joint. The articulating layer of the temporal bone is also covered by a fibrous connective tissue. On average it is 0.5 mm in thickness on the posterior slope of the eminence, varying mediolaterally from 0.36 to 1.08 mm laterally (median 0.72), and 0.44 to 1.30 mm medially (median of 0.87; Hansson et al., 1977). Function in the articulation is always between the condyle and disc (rotation), and the disc and the articular eminence and its extended planes (sliding, Figure 1.6).

The inferior surface of the TMJ disc is concave, and fits like a cap over the top of the condyle (Figure 1.5a,b), with the long axis of the concavity matching the orientation of the condylar long axis. The superior surface of the disc is flatter, with a slight convexity in the frontal plane which matches the gentle concavity of the frontal plane view of the posterior slope of the eminence. The posterior portion of the disc is formed by a thickened band which blends into a loose connective tissue which attaches to the posterior aspect of the condyle as well as the posterior wall of the glenoid fossa (Figure 1.6). A thickened band is also found in the anterior portion of the disc. It too blends into the connective tissue which attaches to the anterior extent of the capsule which is found at the anterior extent of the preglenoid plane (Figure 1.2). When the condyle is seated into the depression in the inferior surface of the disc, the anterior and posterior bands prevent the disc from being dislodged in the anteroposteior direction. The loading of the disc takes place in the thinner intermediate zone of the disc. Hansson et al. (1977) found that the thinnest portion of the intermediate zone of the disc (0.36 to 1.06 mm) was in the lateral portion of the disc. The thickest portion of the intermediate zone (0.44 to 1.30 mm) was in the more central and medial portions of the disc. The disc is attached medially and laterally at the condylar poles, which prevents mediolateral displacement of the disc. Movement between the condyle and the disc is caused by rotation of the condyle which causes sliding between the condyle and disc surfaces. The translation capability of the condyle produces a sliding movement between the superior surface of the disc and the temporal component of the joint (Figure 1.6).

The fibrous connective tissue of the TMJ surfaces and disc is a mixture of a solid matrix and a mobile fluid. The matrix is comprised primarily of type I collagen (Hirschmann and Shuttleworth, 1976, up to 75% dry weight) and proteoglycans (20% dry weight). The fluid, which is 80% of the wet weight of the disc, is made up of water and mobile cationic electrolytes (calcium, potassium, and magnesium).

1.2.2 The fine structure and chemistry of the TMJ disc

The orientation of the collagen fibres in the disc depends on the region of the disc in which they are situated. On the temporal and condylar surfaces of the disc, there is a close network of fine collagen fibrils, which form a dense horizontal mat. The fibres are arranged in all directions within a horizontal plane. There are reports that to some degree there is a greater tendency for an anteroposterior orientation. In the deeper portions of the intermediate zone of the disc, the collagen fibres are more coarse and have a distinct anteroposterior direction. In the thicker anterior and posterior bands, the collagen is also thicker, but has a three-dimensional orientation, with a predominant mediolateral orientation of many of the major fibre bundles. Overall, the collagen fibre orientation gives an impression that the disc is made up of two parts. First, a fibrous core makes up the deeper portions of the disc. This core consists of coarse fibres of collagen, which have a distinct anteroposterior orientation. The collagen has a wavy winding structure, which has been considered as a shock absorbing mechanism (Taguchi et al., 1980). In scanning electron microscopy studies (Taguchi et al., 1980; de Bont, 1985a,b,c,d), the main alignment of fibrils of the core is observed to be in the anteroposterior direction. Under light microscopy (Christen, 1959; Thilander, 1964; Knox, 1967; Scapino, 1983; Isaccson and Isberg, 1985) a similar pattern of anteroposterior orientation of collagen is described. From the intermediate zone, the collagen flares into the anterior and posterior bands of the disc, interlacing with the coarse collagen bundles which run in mediolateral directions. Secondly, an outer sheath of densely matted fine collagen fibres enclose the more loosely arranged fibrous core just described. Taguchi et al. (1980) and de Bont (1985a,b,c,d) both describe the surface as being closely packed collagen, running in all directions within a horizontal plane, but with a tendency toward an anteroposterior direction.

According to Aspden (1986), the orientation of the fibrous component of connective tissue, in general, has a significant effect on the strength of the fibrous matrix. Aspden considers that collagen strength is greatest when forces act along the long axis of the fibre. Bullough et al. (1970) found that in general, for different areas of the meniscus of the knee, the tensile strength of the meniscus was greater when the stress lines were parallel to the fibre orientation rather than perpendicular to the fibres. The differences were generally greater than ten to one in magnitude. Following up Bullough's work, Proctor et al. (1989) reported that the surface of the meniscus of the knee displayed isotropy when tested in tension, but that there was considerable anisotropy displayed by the deeper layers, which was in agreement with Bullough's report. Proctor concluded that the surface of the meniscus behaves isotropically due to the fine woven collagen mat, which is parallel to the articular surface.

The preferential fibre orientation of the inner core of the TMJ disc, as described by Taguchi et al. (1980) and de Bont (1985a,b,c,d), has remarkable similarity to the descriptions of the deeper layers of the meniscus of the knee joint. It is likely that such an organization will produce, in the deeper layers, a greater strength in the anteroposterior direction. The strong anteroposterior orientation of the fibrous core is likely to produce a significant anisotropy in the shear and in the tensile properties of the inner portions of the disc. The mediolateral strength of the disc is probably less in the intermediate zone, but greater in the anterior and posterior bands and the surface layers of the disc due to the collagen bundles which are oriented mediolaterally as well as anteroposteriorly. It is likely there is isotropy of tensile and shear properties of the surfaces of the disc, due to the random orientation of the collagen fibrils.

The other major constituent of the solid matrix of fibrous connective tissue is the proteoglycan component. Proteoglycans are large, polyanionic molecules, composed of long chain glycosaminoglycans and a protein core. The proteoglycan is covalently linked to a hyaluronic acid backbone. The macromolecules are imbedded and immobilized in the fibrous matrix of the articular lining. Due to the polyanionic character and size of the molecules, there is a 0.2 megapascals osmotic pressure (Maroudas, 1979) which causes fluid and free cations to move into the tissue. The result is a swelling of the solid matrix, until the tension on the fibrous component of the matrix balances the osmotic pressure (Venn and Maroudas 1977; Grodzinsky et al., 1981; Tepic et al., 1983; Armstrong, 1986; Harrigan and Mann 1987). The proteoglycan portion is responsible for the unique fluid filled character of the tissue. The ability of the tissue to absorb water accounts for the viscoelastic properties of the tissue (see Appendix A).

The different species of glycosaminoglycans in the TMJ disc, and their topographical distribution in the disc, has been the subject of scrutiny in the literature. The physicochemical characteristics of the proteoglycan species and their concentrations have a significant effect on the response of articular tissues to imposed stresses. The debate continues as to whether or not the earliest event in the development of degenerative joint disease is the reduction in concentration of proteoglycans in the matrix of the connective tissue.

The species of glycosaminoglycans, as described by Kopp (1976, 1978) included chondroitin sulfate and/or dermatan sulfate, and keratan sulfate. Kopp stated that the keratan sulfate was higher in the surface regions. Similar findings were reported by Stockwell (1979) for the hyaline cartilage surface of the femoral condyle. Kopp also found less glycosaminoglycans in the intermediate zone than in the anterior and posterior bands of the disc. This is also the finding of Granstrom and Linde (1973), Hasty et al. (1983), Mills et al. (1988). Immunostaining of rabbit discs (Mills et al., 1988) showed that the glycosaminoglycans were primarily keratan sulfate and chondroitin-six-sulfate. Again the keratan sulfate was found in abundance around collagen fibres. The chondroitin-six-sulfate was located primarily pericellularily.

The proteoglycan component of the TMJ disc is believed to be responsible for the ability of the fibrous connective tissue to resist temporary compressive forces (Mohl, 1983, see appendix A). The ability of the disc to resist compression is due to the imbibition of water by the proteoglycan molecules, which are trapped by the three-dimensional matrix of collagen fibres of the connective tissue. Kopp's (1976) findings suggest that there might be localized concentrations of glycosaminoglycans in the middle and lateral portions of the disc (Figure 1.7). It has not been determined if the degree of sulfation of these local areas affects the local fluid flow during compression.

It is a characteristic of articular tissues that if a load is constantly applied, deformation of the tissue will continue to increase with time as the fluid is squeezed out. Fluid loss during prolonged loading compromises the lubrication by articular cartilage (McCutchen 1962), and thus increases the likelihood of tensile stress on the surface fibres during movement. Mohl (1983) suggested that such stress concentrations and subsequent fluid loss are attenuated during normal function because of the anatomical configuration of the TMJ. Even slight opening and closing movements of the mandible moves the loaded points mediolaterally, which reduces the amount of fluid lost from local areas, and helps to recharge fluid by pushing it in from adjacent areas. The health of the tissues, which is highly dependant on unsustained loading, is facilitated by movement of the area of stress concentration and therefore facilitates fluid movement to all parts of the fibrous connective tissue matrix. However, sustained heavy loading by the condyle against the eminence during eccentric bruxism or clenching, or chronic unilateral mastication potentially compromises the retention of the local fluid of the loaded areas of the disc (Mohl, 1983). The loss of lubrication and fatigue created by this mechanism might explain the development of degenerative joint disease.

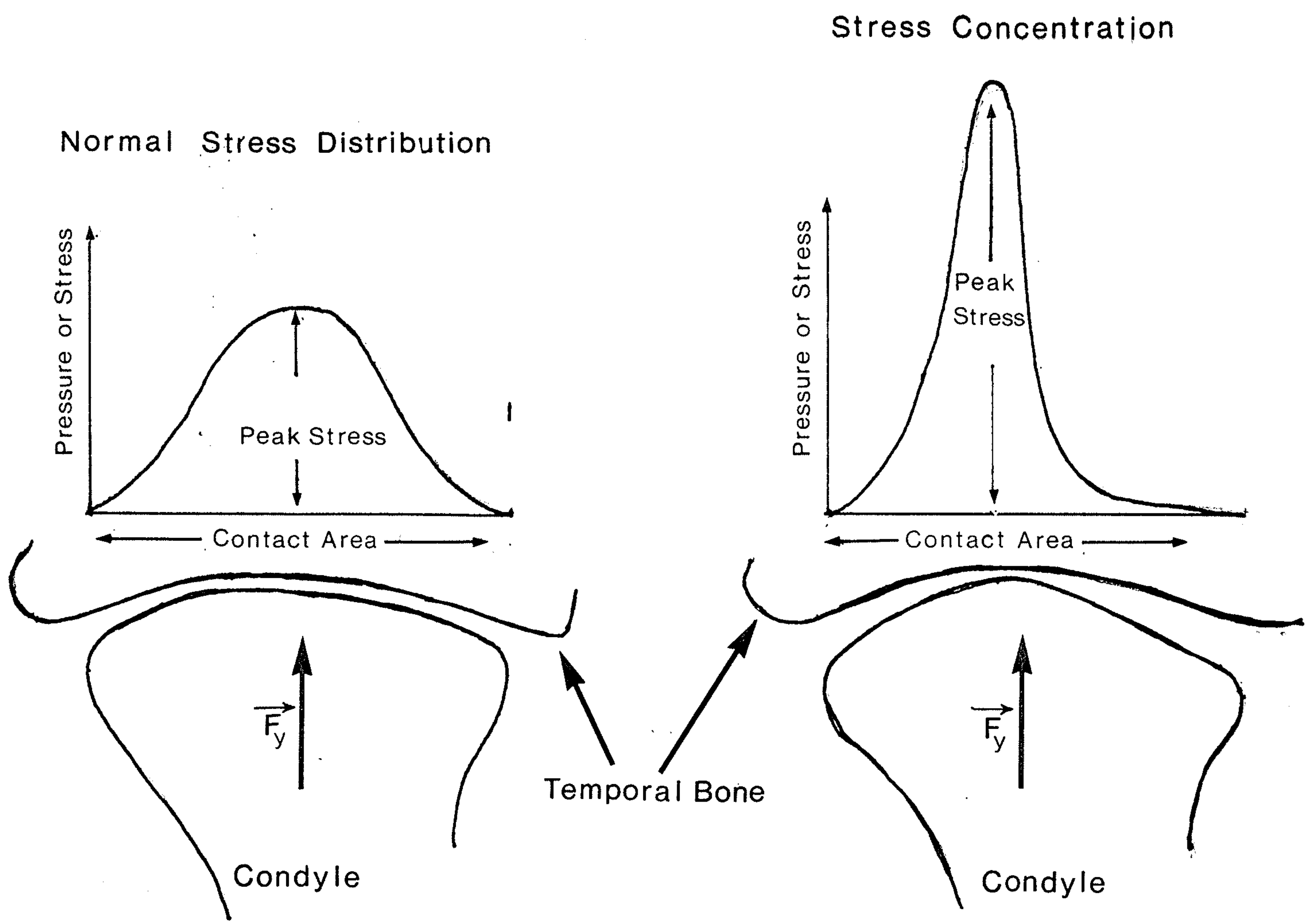

Figure 1.1 **Normal stress distribution and stress concentration**

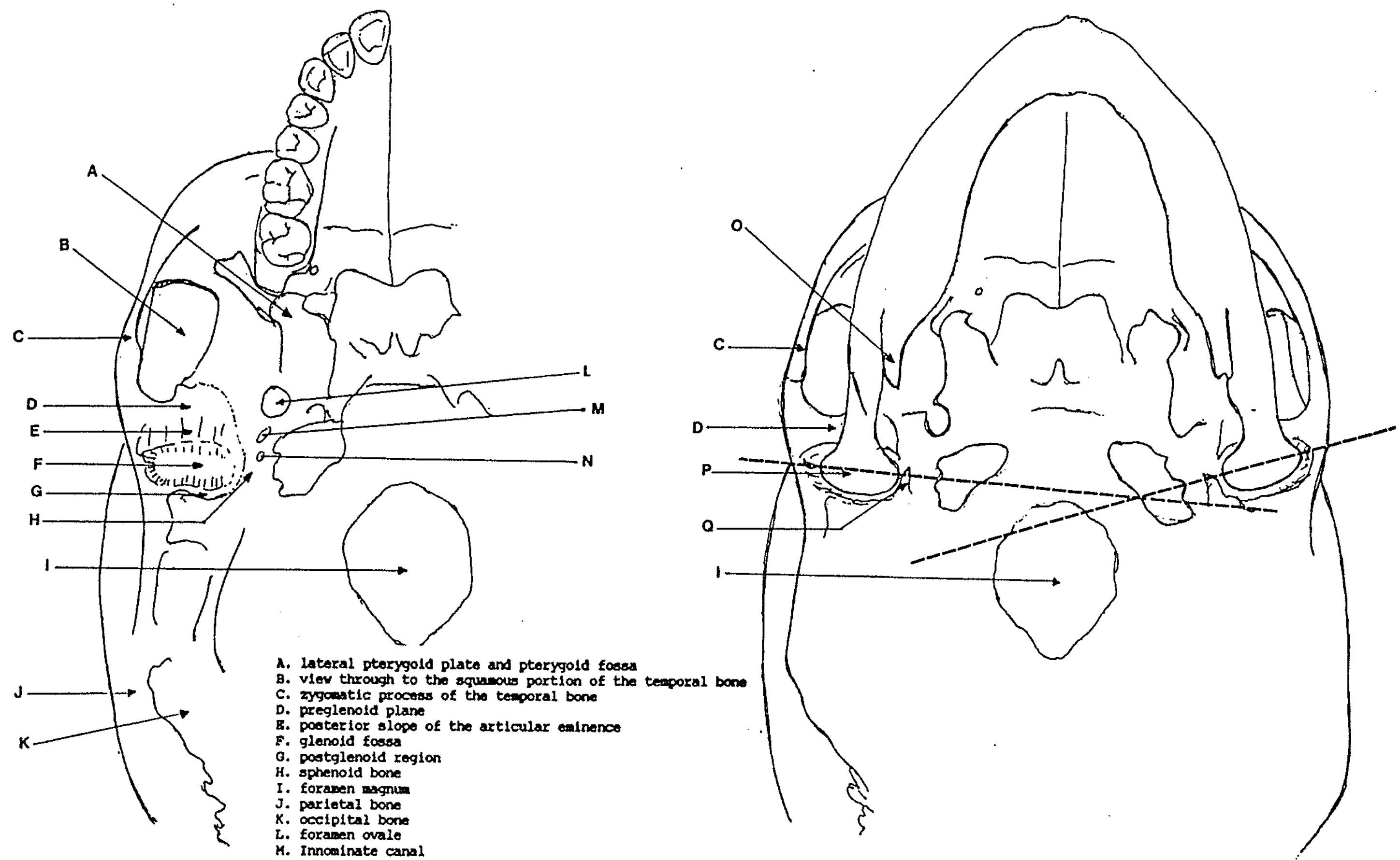

A. lateral pterygoid plate and pterygoid fossa
B. view through to the squamous portion of the temporal bone
C. zygomatic process of the temporal bone
D. preglenoid plane
E. posterior slope of the articular eminence
F. glenoid fossa
G. postglenoid region
H. sphenoid bone
I. foramen magnum
J. parietal bone
K. occipital bone
L. foramen ovale
M. Innominate canal
N. foramen spinosum
O. coronoid process
P. condyle of the mandible (condylar axes indicated)
Q. spine of the sphenoid

Figure 1.2 **Basal plane views of the skull**

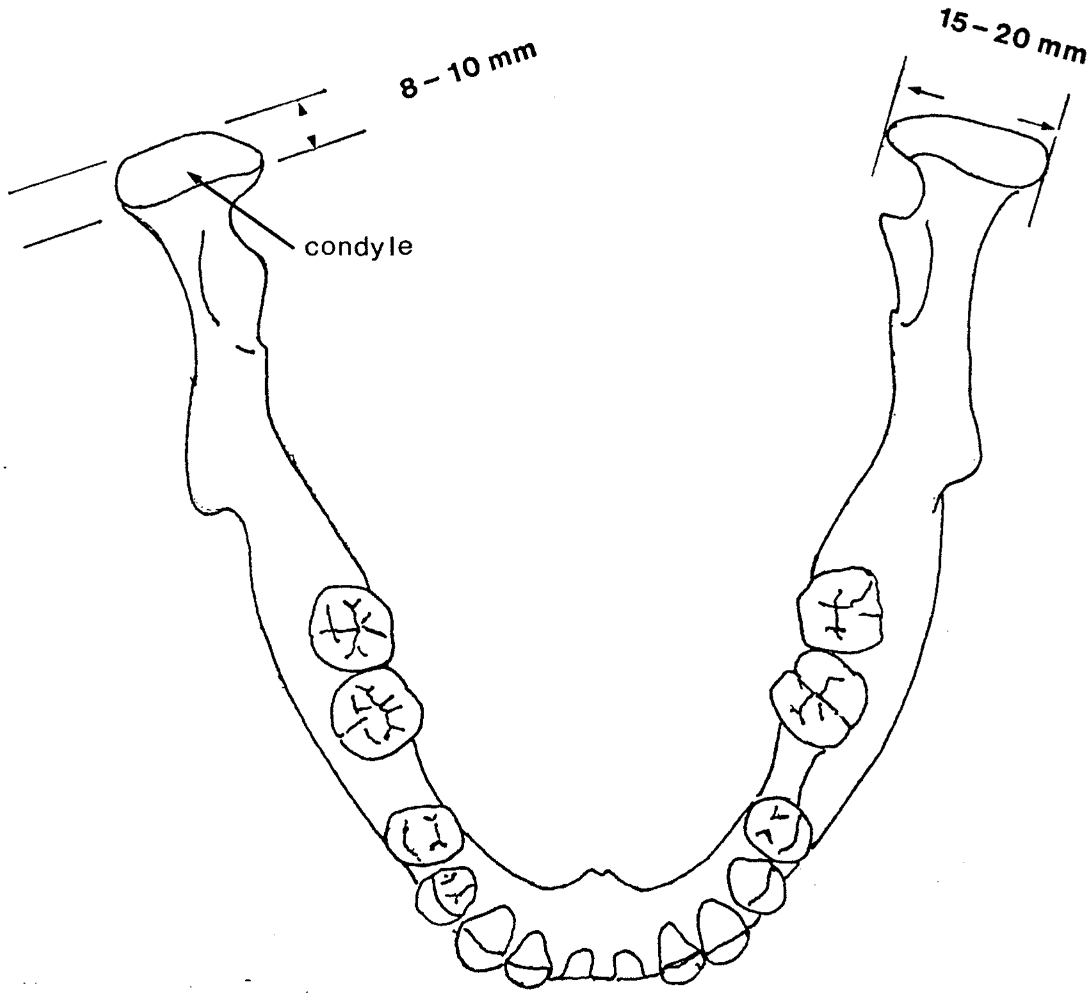

Figure 1.3 Occlusal plane view of the mandible

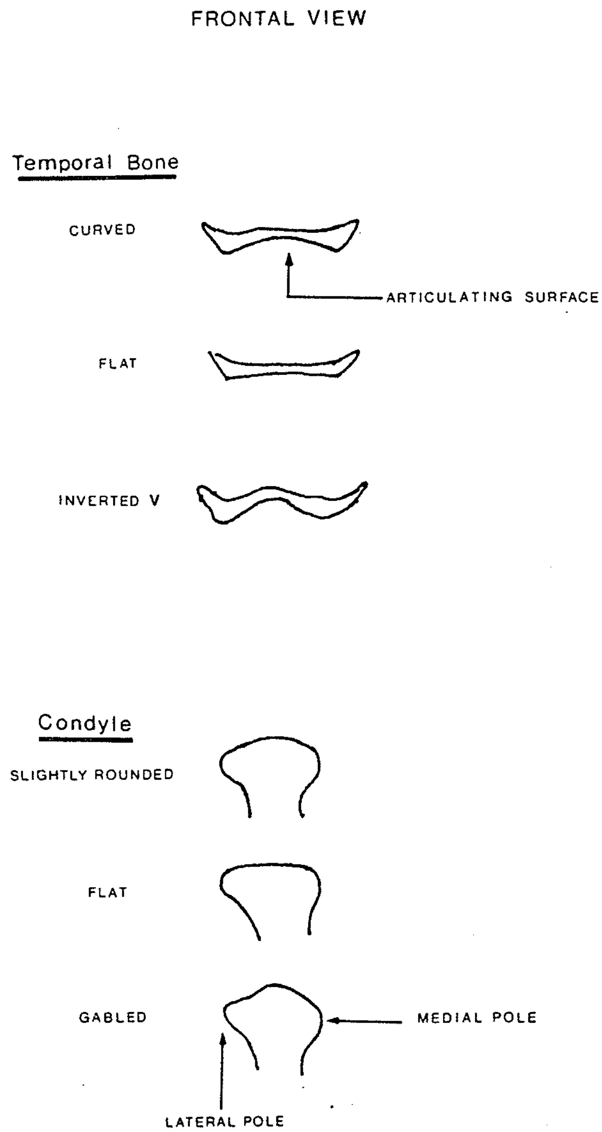

Figure 1.4 Frontal plane views of the shapes of the condyle and temporal bone (adapted from Solberg *et al.*, 1985)

A) Gross Anatomy

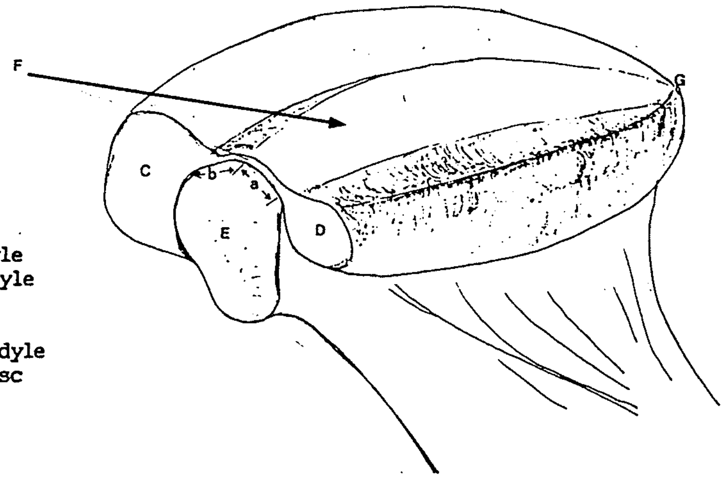

a. anterior slope of the condyle
b. posterior slope of the condyle
C. posterior band of the disc
D. anterior band of the disc
E. cut lateral pole of the condyle
F. intermediate zone of the disc
G. medial pole of the condyle

B) Forces on the disc: deformation and shear stresses

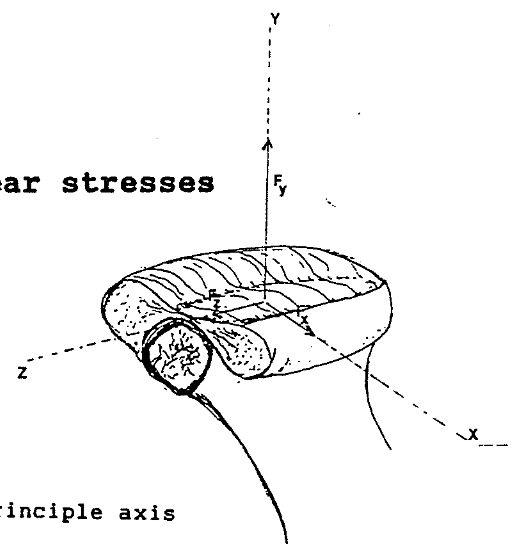

X,Y,Z- orthogonal axis system
Fx,Fy,Fz- forces along the three axis
$\sigma_x, \sigma_y, \sigma_z$- plane stress along a principle axis
τ_{xy}, τ_{zy}- in plane shear stress
a,b- before deformation
a',b'- after deformation

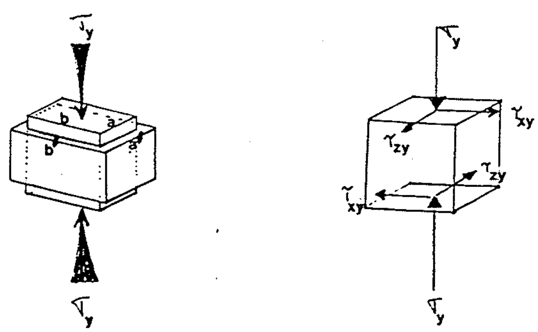

Figure 1.5 The disc-condyle relationship

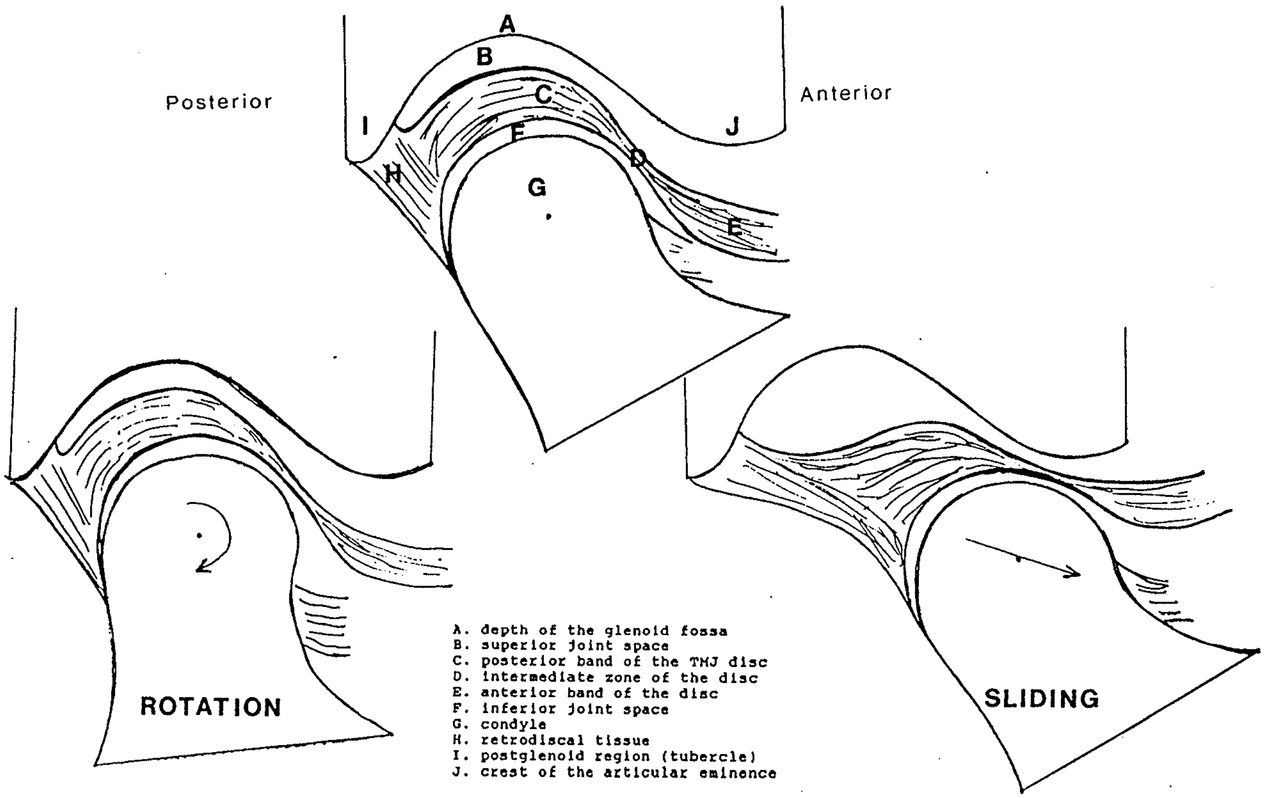

Figure 1.6 Movement of the mandibular condyle

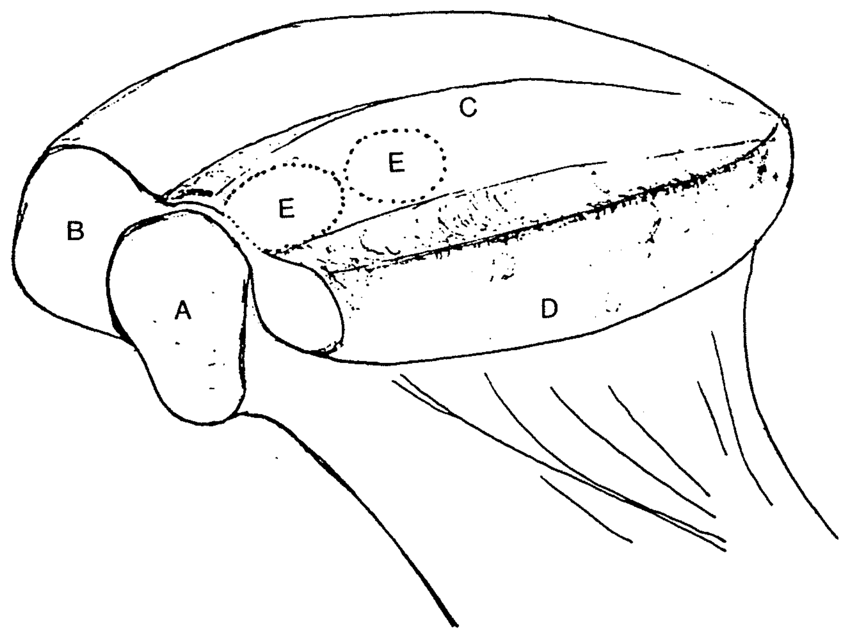

A. cut lateral pole of the condyle
B. posterior band of the TMJ disc
C. intermediate zone of the disc
D. anterior band of the disc
E. areas of glycosaminoglycan concentration

Figure 1.7 Regions of glycosaminoglycan concentration in the TMJ disc

CHAPTER 2

THEORETICAL STRESSES IN THE GROWING TMJ

2.0 Introduction

The development and long term health of the TMJ and other synovial joints is affected by factors determining the magnitude and temporospatial distribution of stress in the articular tissues. As described in Chapter 1, one means of preventing stress concentration and increased local stresses is provided by the coordination of growth of the loading surfaces of the TMJ, together with factors which control the magnitude of joint loads. The following account describes an investigation which demonstrates, theoretically, the age-related changes in the general (average) and local stresses in the growing TMJ. Although this is a theoretical study, the analysis incorporates osteological data describing growth of the loading areas of the joint, congruency of the joint surfaces, and age changes in the bite force, to calculate the theoretical stresses in the growing joint. As well, a numerical model was used to determine how certain factors influence TMJ loads and therefore affect joint stresses. The numerical model had an objective function of minimization of joint loads for conditions of isometric biting. There is evidence (Smith _et al_., 1986; Dixon _et al_., 1990; Trainor and

McLachlan, 1991) that this objective function is a good description of the neuromuscular organization controlling isometric biting. Hence, this study incorporates both the developmental and neuromuscular factors which influence stresses in the TMJ.

This study used a numerical technique to calculate the general and local stress in the growing TMJ. A theoretical approach was chosen since an in vivo experimental method would have required using an animal model to provide the growth data of the joint components, as well as in vivo measurement of joint loads. The results of such an investigation would not have direct applicability to the human TMJ. An in vitro analysis of contact stress, using human temporomandibular joints from autopsy material proved impractical because of the difficulties associated with obtaining unembalmed joints. Instead, a method was used in which human osteological material provided data describing the age-related changes in the dimensions of the human craniomandibular apparatus. Using osteological material made it possible to provide a more complete sample, especially of younger individuals. The osteological sample was also used in calculating the magnitude of condylar loads for each individual. The osteological remains of each individual provided the three-dimensional morphology of the craniomandibular apparatus, which was then used in a numerical model to calculate the magnitude of minimal joint load for isometric biting conditions. Knowing the magnitude of joint load, and the potential area of loading, theoretical stresses were calculated for each individual.

2.1 Description of the Sample

The osteological data used in the study were obtained from the Hamman-Todd Osteological Collection, located at the Cleveland Museum of Natural History. Some of the sample has been described previously (Nickel et al., 1988a,b). Fifty-two (52) specimens were selected for the study presented here. The chronological ages of the specimens ranged between birth and 25 years. Twenty (20) were female, twenty-four (24) were male, and the sex of 8 individuals was not determined. The archival material of the collection made it possible to determine the cause of death for two-thirds of the individuals. Care was taken to find skeletal material of individuals who appeared to be healthy until an acute bout of disease or traumatic mishap resulted in death (Table 2.1). In cases where there was difficulty in determining the cause of death, an attempt was made to screen for gross malnutrition by use of photographs taken at autopsy, height and weight measurements of the cadavers, and notations of the pathologist who had performed the autopsy.

The total sample covered the chronological ages of birth to 25 years. The chronological age of each individual was verified by analysis of the autopsy report, and comparison with dental maturity indicators (Lunt and Law, 1974). The maturity of the individuals was expressed as dental age in years (Table 2.2).

2.2 **Data Collection and Analysis**

2.2.1 Three-dimensional geometry of the craniomandibular system

In the estimation of the theoretical stresses in the joint, data was required describing the magnitude of joint loads, and the areas over which the loads would be distributed. The determination of joint loads was done using a numerical model of minimal joint loading. The calculated joint loads were then divided by the measured area of articular surface assumed to be under load. To use the numerical model in calculations, and to measure the area of loading, required three-dimensional geometric coordinates of the muscles of mastication, dental structures, and osseous structures of the craniomandibular system. Using a previously described photographic technique (Nickel et al., 1988a,b), the positions of the teeth in the dental arch, origins and insertions of the masseter, temporalis, and lateral pterygoid muscles, and morphology of the condyle and temporal component of the joint were defined in three dimensions for each individual. The technique used photographic slide transparencies to facilitate reproduction of the osteological geometries in all three anatomical planes. A computer programme was used to combine the coordinates to produce a three-dimensional geometry of the biting system.

2.2.2 Measurement of loading area

General loading area

In determining the general loading area, the TMJ condyle was considered to be a bent cylinder, with the superior surface of the condyle being the load bearing portion. A rough approximation of the loading area was determined from the anteroposterior and mediolateral dimensions of the condyle. These dimensions were readily derived from 1:1 scale tracings of a coronal plane view (Figure 2.1) of the condyle. Using occlusal tracings of the right and left condyles of each individual, a transverse axis was constructed from the medial pole to the lateral pole of the condyle (Figure 2.1). The distance between the poles along this axis represented the mediolateral dimension of the condyle. At a midpoint in the mediolateral dimension, a perpendicular was constructed which intersected the anterior and posterior boundaries of the traced condyle. The anteroposterior dimension of the condyle was determined by the distance between the anterior and posterior boundaries of the traced condyle (Figure 2.1).

This technique provided the raw data from which the general loading areas were calculated for all individuals in the sample. The following formula was used in the calculations.

$$A_T=[k_1(A_1)][k_2(A_2)]$$

A_T- general loading area (mm^2)
A_1- anteroposterior dimension of the condyle (mm)
A_2- mediolateral dimension of the condyle (mm)
k_1- anteroposterior operator
k_2- mediolateral operator

The operators k_1 and k_2 represent the proportions of the width and breadth of the superior surface of the condyle presumed to be under load. For this study, $k_1 = 0.66$, and $k_2 = 0.80$. These values were a first best guess based on the morphology of the mandibular condyle. The results for the right and left condyles were averaged, and used to give the general area of loading. This technique provided a means of describing a rectilinear loading area, which was used to calculate the magnitudes of general stress. The general stresses were calculated by dividing the applied load by the area.

Stress Concentrations

i. Joint Reconstruction- As stated in Chapter 1, the magnitude of average stress is inversely proportional to the areas of the contacting surfaces, and the distribution of the load is a function of the shape of the contacting surfaces. The general loading area presents a best possible scenario of load distribution. However, the area of loading of the TMJ is not only influenced by the size of the condyle. Equally important is the degree of congruity between the articulating surfaces of the condyle and eminence. With good congruity of the osseous surfaces, the area of loading probably would be of similar shape and size as the general loading area. If, however, there was incongruity of the surfaces so that it was likely that smaller areas of the condyle and eminence would carry the load, then a condition of stress concentration would result. The stresses under these conditions would be higher due to the reduction in loading area over which the load is distributed.

In order to determine if stress concentration occurs in the TMJ, the condyle-eminence relationship was reproduced and analyzed for congruity between the osseous surfaces at condylar positions consistent with incisor biting and molar biting.

A previously reported technique (Nickel et al. 1988a) of reproducing and analyzing eminence growth was modified so that the analysis could be made in the frontal anatomical plane. The technique used fabricated polyvinylsiloxane (Reprosil, Dentsply Limited, Weybridge, Surrey, England) impression records of either the right or left TMJ fossa and eminence. In these impressions, a wire had been bent to produce right angles, and was placed in the impression material before it had set. The impression record was in place over the temporal component of the joint while the standardized photographs were made. The reorientation wire made it possible to reorient each impression record of the eminence to tracings made of the photographic transparencies. For the present study, impression records were made from 39 individuals. Limited facilities and cost factors prohibited making impressions on all 52 individuals.

The impression records were used to make dental stone models of the frontal plane morphology of the articular eminence. For each individual, two sectioned stone models were made. One model was sectioned at the height of the eminence parallel to the transverse axis of the fossa (Figure 2.2). This section of the eminence demonstrated the temporal morphology consistent with a protruded condylar position. Another stone model was sectioned at the midpoint of the posterior slope of the eminence, parallel with the transverse axis of the fossa. This position was consistent with a condylar position during first molar biting (Figure 2.2).

TMJ reconstruction was initiated by making a frontal tracing of the skull of an individual without the mandible <u>in situ</u>. The reorientation wire of the eminence impression record was in place in this view, and was traced on the master tracing. The eminence impression record and appropriately sectioned stone model (posterior slope or height of the crest) were reassembled, and positioned over the tracing using the orientation record as a guide. The eminence impression record was then removed and the stone model was used as a template to trace the frontal morphology of the temporal component on the master tracing. The master tracing was then superimposed on a frontal photograph of the skull with mandible, and the mandible was traced on the master tracing. The tracing was then superimposed on a photograph of the mandible alone, and the details of condylar morphology were traced in correct orientation and scale with respect to the eminence tracings. The reconstruction technique provided good constraints against angular changes in the orientation of the condyle and eminence. Using an overhead transparency projector, the tracing of the condyle and eminence relationship was then enlarged by a factor of five (5). Following this, the enlarged tracing was used in the surface analysis of joint congruity.

ii. <u>Surface analysis</u>- Since the magnitude of stress in the articular tissues is a function of the shape of the contacting surfaces, the purpose of the analysis was to measure the degree of congruity of the osseous surfaces for each individual. An axis system was constructed on the enlarged tracings of the reconstructed joints (Figure 2.3). The origin of the axis system was at the lateral pole of the condyle. The abscissa ("Z") axis was constructed parallel to the occlusal plane, and was divided into ten (10) equal parts, the origin (coordinate #0) at the lateral pole, and coordinate #10 at the point of intersection of a perpendicular which was drawn from the medial pole to the abscissa.

After identifying the coordinates on the Z-axis, perpendicular lines were constructed in a positive (superior) "Y" direction, which terminated at the point of intersection with the superior surface of the traced condyle. These perpendiculars were constructed from coordinates #1 through #9, which represented eighty percent (80%) of the total superior surface of the condyle. This was assumed to be the maximal transverse dimension of the loading area of the condyle (Figure 2.3). On the superior surface of the condyle tracing, midway between each of the coordinates #1 through #9, additional coordinates were marked. This produced a total number of seventeen (17) coordinates, equally spaced on the superior surface of the traced condyle (Figure 2.3). From points #1 through #17 on the condylar surface, a perpendicular line was constructed from the condylar surface, extending towards the traced surface of the temporal component. Each perpendicular was terminated at the point of intersection with the traced surface of the eminence. These perpendiculars represented the loci specific vertical dimension between the condyle and eminence.

To demonstrate variation in congruency, the average distance between the condyle and temporal component was calculated and the differences between the average distance and the distance at each of the coordinates #1 through #17 was plotted. For any individual, the average vertical distance was determined by summing all the perpendicular dimensions for coordinates #1 through #17, and dividing by 17. A normalized congruency plot was then constructed (Figure 2.4). The surface coordinates #1 through #17 were plotted on the horizontal axis. Coordinate specific differences in vertical dimensions were plotted on the vertical (Y) axis. The end result was a normalized plot of joint surface congruity. Widening of the distance between the surfaces was reflected in positive (+) vertical scores, and negative vertical scores (-) reflected a narrowing of the distance between joint surfaces (Figure 2.4).

iii. <u>Calculating area of stress concentration</u>- The anteroposterior boundaries of the loading area were determined in the same manner as the general loading area, and were assumed to be 66% of the anteroposterior width of the condyle. Any variation in the concentration of loading, therefore, was influenced by the widening and narrowing of the vertical distance between the joint surfaces. The mediolateral boundary limits of the local loading area were defined by a positive two (+2) millimetre (mm) addition to the minimum vertical distance (Y minimum) on the enlarged tracing of the reconstructed TMJ. The value of +2 mm was chosen for it represented a 30% normal displacement of the fibrous articular coverings of the condyle and eminence. The magnification of the enlarged reconstruction tracings was by a factor of five, which means that 2 mm on the tracing was a 0.4 mm displacement _in vivo_. Hansson and Nordstrom (1977) and Hansson _et al_. (1977) found that the average combined soft tissue thickness of the central portion of the condyle and eminence was 1.5 mm. Therefore, 0.4 mm of displacement is about 30 % of the total tissue thickness of the condyle and temporal component of the joint. This value seemed to be a reasonable starting point from which to define the local stress areas. A 30 % displacement limit was an optimistic value. Strain values of 20% have been measured in hyaline cartilage of the hip (Rushfeldt _et al_. 1979, 1981). It should be noted that the lateral boundaries were determined by the displacement of the soft tissue covering of the condyle and the temporal bone. The potential effects of the TMJ disc in increasing the loading area were not considered at this stage. This was acceptable for the time being, since the objective of this portion of the investigation was to determine the capability of the developing surfaces and mechanisms of load control in preventing high magnitudes of local stress. In Chapter 3, the role of the disc in load distribution is explored.

The local loading area, as determined by the described technique, was calculated as a percentage of the transverse width of the condyle. If there was good joint congruity, the calculated value approached unity, which meant that the transverse width of the loading area was the same as that in the general loading area calculations. With poor congruence, the percentage of the transverse dimension was reduced. Multiplying this value by the actual transverse dimension of the condyle, as measured from the occlusal photograph of the mandible, provided the mediolateral dimension of the local loading area. This value in turn, when multiplied by the anteroposterior dimension, gave the local rectilinear loading area in mm^2. The equation used to calculate the local area of loading is as follows:

$$[\frac{\Sigma}{17}(k_1\gamma)]\,[k_2\epsilon]=A_L$$

Σ - number of coordinates in the local loading area
γ - anteroposterior width of the condyle (mm)
ϵ - mediolateral width of the condyle (mm)
k_1,k_2 - anteroposterior and mediolateral operators (see section 2.2.2- General loading area)
A_L - local loading area (mm^2)

2.2.3 Calculation of joint load

Mechanical stress is defined by the equation:

$$Stress = \frac{Load(N)}{Area(mm^2)} \qquad (MPa)$$

The method of measurement of general and local loading areas were described in sections 2.2.1 and 2.2.2. The magnitudes of condylar load was left to be determined using a numerical modelling technique as described by Smith et al. (1986) and used by Nickel et al. (1988b). Using a numerical model in combination with reported bite force magnitudes, the joint loads were calculated and expressed in Newtons (N).

Numerical analysis of joint loads

i. Description of the model- The numerical model used in this project has been described by Smith et al. (1986) and Trainor and McLachlan (1991). Dixon et al. (1990) and Nickel et al. (1988b) have used the model in experiments to describe the muscular control of the mandible, and the growth of the eminence of the TMJ. An abbreviated description will be presented here to introduce the terminology used in the model.

In the numerical model, bite force direction, magnitude, and point of application were defined. Three muscle pairs (masseter, temporalis, and lateral pterygoid) were identified by points of origin and insertion, which were defined by the estimated centroid of each muscle attachment. The magnitude of force contributed by each muscle, for a given biting condition, was left to be determined by the modelling processes.

The method used in the numerical model was an iterative or "trial and error" technique. This technique enabled calculation of six muscle forces (three muscle pairs) and six condylar forces (right and left F_x, F_y, and F_z). The final solution was calculated on the basis of producing minimal joint loads, as well as producing static equilibrium. The iterative method varied each muscle, in turn, to find the combination of muscle forces that would result in static equilibrium and minimal condylar forces.

ii. Numerical Calculations- The numerical model was used to calculate the magnitudes of condylar loading for mandibular positions consistent with isometric biting on the first molar and on the incisor teeth. The method used in this study was the same method described by Nickel et al. (1988b). In the previous study, the analysis focussed on the directions of condylar loading. The primary concern in the present study was the magnitude of the load on the condyles.

In order to use the numerical model, craniomandibular geometries consistent with mandibular positions for first molar biting and incisor biting were developed. Different geometries were used for molar and incisor biting since movement of the mandible from a retruded (molar biting) position to a protruded (incisor biting) position altered the three-dimensional relationship of the muscles of mastication. This resulted in different magnitudes and directions of condylar loads between the two positions.

The results of calculations of the numerical model were expressed as a percentage of a theoretical bite force.

$$C_T \times B_F = C_L$$

C_T- predicted condylar load for a unit bite force
B_F- age-specific bite force (N)
C_L- condylar load (N)

For the purposes of the calculations, a maximal theoretical bite force was prescribed before calculations began. To convert the calculations of the numerical model to N, the magnitude of theoretical condylar load (which was expressed as a percentage) was multiplied by the bite force (N) appropriate to the age of the individual (see following section).

Maximum isometric bite force

The values of age-related bite forces, as used in the equation above, were established from reports in the literature. Isometric bite forces for molar biting in adults has been reported by Proffit et al. (1983), Mansour and Reynik (1975), Sasaki et al. (1989), Lundgren and Laurell (1986), and Howell and Manly (1948). Proffit and Fields (1983) were the only source of isometric bite forces for children. These children were between the ages of six and eleven years (mean of 8 years). Peiper (1963) provided data on suckling "bite forces" of the new born child. Figure 2.5 shows the ranges of bite forces cited in the previously mentioned literature. Figure 2.5 also shows the age relationship of the bite force values used in the theoretical calculations of joint load. For the purposes of this project, it was assumed that there was a linear increase in molar bite force with increasing age (20 N/year). This increase in bite force was derived from the slope of the line intersecting the average bite force of 170 N at 8 years of age (Proffit and Fields, 1983), and approximately 10 N at birth. The bite force chosen at birth was done on the basis that it was slightly higher than the protruded bite force described by Peiper (1963). The assumed linear relationship of the molar bite force was continued through to adulthood, where at 25 years the extrapolated molar bite force was 500 N.

The average maximum isometric molar bite force in the younger age groups is in reasonable agreement with the reported bite force found in the literature. A bite force of 500 N in adults is high with respect to an average of the reports in the literature (see Table 2.3, Figure 2.5). This feature should be taken into consideration when interpreting the results for stresses during molar biting in adults.

Information concerning the variation of isometric incisor biting with age is scarce. In adults, Mansour and Reynik (1975) measured isometric incisor bite forces at about one-fifth that of isometric molar bite forces. In the absence of experimental data, a first approximation of incisor bite forces in adults was determined as twenty percent of the given molar bite force. In the youngest age groups (birth to six months), a starting anterior bite force of 8 N was chosen, based on Peiper's work (1963) in which he described the suckling bite force of a newborn as increasing to above eight hundred grams in a few weeks after birth.

2.2.4 Sources of error

Data Collection Errors

i. Errors due to an osteological sample. It is not ideal to use a cross-sectional sample to investigate growth phenomenon. However, the problems associated with obtaining a longitudinal human sample are prohibitive. The invasiveness and lack of detail of available imaging techniques outweighed any potential benefit to the individual. An animal model could have been used to study longitudinal growth characteristics; but the results would have limited application in the description of the growth and development of the human joint. Therefore, a cross-sectional sample of human remains provided the best way to describe the growth and development of the joint, but its limitations are acknowledged.

ii. Photographic technique errors. The photographic technique used to collect data has been evaluated for errors in photographic perspective (Nickel et al., 1988b). Corrections for these errors were calculated to determine if there were large differences in the magnitudes of condylar load when using a perspective-corrected geometry as opposed to an unaltered geometry. The mean difference in condylar loads between the two geometries was approximately 8%. This amount of error was small enough that unaltered geometries could be used in this study to give a reasonable approximation of the magnitude of condylar load.

Photographic perspective was also a potential source of error in the calculation of the loading area of the TMJ, especially in the calculation of stress concentration. In the frontal plane view, the condyle was always behind the focal plane. Therefore, there was a perspective error in the dimension of the condyle in this view. To correct for this error, prior to joint reconstruction, a frontal plane photographic projection was enlarged so that the mediolateral dimension of the condyle matched the mediolateral dimension measured from an occlusal tracing of the mandible (Figure 2.1). In the occlusal view of the mandible, the condyles were always on the focal plane. This view always gave an accurate measurement of the true mediolateral dimension of the condyle. By enlarging the mediolateral dimension of the frontal plane projection, photographic perspective errors of the mediolateral dimension were corrected. It should be noted, however, that the mediolateral angulation of the condyle in adults caused the medial aspect of the condyle to be behind the lateral pole. To determine the magnitude of the difference in perspective between the medial and lateral aspects of the condyle, a worst-case situation was chosen (specimen #052) in which the medial pole of the condyle was approximately 10 mm posterior to the lateral pole. The distance of the lateral pole to the focal plane was in excess of 90 mm. The correction formula,

$$Y_{actual} = Y_{measured} \left(1+\frac{X_{measured}}{D}\right)$$

Y_{actual} - real vertical dimension (mm)
$Y_{measured}$ - vertical dimension (mm) measured from the photograph
$X_{measured}$ - distance (mm) of measured point behind the focal plane
D - distance (mm) from camera to focal plane

was used to determine the correction factors for the medial and lateral poles of the condyle. The correction factor for the lateral pole was 1.09, whereas the factor for the medial pole was 1.10. The mediolateral difference in magnification was approximately 1%, and therefore considered not to be significant in the calculations of local loading area.

iii. Tracing technique errors. Superimpositions of the tracings of osteological morphology were easily accomplished, which indicated that tracing errors were not greater than one line thickness, or approximately one-half of one millimetre.

Errors in Calculation of Loading Area

i. Joint reconstruction errors. When determining the area of loading of the joint surfaces, the most significant source of error in this study was introduced by the reconstruction technique. The reorientation wire provided good constraint against rotation (angulation) variation between the condyle and stone model made from the eminence impression record. However, the correct mediolateral relationship between the eminence and condyle was not as easily defined. The method chosen in deciding the mediolateral relationship between the two components was a "best fit" approach which optimized the mediolateral dimension of the loading area. To determine the best-fit between the condyle and eminence, at least two reconstructions of the condyle-eminence relationship were done. Each reconstruction had a slightly different mediolateral position of the condyle with respect to the eminence. The local loading area for each reconstruction was then measured. The condyle-eminence relationship which maximized the local loading area was then used in the calculations of local stresses.

To test the reproducibility of the reconstruction technique, twenty-one randomly selected individuals were reconstructed on two different occasions, and were analyzed for discrepancies in the mediolateral dimension as determined by the congruency plots. The range of differences between the two reconstructions was from 0% to 18%, with the average difference being about 6%. This amount of variability was considered acceptable for describing the relationship between local stress and age. In the future, in order to determine accurately individual local stresses, a more rigourous technique will be required to reduce the variability of the mediolateral dimension of the local loading area.

ii. Error in the boundary limits of loading areas. The size of the general loading area was determined by 0.66 of the anteroposterior width (k_1 operator) and 0.80 of the mediolateral length (k_2 operator). These values were chosen based on the estimation of the loading area on the superior surface of a bent cylinder. In the future, a better measurement of general loading area may be made using in vitro techniques such as dye exclusion during loading of intact joints (Seedhom and Hargreaves, 1979) or intraarticular castings using polymethylmethacrylate (Walker and Erkman, 1975). Unfortunately, testing of intact joints will still encounter the problem of finding adequate cadaver material from ages birth to adult. For the present study, the described technique provided an acceptable means of establishing the relationship between general stress and age.

With respect to the local loading areas due to surface incongruity, the method of defining the boundaries was chosen so that the result was optimistic in magnitude, thereby giving lower local stresses. Strains of 20% of fibrous connective tissue have been reported (Rushfeldt et al., 1979, 1981), but are likely to produce early fatigue failure of the fibrous component of the tissue matrix (Weightman et al., 1973). Therefore, using a peak maximal displacement of 30% of the soft tissue to define the boundaries resulted in a larger loading area than might otherwise occur in vivo. At this time, we can only estimate local stresses. In the future, the direct measurements of local stresses will require the use of techniques such as those described in Chapter 3, in which microinstrumentation can measure stresses with high topographical resolution; better than presently reported for larger synovial joints.

Errors in the Calculation of Joint Load

i. Errors in age-related bite force. This study examined the stresses during theoretical maximal isometric biting. Given the nature of the sample used in this study, it was not possible to determine the bite forces that each individual could produce. The assumption was made that a particular bite force was possible, based on reported bite forces found in the literature. The bite forces in the younger age groups were biased toward the low end of the range of bite forces cited in the literature. The bite force was assumed to increase linearly from birth to adult (Figure 2.5). The assumption is likely to be incorrect. The rate of increase in bite force probably reflects a function similar to the rate of increase in muscle mass of the individual (Tanner, 1977). The growth of muscle mass is not a linear function, but shows a very high rate of increase in the younger years, and slows during adolescence. Therefore, assumption of a linear increase in bite force probably overestimates the bite force in the older age groups.

The decision to model incisor bite force as 20% of molar biting was based on evidence of Mansour and Reynik (1975). There is no evidence to fully support this assumption for young individuals. For the time being, it is not unreasonable to believe that the control of bite forces is similar in children and adults. Further data is required before a more accurate description of age changes in incisor biting is possible.

ii. <u>Validity of the numerical model</u>. There is phylogenetic as well as electromyographic evidence to support the hypothesis used in the model, that minimization of joint loading is a reasonable objective function of neuromuscular organization during isometric biting. Evolutionary evidence to support the hypothesis has been presented by Crompton (1963). Further validation of the model has been reported by Dixon <u>et al</u>. (1990) in which electromyography was used to test the numerical model calculations of muscle force values for a series of biting conditions. Experimental results on humans indicated that for isometric biting, EMG activity of the masseter and temporalis muscles correlated well with model-calculated muscle forces. As well, the calculated relationship between arch position, and bite force magnitude match the in vivo measurements made by Howell and Manly (1948).

It may seem that the use of a single vector to represent a muscle force is an oversimplification, given that the muscles of mastication are multiply pinnate. A muscle may be theoretically modelled by any number of vectors, which, in turn, may be summed to produce a single vector of known direction and point of application. It has been demonstrated (A. Hannam, personal communication) that the muscle fibres innervated by a single motor neuron were found throughout the breadth of the superficial masseter. It seems unlikely that a single portion of the muscle could produce an unusually large contribution to the overall force. Jimenez (1985) also found that in general, during normal biting, portions of the temporalis muscle were not isolated in terms of which portion produced the force. Wood (1986) used fine needle electrode electromyography, and found that all areas of the temporalis were always active during normal biting tasks, which supports the assumption that a single vector may be assumed to produce a general force direction and point of origin. The electromyographic evidence presented by Blanksma and van Eijden (1990) shows that for a very large gape of 18 mm, there is some discrepancy in the direction of the temporalis muscle vector, depending on the direction of the bite force.

However, the largest difference shown by the author was 8 degrees change in the temporalis muscle vector. It seems reasonable that the single muscle vector is a useful simplification for the purposes of modelling.

The numerical model is also supported by some of the recent work of Appenteng and co-workers (1989, 1990). Their results show that interneuron connectivity, starting from periodontal afferents, results in differential activation of ipsilateral and contralateral motoneurons. The excitatory post synaptic potentials (EPSP's) were stronger in the masseter and temporalis motoneurons on the side which was ipsilateral to the stimulated periodontal mechanoreceptors. Appenteng and co-workers suggest that synaptic characteristics such as the number of boutons which synapse on contralateral motoneurons are responsible for this differential ipsilateral-contralateral activation of masticatory muscles. The numerical model calculations also predict a differential ipsilateral vs. contralateral muscle activation, as reported in the EMG literature (Dixon et al., 1990) and reported by Appenteng and co-workers. Ter Horst et al. (1990) have studied contralateral projections of interneurons to the trigeminal motor nucleus, and have noted that there was the requirement of a differential right-left activation of the masticatory adductor muscles. However, Ter Horst et al. (1990) stated that the contralateral muscles were activated more than the ipsilateral. This is not borne out for the conditions of isometric biting (Dixon et al., 1990) or for the final closing phase of mastication (L.R. Iwasaki, personal communication).

2.3 Results

2.3.1 General stresses

As shown in Figures 2.6, general stress for molar biting starts at approximately 0.5 Mpa at birth, and increases to approximately 3.0 Mpa by age 25 years. During this period, the bite force for molar biting increases from 10 N to 500 N (Figure 2.5). The increase in bite force compared to the increase in general stress is about 8 to 1. The increase in general stress was limited by two factors. First, there is an increase in the general loading area (Figure 2.8) which increased from approximately 25 mm^2 at birth to approximately 70 to 75 mm^2 by age 25 years. The second factor limiting the increase in general stress during molar biting is the limited increase in joint loads (Figure 2.9). Condylar loading during molar biting increased from 6 N at birth to an average of 150 N at age 25 years. The increase in the bite force compared to the increase in condylar load was about 2 to 1. The combination of increase in general loading area, with the control of increases in condylar load, limited the increase in general stress during molar biting.

With respect to the general stresses during incisor biting, general stresses increased from 0.5 MPa at birth to about 1.5 MPa at age 25 years (Figure 2.7). Incisor bite forces increased by a factor of 17, from 8 N to 140 N. The increase in bite force compared to the increase in general stress during protruded biting is about 6 to 1. The limited increase in general stress during incisor biting was due to an increase in the size of the condylar loading area (3.5:1), as well as a limitation in the age-related increase in condylar load during incisor biting (Figure 2.10). Condylar loads increased from 8 N at birth to about 80 N at age 25 years. The increase of bite force compared to increase in condylar load during protruded biting is about 2 to 1.

2.3.2 Local stresses for molar and incisor isometric biting

Figures 2.11 and 2.12 show frequency distributions of the size of the mediolateral dimension of the localized loading area for each individual. The skewness of the frequency distribution for molar biting (Figure 2.11) indicated that good congruity occurred more often when the condyle was positioned against the posterior slope of the eminence. This resulted in local stresses being nearly equal to general stresses for the majority of individuals (Figure 2.6). Opposed to this, the frequency distribution associated with protruded or incisor biting (Figure 2.12) shows that there is considerably less congruity and hence smaller mediolateral dimensions in the local stress area. The results were that local stresses were more often higher than the general stresses (Figure 2.7).

There were exceptions to these results. There were four individuals who exhibited very high local stresses during molar biting (specimens #028, 031, 087, 091; as indicated by black squares, ■, in Figure 2.6). These individuals had retruded local percentages of loading areas which were less than the protruded local percentages. These individuals had better TMJ surface congruency in the protruded biting position compared to the retruded biting position. The congruency in the protruded position was between 1.3 and 3.9 times better than for retruded biting. Examination of the stone models showed that in these individuals the surface was remodelled in a fashion similar to the descriptions reported by Moffett _et al_. (1964). The stone models in this study exhibited erosions at the height of the crest of the eminence. It may be that these individuals were functioning more frequently in a protruded position. This would result in an increase in stress in the area of the crest of the eminence. However, looking at the occlusions and skeletal patterns of these individuals, it was not evident why protruded biting would be more common in these individuals. No evidence of wear or other factors could account for the evidence in the joints that "habitually" protruded function had occurred.

2.4 **Discussion**

The objective of this component of the research was to determine if there was evidence of developmental and neuromuscular mechanisms which reduced the magnitude of stress in the TMJ. If these mechanisms were functional, there would be a limited increase in the stresses in the joint because of growth of loading areas of the joint, and controlled increases in the condylar loads. The results showed that the general growth of the condyle, together with an objective function of minimization of joint load, resulted in an increase in general stresses which were at least 6 to 8 times less than the increases in the age-related bite force.

There has been increasing interest in the developmental aspects of degenerative joint disease (Carlson et al., 1985). The results of this study have shown that although the general stresses were well controlled, stress concentrations occurred very early in the developing joint. Although the expression of degenerative joint disease is more likely to be found in the adult, the events which precipitate the disease could occur during the development of the joint. As reported in the orthopaedic literature (Malemud and Shuckett, 1987; Sokoloff, 1969; Rushfeldt et al., 1979, 1981; and Spoor et al., 1989), factors such as growth and congruency of the articulating surfaces and the neural organization controlling the joint loads influence the long term health of the joint. In the TMJ, the present results have established one component of the process, that being the growth mechanism of the eminence, which appears to produce, in some cases, site specific stress concentrations between the articulating surfaces. Theoretically, the articular eminence appears to be developed in consequence of a temporospatial loading of the condyle against the temporal component of the TMJ (Nickel et al., 1988b). This loading results in a secondary cartilage and osseous growth on the temporal component of the immature joint. The process begins in utero, with the greatest velocity and with at least fifty percent of eminence development occurring before the age of three years. Such a mechanism of bone growth would seem to create instability in the control of local stresses, for it is likely to produce significant site specific incongruities between the joint surfaces. Such an interpretation is supported by the results of this study and by the autopsy reports of Solberg et al. (1985) and others (Carlsson and Oberg, 1974). These latter authors suggest that degenerative joint disease is most commonly found on the lateral portion of the crest of the eminence. The results of the present study show that the local stresses during incisor biting are at least equal to if not higher than during molar biting, even though the protruded bite forces are one-fifth that of molar biting.

The general and local stresses calculated in this study are of similar magnitude to the stresses reported for in vivo and in vitro studies of other synovial joints (Rushfeldt et al., 1979, 1981; Walker and co-workers, 1972, 1975; Hayes et al., 1972; Brown and co-workers, 1980, 1983; Mizrahi et al., 1980). The general stresses have averaged between 2 and 4 MPa in the adult hips and knees, and peak local stresses on the average of 4 to 6 MPa, but as high as 18 MPa in the hip (Hodge et al., 1986). Paul (1980) has estimated that the general stresses in the elbow are about 3 MPa, and 2.9 to 4.3 MPa in the fingers. In retrospect, it is not surprising that the stress levels of the TMJ are like other synovial joints. The mechanisms of tissue nutrition are likely to be the same as other articular tissues (Mohl, 1983). With all the similarities of the TMJ to other joints, the TMJ has some unique features which are likely to have an effect on the mechanics of the articulating surfaces. The translational ability of the condyle imparts a remarkable mobility to the joint. A consequence of this mobility is a significant potential for variation in the congruity between the articulating surfaces, as demonstrated in the results presented here. The potential for surface incongruity is enhanced by the unusual phenomenon of the development of the articular eminence. For protruded biting, it is fortunate that there is neural control limiting the bite force (Lund and

Lamarre, 1973). In most of the cases analyzed, although the protruded bite forces were one-fifth of molar biting, the local stress levels were of equal or greater magnitude to that of the local stresses during molar biting. Clearly, significant reduction of loading area exists in the protruded position. The exceptions to these results (specimens # 028, 031, 087, 091) are interesting for upon inspection of the stone model reproductions of the temporal components it became obvious that the surfaces were remodelled; even in these very young individuals (ages 12 to 24 years). Significant remodelling of the joint has been previously reported for this age group by (Solberg et al., 1985; Pullinger et al., 1990; Irby and Zetz, 1983). The osseous changes were consistent with regressive remodelling as described by Moffett et al. (1964). Due to the changes in the surface of the eminence, congruity of the surfaces became better in the protruded position than in the retruded condylar position.

The evidence of stress concentration in the TMJ is an important result. During translation, the position of stress concentration changes mediolaterally as the condyle moves anteroposteriorly (Mohl, 1983). A local deformation of the cartilage, therefore, must move mediolaterally, pushing water through the cartilage matrix. This occurs as the loaded condyle is translating anteroposteriorly. The tractional forces produced by this "ploughing" may be the principal means of fluid movement and nutrition to the loaded areas of the disc and to the surfaces of the condyle and eminence.

In the calculation of theoretical stresses, the role of the TMJ disc was not taken into account. The disc has been considered as an intracapsular mechanism which facilitates load distribution (Okeson, 1985; Gillbe, 1975; Gerber and Steinhardt, 1990; Saegesser, 1990). Unfortunately, there is no evidence as to how good the disc is at load distribution. It might be possible that the disc is capable of reducing local stresses, for this would be useful for the continued health of the fibrous matrix of the articular tissues. By reducing the local stresses there is a reduction in the potential for fatigue failure of the fibrous connective tissue matrix (Weightman et al., 1973). As well, lubrication of the joint surfaces would be enhanced. McCutchen (1978) states that boundary lubrication fails at 1 MPa. Theoretically, this would mean that most of the general and local stresses exceed the limit of boundary lubrication. McCutchen also notes that a weeping lubrication mechanism (see chapter 4) relies on congruent surfaces, with a ready supply of fluid. The disc might also play a role in not only increasing the congruity between the joint surfaces, but also as a reservoir which supplies fluid to the weeping bearing. The weeping bearing is the third mechanism by which stresses are reduced in synovial joints, and an essential one for the elimination of tensile forces on the surface due to friction between the sliding surfaces.

2.5 **Summary**

The results, as presented in this chapter, show that with respect to reducing the general stress in the TMJ, there is coordination between general growth of the condyle and the control of joint loads. The age-related increase in bite force was 6 to 8 times greater than the increase in general stresses. However, the mechanism of eminence development produced instability, in that the osseous development of the articular eminence increased the degree of stress concentration in the protruded mandibular position. In the earlier ages, the local stresses during protruded biting were equal to or greater than the stresses during molar biting, even though the bite force in the protruded position was reduced to 20% of the retruded bite force. In some individuals of the older age groups the local stresses during protruded biting were not as great as compared to molar biting. There was physical evidence to indicate that surface erosions had occurred between the articulating surfaces of the protruded biting position.

Neural control of bite force reduces the maximum bite force in the protruded position (Lund and Lamarre, 1973). This prevents a catastrophic increase in the local stresses. Coupled with this, the morphology of the anterior dentition can produce significant stresses in a bolus without having to resort to maximum incisor bite force. The role of the disc in reducing local stresses by increasing the loading area is still in question. By decreasing local stress, there would be reduced risk of fatigue of the cartilage matrix, as well as enhanced lubrication of the joint.

The following chapters describe experimentally derived data through which the mechanics of the TMJ disc is examined. In chapter 3, the disc is analyzed for properties in distributing normal loads over surfaces of varying congruity. Chapter 4 addresses the lubrication properties of the disc, and evaluates changes in disc lubrication due to factors such as stress concentration and damage to the disc.

Table 2.1 **Causes of death of the individuals in the sample**

Cause of Death	Number of Individuals
Trauma	6
Acute Infection	12
Debilitating Diseases (eg. tuberculosis, emphysema)	16
Unknown Cause	18
Total Number	52

Table 2.2 **Dental age range of the selected sample**

Dental Age Range (years)	Number of Individuals
Birth - 0.5	3
0.6 - 0.75	1
0.76 - 1.5	4
1.6 - 2.0	1
2.1 - 2.5	0
2.6 - 5.0	8
5.1 - 11.0	11
11.1 - 15.0	5
15.1 - 20.0	10
20.1 - 25.0	9

Table 2.3 **Cited isometric bite forces in adults**

Authors	Average Isometric Bite force (N)	Range (N)
Howell and Manly (1948, 3 closest subjects)	414 N	361-474
Proffit and Fields (1983, normal adults)	343 N	157-529
Sasaki, Hannam, and Wood (1989)	190 N	+/- 78
Lundgren and Laurell (1986)	211 N	+/- 77
Mansour and Reynik (1975)	630 N	

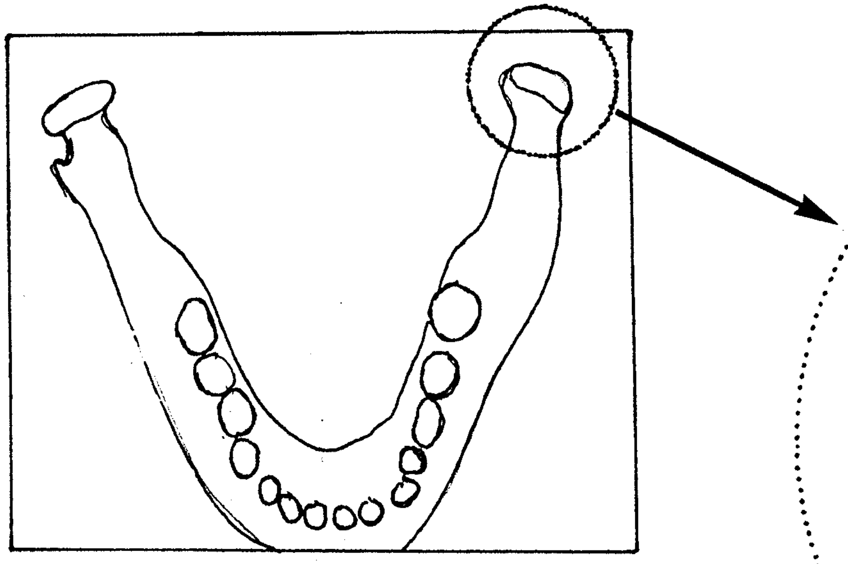

OCCLUSAL VIEW OF THE
MANDIBLE

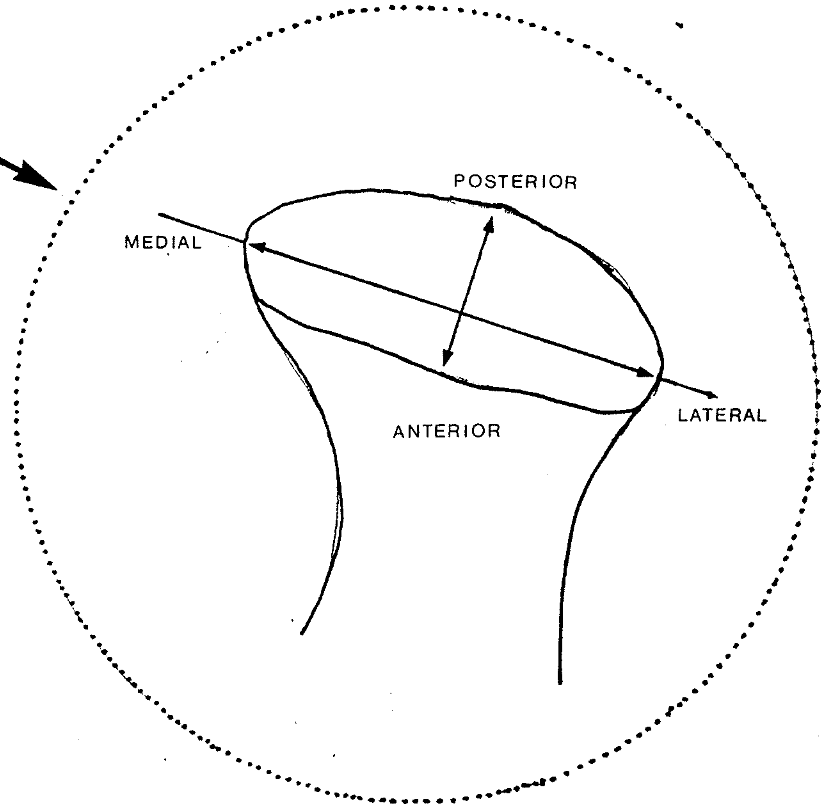

AXIS SYSTEM USED TO MEASURE
CONDYLAR DIMENSIONS

Figure 2.1 **Axis system used to measure general loading area of the condyle**

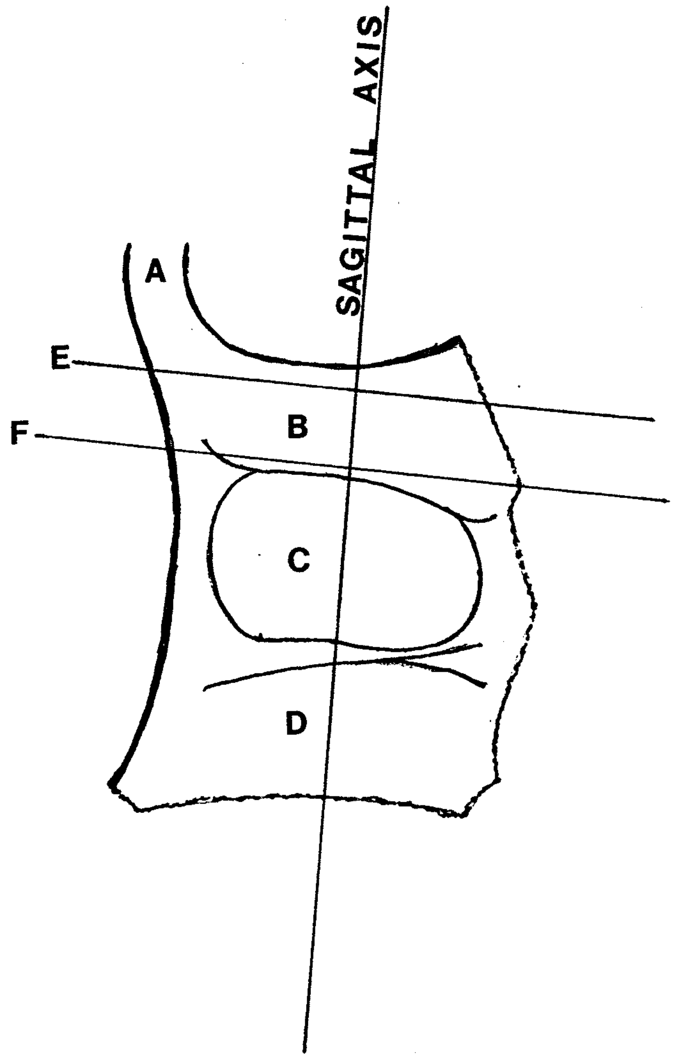

A. zygomatic process of the temporal bone
B. posterior slope of the eminence
C. depth of the glenoid fossa
D. postglenoid region
E. plane of section at the crest of the eminence
F. plane of section on the posterior slope of the eminence

Figure 2.2 Planes of section of the eminence of the TMJ

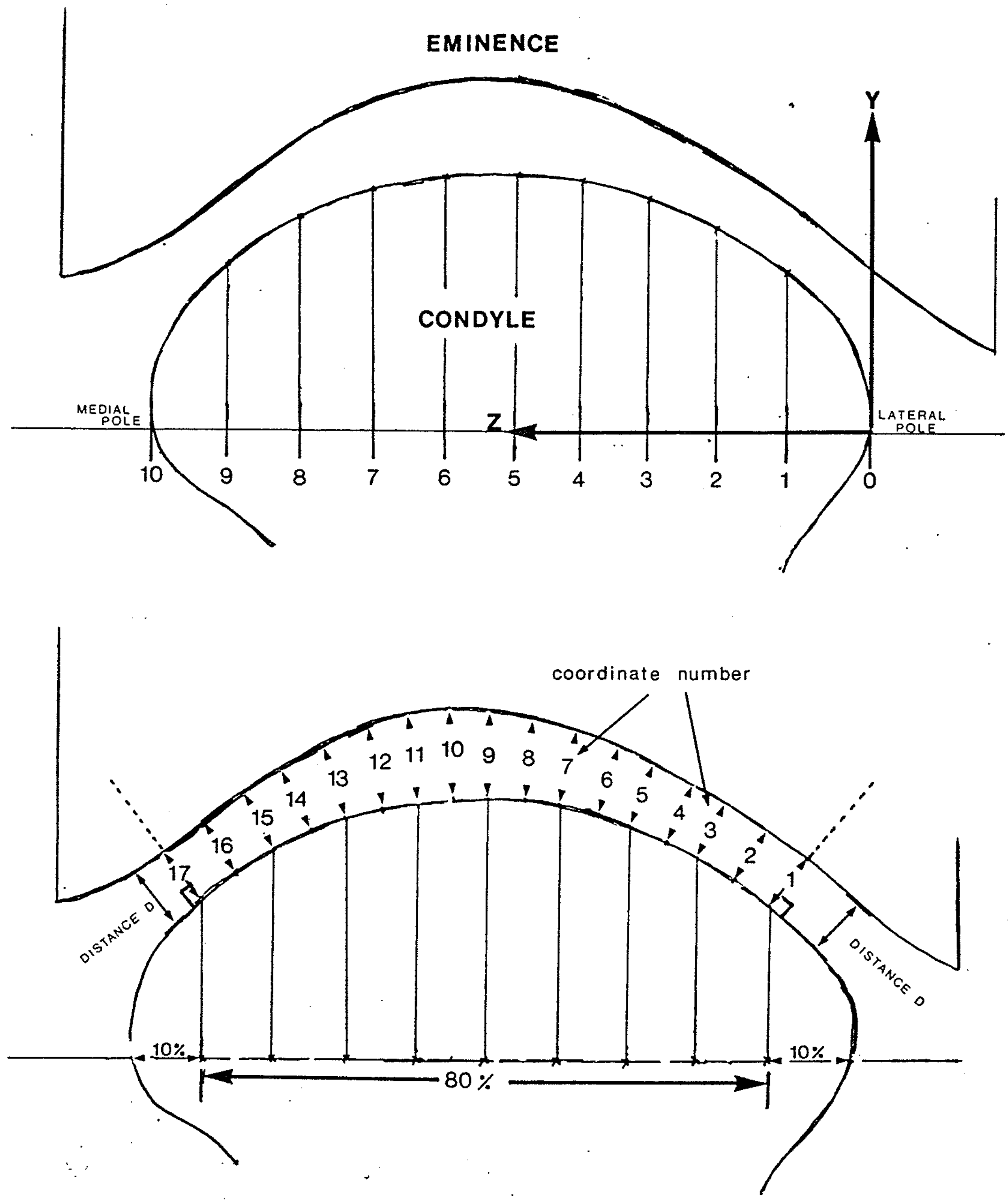

Figure 2.3 Frontal view of the condyle-eminence reconstruction

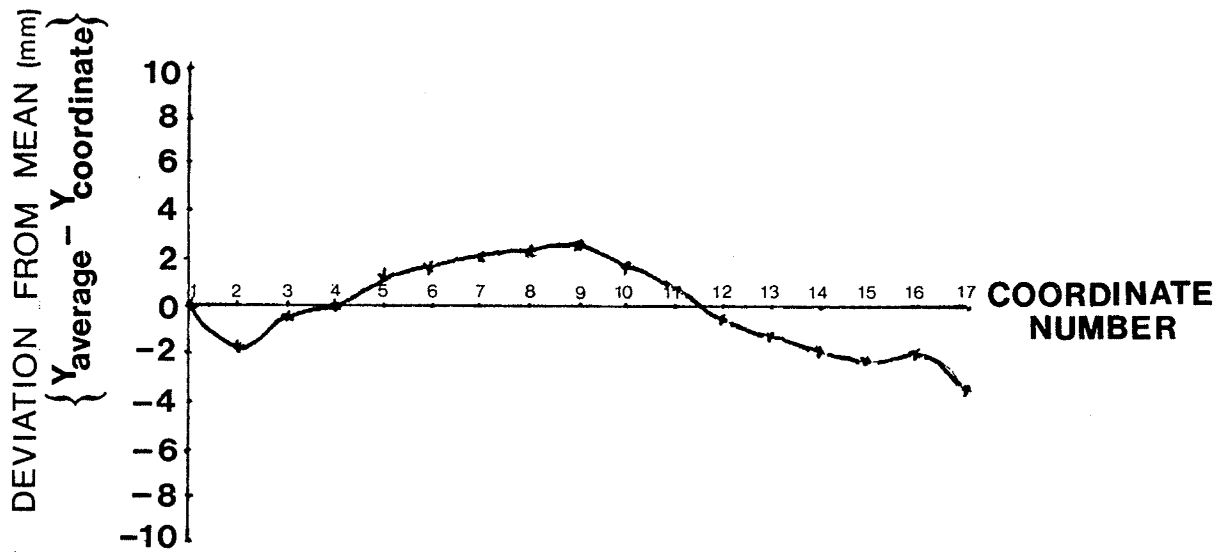

Figure 2.4 Condyle-eminence congruency plot

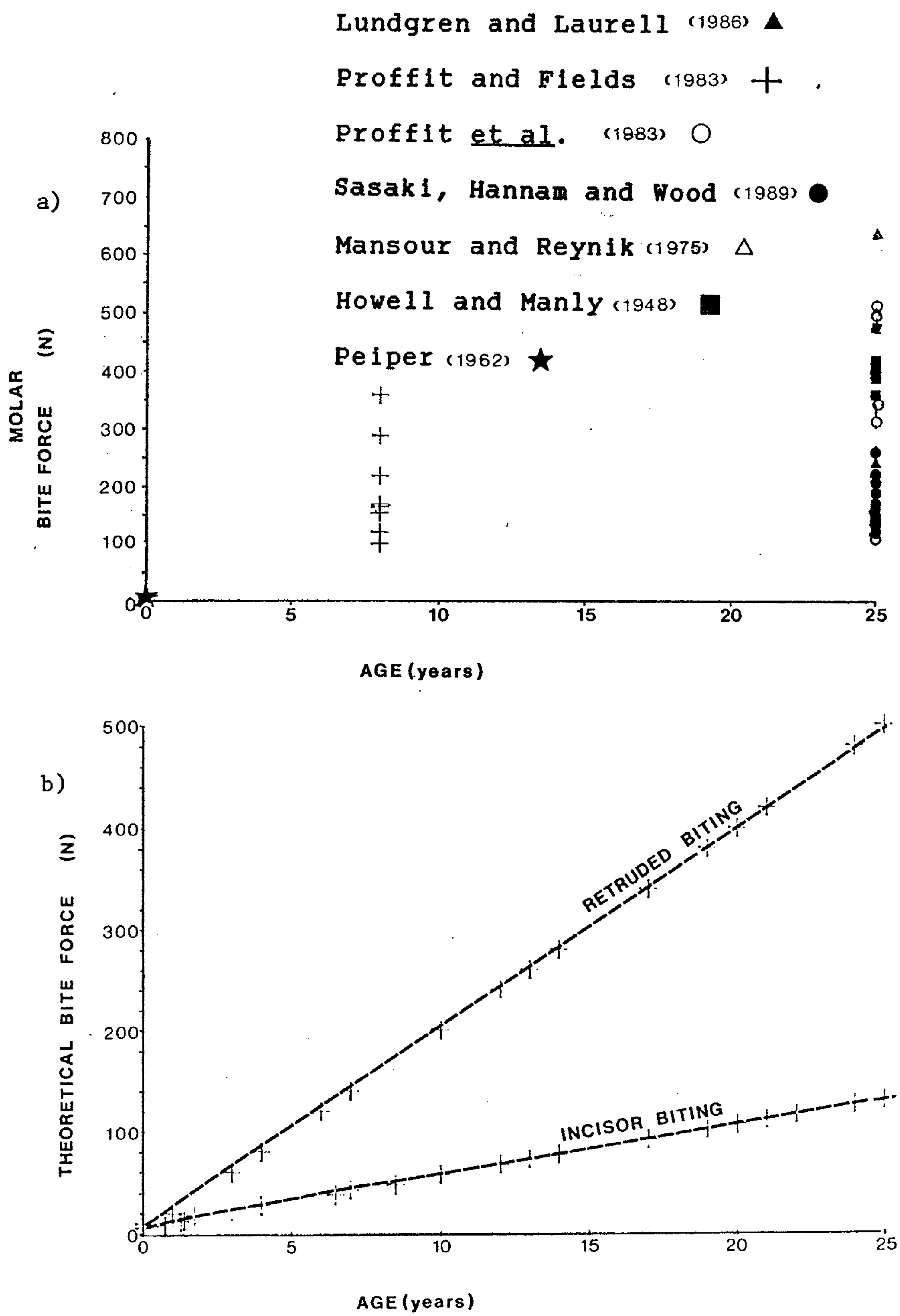

Figure 2.5 Isometric bite forces: a) reported in the literature, b) theoretical forces used in the numerical model

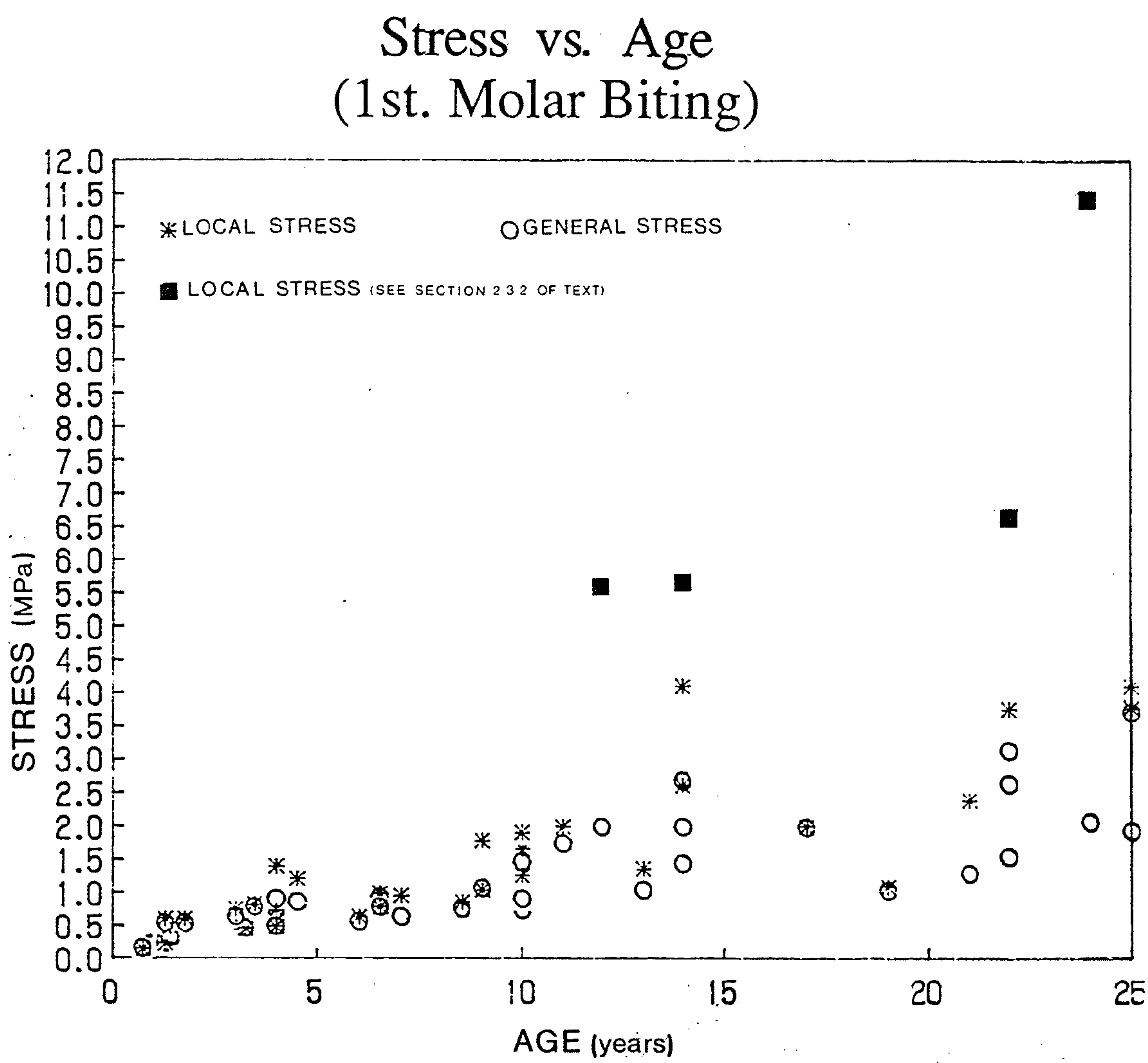

Figure 2.6 **General and local stresses during retruded biting vs. age**

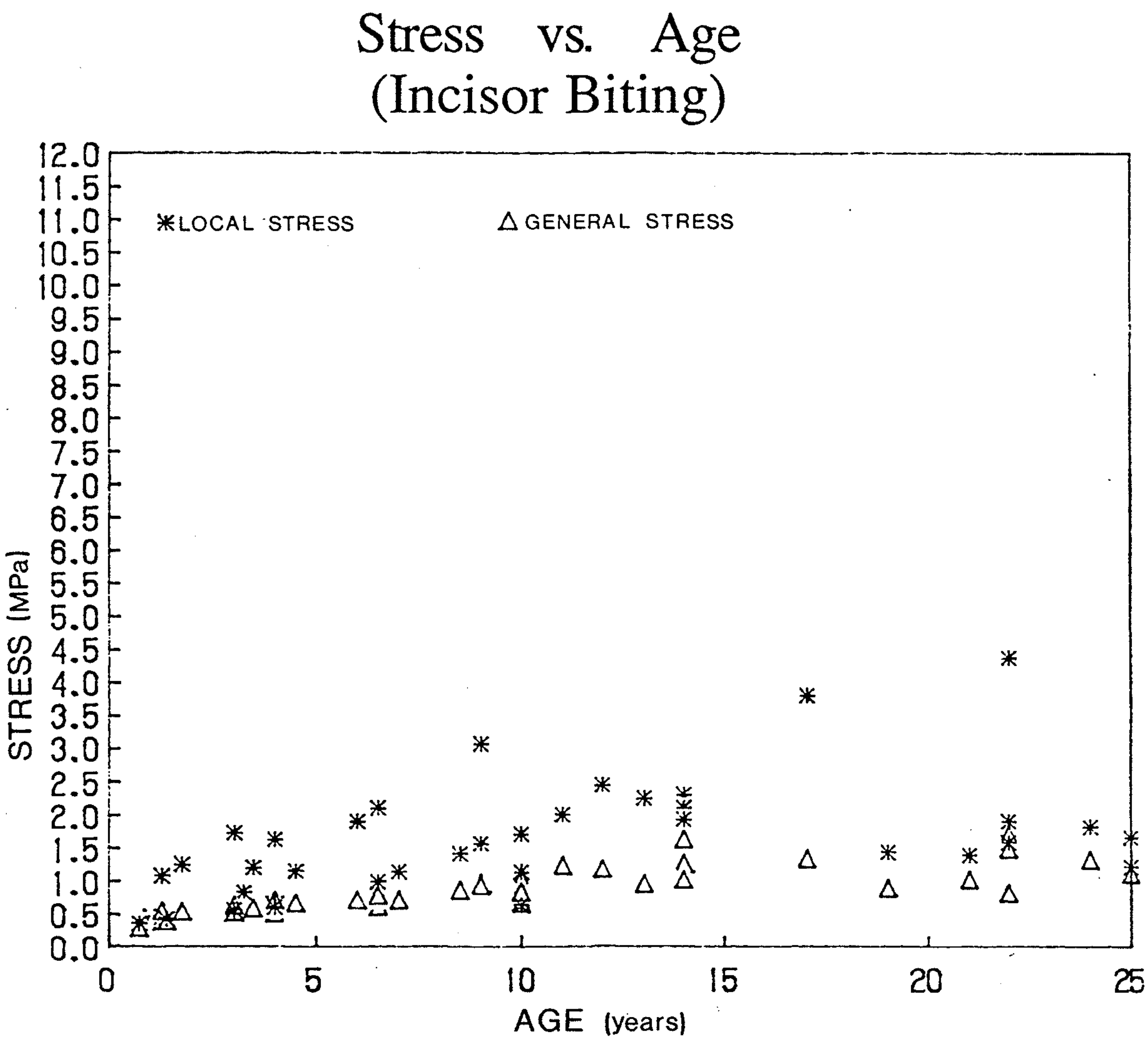

Figure 2.7 General and local stresses during protruded biting vs. age

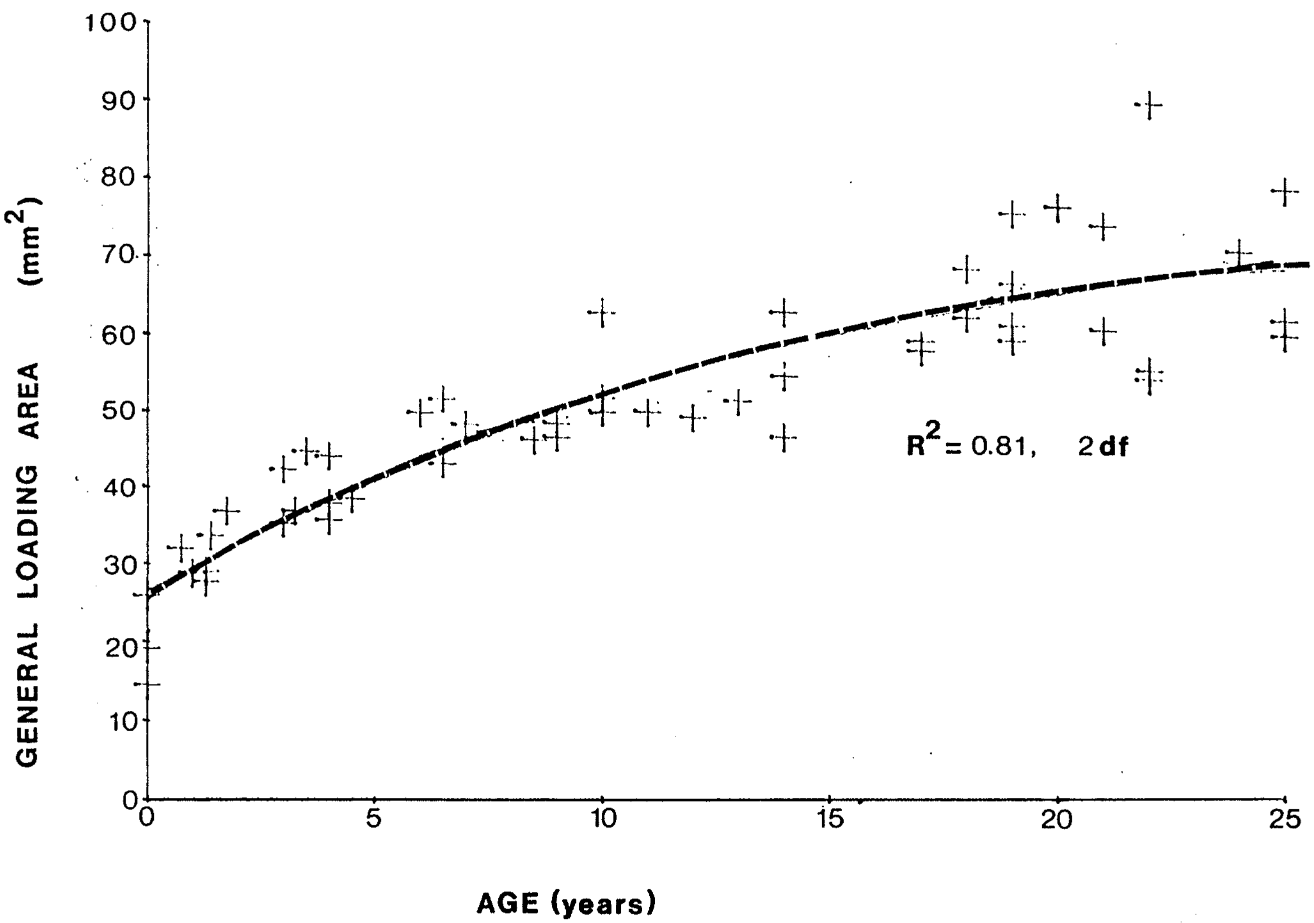

Figure 2.8 Size of the general loading area of the condyle vs. age

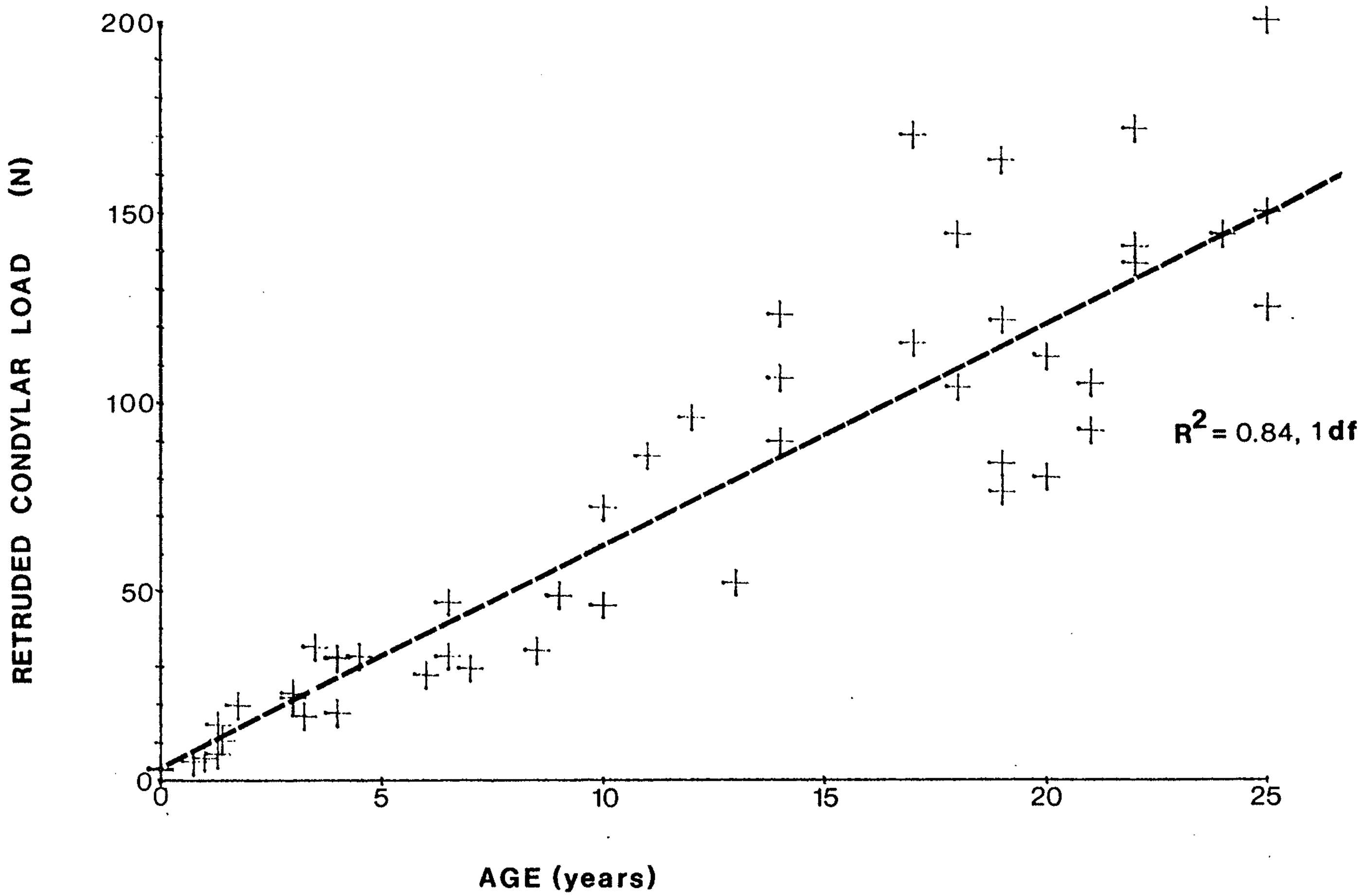

Figure 2.9 Magnitude of condylar load during molar biting vs. age

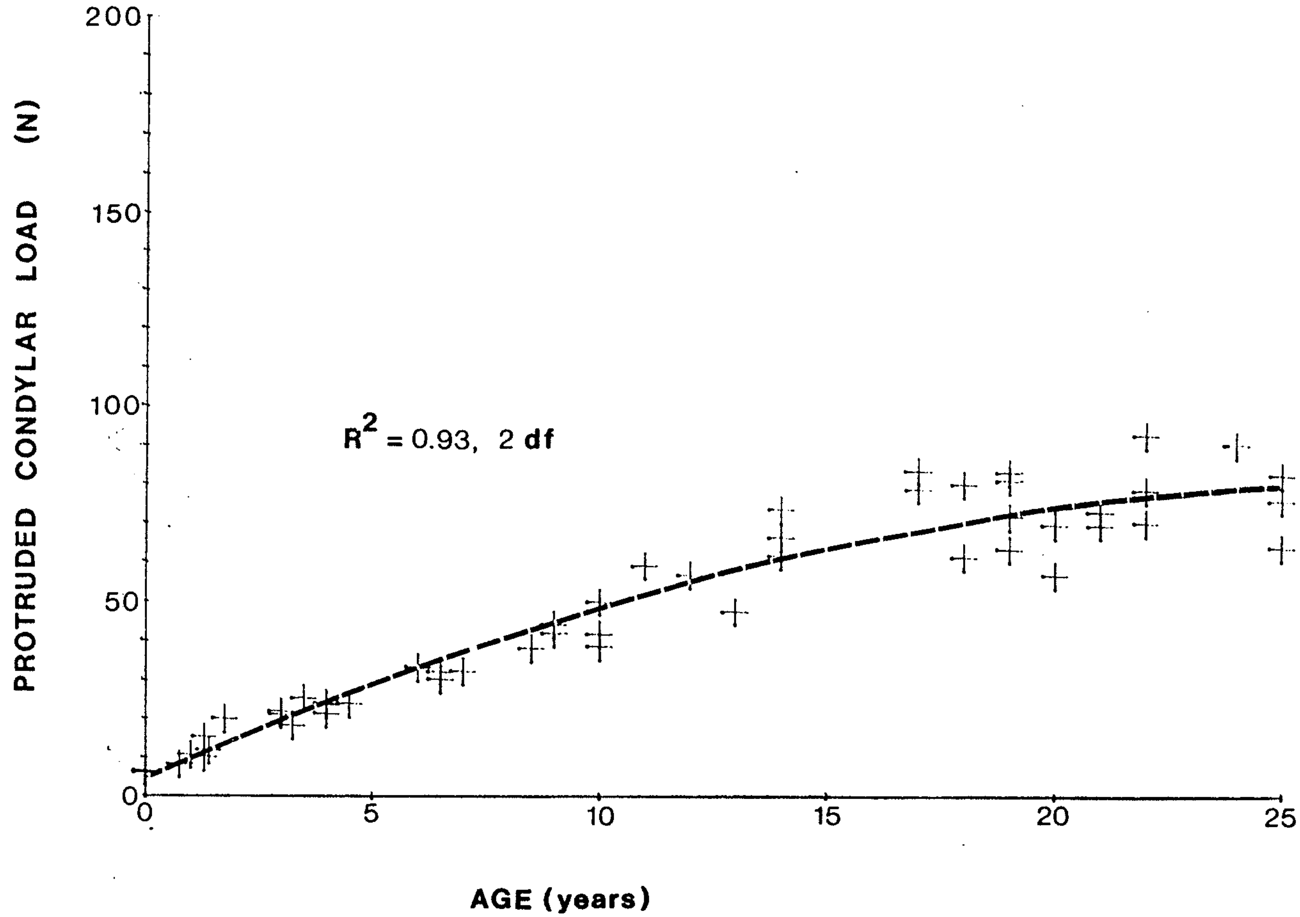

Figure 2.10 Magnitude of condylar load during protruded biting vs. age

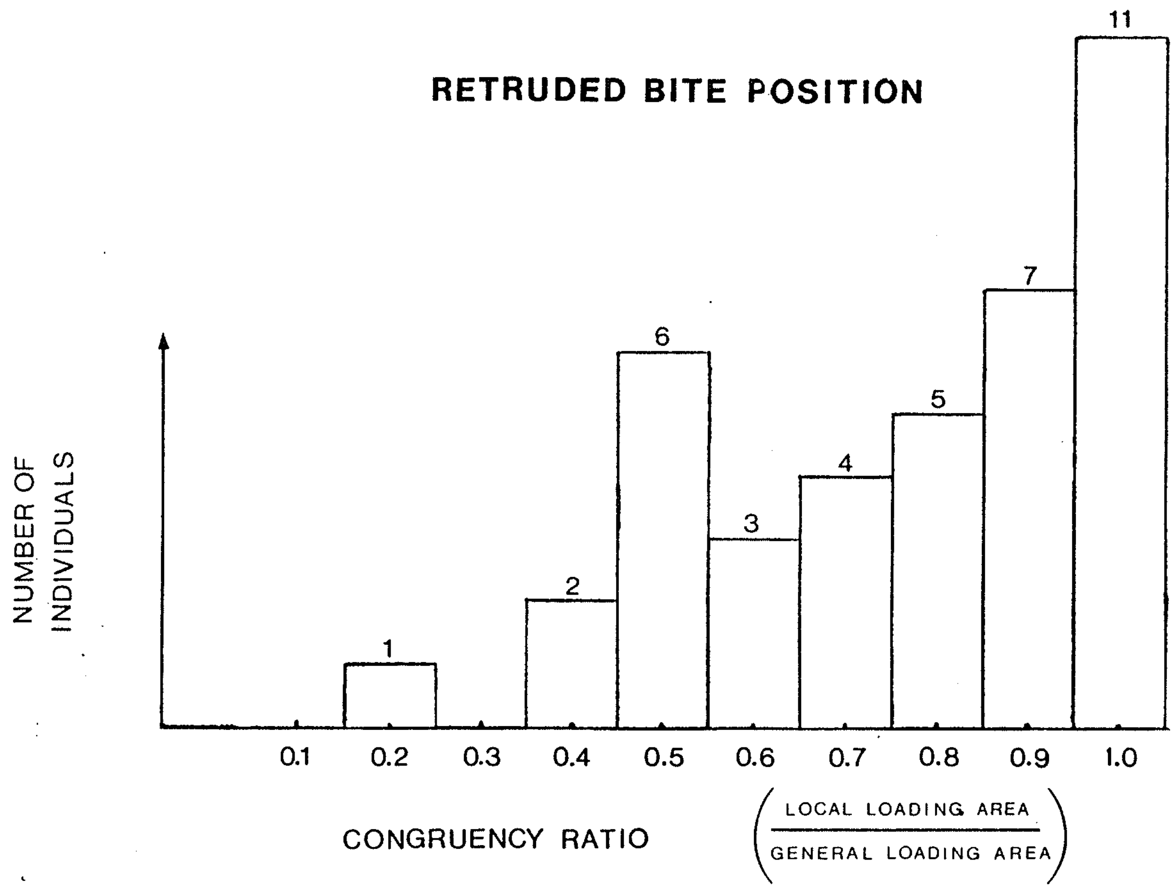

Figure 2.11 Condyle-eminence congruency in a retruded biting position

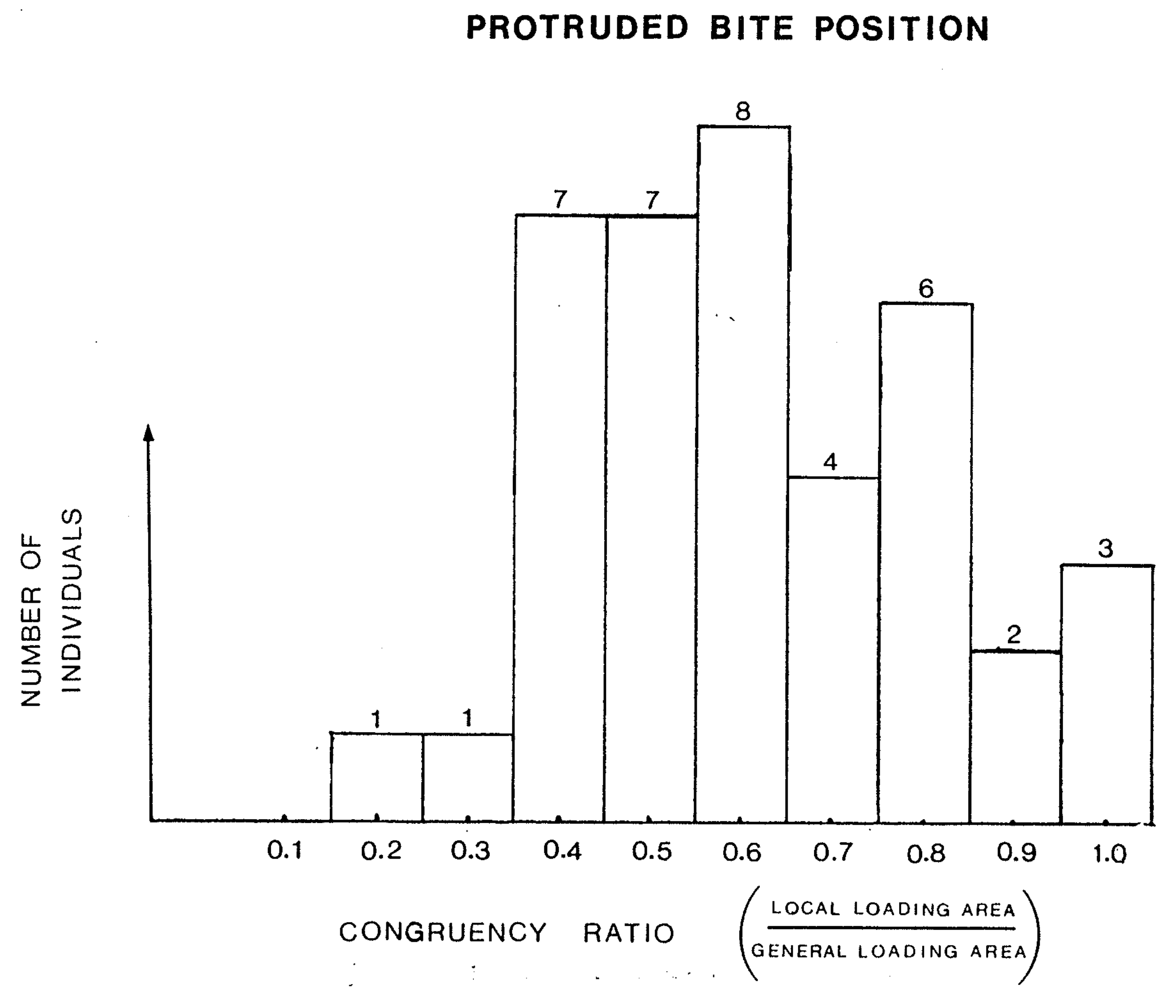

Figure 2.12 Condyle-eminence congruency in a protruded biting position

CHAPTER 3

AN ANALYSIS OF THE LOAD DISTRIBUTION PROPERTIES OF THE TMJ DISC

3.1. Introduction

In chapter 2, it was shown that with age, there is an increase in the theoretical general stresses in the joint, but that the increase was six to eight times less than the age-related increase in bite force. The increase in average stress, with age, was limited by the combined action of growth of the surfaces of the TMJ which increased the effective contact area of the joint, and by theoretical evidence of factors which minimized condylar loading during isometric biting. In certain individuals, however, significant local stresses would likely have occurred due to incongruity of the articulating surfaces of the condyle and articular eminence. As a consequence of these incongruities, the theoretical magnitudes of local stresses were two to three times that of the general stresses. High local stresses are potentially detrimental to the growth of the joint components (Copray <u>et al</u>., 1985a,b,c,d). As well, high stresses compromise lubrication (McCutchen, 1983) of the joint surfaces and potentiate the fatigue of the collagen fibres in the articular tissues.

The theoretical evidence of high local stresses between the condyle and temporal bone brings to focus the principal issue of the role of the TMJ disc as an intracapsular mechanism of reducing stress concentration. Descriptions of the TMJ disc (Gillbe, 1975; Couly and Vaillant, 1975; Okeson, 1985; Gerber and Steinhardt, 1990), like the meniscus of the knee (Walker and Erkman, 1975; Seedhom and Hargreaves, 1979), have considered the disc as the local mechanism which smooths out stress concentrations due to joint surface incongruities. The assumption is that the physical structure of the disc is capable of transmitting loads over larger areas of the articular surfaces. No quantitative evidence could be found in the literature to support this view.

One of the objectives of this chapter is to present experimental evidence of the stress distribution characteristics of the TMJ disc. In these in vitro experiments, the pressure distribution underneath the disc was measured and analyzed for a series of conditions representing a stepwise increase in stress concentration on the disc. The aim was to determine the efficacy of the disc to distribute loads (ie. to reduce stress concentrations).

To contrast the properties of the natural disc, an identical loading regimen was used on synthetic materials which, until recently, have been used as disc substitutes. As well, the results of a preliminary analysis are presented which show changes in the load distribution properties of several discs after exposure to unusually high stresses.

3.2 **Description of the Sample**

3.2.1 The porcine TMJ disc

In ideal terms, the study of the mechanics of the human TMJ disc requires healthy human TMJ discs. The success of mechanical tests performed on TMJ discs depends on hydration of the disc (Parsons and Black, 1979) without alteration of the proteoglycans or collagenous matrix (Malcom, 1976). Due to the difficulty in procuring and maintaining unpreserved healthy human TMJ discs, it was decided that a pig model would be used to study TMJ disc mechanics. The criterion used in choosing the pig as a model were based on joint function (Herring, 1976) and in the structure and chemistry of the connective tissue (Strom et al., 1986). Preliminary measurements indicated that the dimensions of the pig disc were similar to the dimensions of the human disc, as described by Hansson et al. (1977). The gross morphology of the TMJ disc of the pig is similar to humans in that there is an anterior and a posterior band, as well as a thinner intermediate zone which fits over the condyle (Figure 1.5). Macroscopically, there is a detectable anteroposterior fibril orientation of the collagen fibres of the disc. This orientation has also been described in the human disc (Taguchi et al., 1980). A mechanical analysis of the pig disc

(Fontenot, 1985) has suggested similarities in material properties between human and porcine discs. The relative ease of procurement, as well as the points noted above, were taken into account in making the selection of the pig as a model for the study of the mechanics of the TMJ disc.

Pig TMJ discs were made available courtesy of Burns Meats Limited (Winnipeg, Manitoba). Approximately twenty minutes after death, the pig was decapitated and made ready for dissection. A posterior capsular approach was used to gain access to the intracapsular tissues. After identifying bony landmarks, sharp dissection was used to enter the inferior joint space at the disc attachment on the posterior aspect of the condyle. Using blunt dissection, the medial and lateral extent of the inferior joint space was identified. Sharp dissection was then used to enter the superior joint space, at the posterior attachment of the disc to the temporal bone. Blunt dissection was used to identify the medial, anterior, and lateral disc attachments to the temporal bone. After identifying the anterior extent of the superior joint space, blunt dissection was used to extend the inferior joint space to the anterior attachment of the disc on the condyle. Sharp dissection was used to cut the medial, anterior, and lateral attachments of the disc to the temporal component. Then the medial and lateral attachments of the disc to the condyle were cut. Finally, the anterior attachment of the disc to the condyle was cut with curved scissors, and the disc was extirpated from the articulation. During the entire dissection, gentle posterior traction was used to hold the disc steady.

A key factor in maintaining the mechanical character of the disc was keeping the disc hydrated by using a physiological salt solution. A Krebs-Ringer, bicarbonate buffered (pH = 7.0-7.2) salt solution (Sigma Chemical Co., St. Louis, MO) was used. The solution contained 0.18 grams per litre (g/L) glucose, 0.1 g/L magnesium chloride, 0.34 g/L potassium chloride, 7.0 g/L sodium chloride, 1.23 g/L sodium bicarbonate, 0.10 g/L anhydrous dibasic sodium phosphate, and 0.18 g/L anhydrous monobasic sodium phosphate. After preparation of a fresh solution and balancing the pH, the solution was stored at 4 degrees centigrade until needed. Immediately after dissection, the disc was placed in a warmed salt solution bath (37 degrees centigrade, ± 3 degrees). The specimens were then taken to the laboratory for analysis. During the testing period, the discs were kept hydrated and warm.

3.2.2 Synthetic discs: Proplast and Silastic

To contrast the stress distribution properties of the TMJ disc, a comparison was made between the properties of the TMJ disc and properties exhibited by commonly used disc replacement materials.

Proplast II (registered trademark, Vitek INC, Houston

Texas) has been used for meniscal repair or replacement. The implant material is a bilaminar wafer of porous three-dimensional fibrous polytetrafluoroethane (Teflon, registered trademark, DuPont Company, Wilmington, Delaware) which is stabilized by bonding to a non-porous sheet of Teflon. The porous backing of the implant is sutured against the temporal component of the joint, where it eventually stabilizes by tissue growth into the porous back of the graft. The condyle articulates against the Teflon surface of the implant. The sample of Proplast used in this study was 1.3 millimtres (mm) thick. The tensile modulus of elasticity of polytetrafluoroethylene is approximately 400 megapascals (MPa) (Flinn and Trojan, 1981).

The other implant material used in this study was Silastic (registered trademark, Dow Corning Corporation, Midland, MI). Silastic is a non-reinforced medical grade silicone rubber. A sample of this rubber, 1.5 mm in thickness, was used to evaluate its stress distribution properties. The modulus of elasticity of rubbers are not usually determined because of non-linear behaviour. However, an estimate of the tensile modulus suggests that it is about an order of magnitude less than that of polytetrafluoroethane (Flinn and Trojan, 1981).

The only documented tensile tests done on TMJ discs have been performed by Tanne, Tanaka, and Sakuda (1991), who studied the tensile properties of the TMJ disc of dogs. They found that the disc demonstrated non-linear behaviour, with an initial low modulus of elasticity of about 45 MPa at 2 percent strain, followed by a higher modulus of about 95 MPa at 5 percent strain. Overall, the modulus varied from approximately 30 MPa to as high as 120 MPa. The modulus of elasticity of the TMJ disc is very similar in magnitude to the estimated range for Silastic. Teflon (Proplast) on the other hand is anywhere from 4 to 10 times stiffer than either Silastic or the natural disc.

3.3 Testing Apparatus

3.3.1 Overview

Measurement of the stress distribution characteristics of the TMJ disc and disc analogues required the development of an apparatus and techniques to measure stresses under the disc, or disc analogue, with a high degree of topographical resolution. A more detailed description of the apparatus and techniques used is found below. In general, an electromagnetic force generator was used to load the disc. The rate of loading, frequency, and magnitude of loads were controlled and altered according to a specific regimen. The force generator was attached to one end of a hinged beam (Figure 3.1). At the other end, a curved acrylic indentor was attached to the beam, and was used to place the load on the TMJ disc. A specially designed transducer made it possible to measure pressure (stress) at locations under the mediolateral axis of the TMJ disc, and thus to estimate the stress distribution. A high degree of topographical resolution of the stress distribution was achieved by close spacing of the transducers. A linear voltage differential transformer (LVDT) measured the displacement of the indentor into the TMJ disc. Data from the pressure transducers were collected and stored digitally on magnetic tape, and later transferred to a microcomputer for analysis. The data from the LVDT was plotted directly using an X-Y plotter.

The apparatus and technique provided a means of in vitro measurement of the mechanical properties of the isolated TMJ disc. The apparatus and technique can be modified so that future studies can examine the stress distribution of natural condyles and TMJ discs.

3.3.2 Measuring the stress distribution

As stated by Brown and Shaw (1983),

> ".. it is not difficult to show, however, that computed internal stress patterns in the natural joint depend intimately upon the assumed contact stress distribution (Brown and Ferguson, 1980). Also, it is widely recognized that intrinsic pathomechanical changes in articular cartilage depend on local stress levels rather than upon global joint loading."

Even for the largest of synovial joints, the measurement of local stress distribution in cartilage has posed technical problems. Several methods of measurement have been reported, each with advantages and disadvantages (see Table 3.1). With respect to the TMJ, it was of advantage to make the pressure sensing areas small and sensitive. These characteristics were desirable for the temporospatial measurement of the stresses under the disc. It was essential that the technique not interfere with the lubrication of the disc surfaces which would disrupt the normal mechanics of the disc (Spilker et al., 1990).

The design of the pressure transducer was based on the measurement of the buckling strain of a pre-curved brass strut (0.003 in. thick) as seen in Figure 3.2 (marked "E"). Strain measurement was accomplished using foil strain gauges luted to the compression and tension surfaces of the strut. Loads were transmitted to the transducer by a 1.12 diameter aluminum pin (marked "A", Figure 3.2). The top surface of the pin was congruent with the articulating surface of the base of a bath (marked "B", Figure 3.2). The pin was housed in a channel which was drilled through the acrylic base. During the experiments, the disc was kept moist by immersion in Ringers solution. To prevent leakage of the bathing solution through the pin holes, a thin polyethylene film (Saran Wrap trademark, Dow Chemical Company/ Dowbrands Canada Inc., Paris Ontario, Canada) was luted over the acrylic surface, and rested on the head of the aluminum pin. The point of the pin rested on a hinged aluminum beam (marked D, Figure 3.2) which was supported by the brass strut. The amount of vertical displacement was determined by the magnitude of load applied to the top end of the pin. With knowledge of the voltage output per unit load of each transducer, it was possible to calculate the loads for a given strain, and thus derive the pressure (normal stress) since the loading area was constant (0.98 mm^2).

A linear array of 10 transducers measured the mediolateral distribution of pressure beneath the TMJ disc (Figure 3.2). Each framework was supported by a central bearing rod, and by brass bushings on each side of the framework. The bushings provided 6 mm of separation of the transducer frame from neighbouring frameworks (6 mm from centre to centre of frameworks, Figures 3.2). By interleaving the transducer frames, alternating transducer frames were separated by 3 mm. The staggered arrangement gave each transducer freedom from interference from the lead wires of immediately adjacent transducers (Figure 3.3).

The frameworks (Figure 3.2) were held firmly in place by the brass bushings, but were capable of rotation about the central bearing rod (marked "H", Figure 3.2). Slight adjustments of the height of the aluminium pin (marked A, Figure 3.2), were produced by changing the height of the tail of the transducer frame (marked "G", Figure 3.2).

There was some variation in voltage output per unit load between transducers. Each transducer was individually calibrated in terms of output per unit pressure. The calibrating pressure (0.05 MPa) was produced by loading latex rubber with a steel platform. The maximum error of transducer output for consecutive calibration pressures was ± 0.005 MPa. Calibration of the transducers was done before and after each experiment to determine if there were changes in transducer sensitivities. Any changes in transducer sensitivity were within ± 5.0 percent.

3.3.3 Loading mechanism and loading regimen

This study required the control of the magnitude of the applied load. An apparatus was developed which used an electromagnetic force generator with known force/current characteristics. The force could be increased by increasing the current to the electromagnet, with the amount of force being measured by a load cell employing electric strain gauges in a bridge configuration. Thus, by changing the magnitude and the rate-of-change of the current to the force generator, the force and rate-of-application of force delivered by the indentor could be controlled.

The size and form of the electromagnetic force generator together with the need for rapid placement of the disc under the indentor required that the force be transmitted via the beam shown in Figure 3.1. The overall design provided for easy disconnection of the beam from the force generator to allow for rapid removal and replacement of discs. A small pin coupling between the beam and the force generator permitted adjustment of the indentor relative to the "at rest" height of the force generator. The coupling (labelled "C", Figure 3.1) was attached to a brass connector which had a calibrated load cell. The load cell measured the force applied to the beam by the force generator. At the other end of the beam, indentors of the form shown in Figure 3.4 were fixed by a locking screw after self-centering had taken place under a light load. Eight indentors were constructed, with the variable radius ranging from 5 mm to 125 mm (Figure 3.4).

Loading of the disc involved removing the disc from the reservoir of saline solution, and placing the disc in the bath of the testing apparatus. The superior surface of the disc was chosen as the surface to contact the acrylic indentor. A brief light load was gently applied using finger pressure to determine if the disc was stable under the indentor. If the disc moved laterally, it was repositioned in another location and tested for stability. After establishing stability, the beam was passively attached to the brass connector to prevent additional load on the disc. The first set of voltages from the pressure transducers were then measured by the voltmeter. Following this, the load was applied, at a ramp rate of 0.5 seconds to full load. The load was then kept constant for ninety seconds. After completion of the loading, the disc was removed and placed back in the bathing solution. The disc was given about 30 minutes to recover in the saline solution before retesting. For the measurement of the load distribution character of the disc, loading of the discs started with the largest indentors and the lightest loads. The magnitude of loads were increased in 3 Newton (N) increments, from 3 N to 9 N. This was followed by further loading with an indentor having a smaller radius, and another loading iteration starting from 3 N up to 9 N.

In another series of experiments, TMJ discs were exposed to high normal stresses to test if high magnitudes of pressure changed the average stress distribution pattern of the TMJ disc for low magnitudes of load. Loading of the discs involved an initial series of three loadings on the same area of the disc. After each of these loads, the disc was resoaked for 30 minutes. The loads were imposed on the disc using either a 62 mm or a 15 mm indentor, under a 3 N load for 90 seconds. These loadings produced a normal or bell-shaped pressure distribution curve. Following these initial loads, one of the following high stress regimens was used on each disc.

(a) 12 N load with a 62 mm indentor, for 90 seconds.

(b) 9 N load, with a 15 mm indentor, for 90 seconds.

After exposure to these high stresses, the disc was placed back in the saline reservoir for 30 minutes, and then retested for changes in the average pressure distribution. Changes were determined by comparing the pressure distribution before and after the high stress episode. The disc was placed back in the saline reservoir for another 30 minutes, after which another high stress was placed on the disc. This was followed by the same regimen as described before to test for further changes in the pressure distribution profile.

3.3.4. Data collection and storage

The collection and storage of data for all tests was accomplished by converting the analogue signals to digital form, with a resolution of 0.05% of full scale. Sampling rate varied according to the number of monitored channels. The sampling rate when monitoring all 10 channels was 0.7 samples per second per channel. Single channel sample frequency was 10 per second. All data were stored in digital form for further analysis.

3.4 Data Analysis

3.4.1 Stress distribution plots

Using a computer plotting programme, the recorded transducer signals, in millivolts, were plotted against sample number (time, seconds). The ordinate axis was then converted to MPa, using a 0.05 MPa conversion calibration (section 3.3.2). The resulting plot showed pressure output (MPa) for each channel (Figure 3.5). The computer programme corrected for the differences in transducer sensitivities before plotting the results.

Comparison of the load distribution properties of the discs was enhanced by using the data to make quasi three-dimensional plots of the pressure envelopes for each disc (Figure 3.6). This type of plot helped in making qualitative identification of changes in the pressure distribution consequent to changes in magnitude of load or size of indentor.

3.4.2 Pressure gradient analysis

The probability of cartilage failure under load is likely to be dependent on the rate of change of pressure with respect to distance, as well as magnitude of applied surface pressure (Weightman et al., 1973; Armstrong et al., 1984; Armstrong, 1986). Since the distribution of stress under the disc generally forms a bell-shaped curve, the rate of change of stress may be indicated by the flatness or peakedness (kurtosis) of the curve. Thus, the kurtosis of the stress curve was taken as an initial measure of the effectiveness of load distribution. Using a statistical package for the computer, the kurtosis of each pressure distribution profile was calculated, and evaluated with respect to the radius of indentor and magnitude of load. A normal bell shaped stress distribution curve has a kurtosis of 3.0 (Figure 3.7). Higher values of kurtosis indicates a more peaked pressure distribution, and a faster rate of change of pressure with respect to distance. Values of kurtosis less than 3.0

indicates a lower rate of change of pressure with respect to distance characteristic of a flatter stress distribution curve. Identification of changes in the pressure gradients was made easier using the kurtosis measurement. Where kurtosis measurements indicated significant changes were occurring, the steepest pressure gradients of the pressure distribution curve were then measured using the units of megapascals per millimetre (MPa/mm).

3.5 Results

3.5.1 Effect of load on peak stress and kurtosis

The principal factors of interest, as identified by Weightman et al. (1973) and Armstrong (1986), are peak stresses and pressure gradients. The ability of the disc to limit these factors for a given load is a reflection of the ability of the disc to act as a stress distributing mechanism.

The results, as seen in Figure 3.8, show that there is a near linear increase in peak stress with increase in load from 3 N to 9 N. This was true for all indentors. For an increase in load by a factor of 3, peak stresses also increased by approximately 3 times. Likewise, the pressure gradients were affected by the magnitude of the load as well as the radius of the indentor. With smaller radius indentors, the increase in the pressure gradient was greater. Figure 3.9 shows this feature, where the increase in the pressure gradient was higher for a 31 mm indentor than for a 62 mm indentor.

Overall, the results suggest that the disk does not seem to prevent a matching increase in peak stress for a given increase in load. As well, there is an increase in the pressure gradient as the load increases. The increase in pressure gradient is faster when the radius of the indentor is reduced.

3.5.2 Effect of disc thickness on peak stress

In Figures 3.10a and 3.10 b, a clear relationship was found between disc thickness and peak stress for a given applied load to the indentor. The results show that there is bilateral symmetry, for right and left discs from the same animal. The results shown in Figure 3.11 show the extremes of peak pressures due to differences in disc thickness. Although the kurtosis of the discs from two animals were not very different, considerable differences in peak stresses were evident. The differences in peak stress were due to the differences in thickness between the discs of the two animals. Discs #2 and #4, which came from the same pig, were 3.25 and 3.35 mm in thickness respectively. Discs #1 and #3, which were taken from another pig, were 1.15 and 1.10 mm thick. Figure 3.12 shows the effect of disc thickness on the peak stress for a 31 mm indenter and 9 N load. Plotted in this Figure are five matched pairs (10 discs), from five pigs, and four single discs recovered from four pigs. As there is a reduction in the thickness of the disc, the peak stresses increase, with the rate increasing as the disc approaches 1.0 mm in thickness. This phenomenon has been reported before for hyaline cartilage (Mow et al., 1984). Figure 3.13 shows the linear relationship between peak stress and normalized displacement of the disc. For a given load and indentor geometry, thinner discs exhibit a greater percentage deformation than thick discs.

3.5.3 A comparison of kurtosis and peak stresses for the TMJ disc and disc analogues

Figure 3.14 presents data describing kurtosis for various indentor radii. The test materials were pig TMJ disc, Silastic (registered trademark) silicone rubber and Proplast (registered trademark) implants. The most notable results were the similarities of the distribution of the kurtosis for Silastic and the TMJ disc, and the significantly higher values of kurtosis for loads on Proplast. As noted in section 3.2.2, silicone rubber (Silastic) and the natural TMJ disc have similar tensile moduli, whereas polytetrafluoroethane (Proplast) has a tensile modulus which is 4 to 10 times greater. The results show that the pressure distribution characteristics of the TMJ disc is not any better than the pressure distribution by Silastic, but both were better than

Proplast. The Silastic and natural disc showed an increase in kurtosis from approximately 2.5 to a peak kurtosis of slightly less than 5.0, for an indentor radius reduction of 125 to 15 mm. This represents an approximate change in pressure gradient from about 0.023 MPa/mm to 0.045 MPa/mm. Similar reduction in the radius of the indentor produced an increase in Proplast kurtosis from about 7 to 13. This represents an approximate increase in pressure gradient from about 0.054 MPa/mm to 0.083 MPa/mm.

Equally important for the health of the collagen network of the articular tissues is the control of peak stresses in the tissues. Figure 3.15 shows the relationship of peak stress for Silastic, and average peak stress and the range of peak stresses for the TMJ disc. There is not much difference in the averages between the Silastic and the TMJ disc, although of the two the range for the TMJ disc shows greater variability. For the sake of clarity, peak stresses for Proplast were not plotted in Figure 3.15. On average, the peak stresses for Proplast were twice the magnitude of the peak stresses for Silastic. Peak stresses for Proplast were always higher than the highest peak stresses of the natural discs.

3.5.4 Stress concentration effects

It has been suggested (Copray et al., 1985b) that local stresses on the condyle will influence the growth of the condyle. It is possible that the TMJ disc can alter local pressures, thereby creating the potential for local changes in the growth of the condylar surface. To this end, the effects of high stresses on the normal pressure distribution of the disc were investigated.

As seen in section 3.5.1, for the normal stress distribution curve of the TMJ disc, the pressure gradient was directly related to both load and stress concentration. The pressure gradient has been identified as the primary factor in causing the movement of water through the matrix of articular cartilage (Mow et al., 1984). The ability to move water through the disc makes it possible to increase the contact area between the indentor and disc, and thereby increase the area of loading under the disc. This phenomenon of water redistribution can be shown by measuring changes in the pressure distribution curve of the disc after exposure to steep pressure gradients.

Four discs from four animals were used in this experiment. An outline of the steps taken to test for changes in the stress distribution properties of the disc is as follows:

1. Three (3) initial loadings used either a 62 mm indentor under a 3 N load (Discs H1 and H6), or a 15 mm indentor under a 3 N load (Discs I4 and I6). This produced a series of pressure distribution curves which represented the average pressure distribution under light loads. Thirty (30) minutes of recovery was permitted between each light loading, and at the end of the third loading episode.

2. High stresses were then imposed on the discs using either a 62 mm indentor under a 12 N load (Discs H1 and

H6), or a 15 mm indentor under a 9 N load (Discs I4 and I6). The load was kept on the disc for 75 seconds. This step is identified as Trial 1 in Table 3.2. Thirty (30) minutes of recovery was permitted before proceeding to step three.

3. The pressure distribution profile of the discs was retested under light load as described in step 1. Thirty (30) minutes of recovery followed before proceeding to step 4.

4. High stresses were once again imposed on the discs using one of the regimens described in step 2. This step is identified as Trial 2 in Table 3.2. Thirty (30) minutes of recovery was allowed before proceeding to step 5.

5. There was a final testing for changes in pressure distribution of the disc, using light loads as described in step 1.

The results of these tests can be found in table 3.2. The high stress profiles from all the experiments had peak maximum stresses between 0.12 and 0.19 MPa. The pressure gradients varied between 0.022 and about 0.046 MPa/mm. Two of the discs from two different animals (H1 and H6) were loaded with the 62 mm indenter under a 12 N load. This regimen resulted in peak stresses between 0.13 and 0.19 MPa. The pressure gradients ranged from 0.032 and 0.037 MPa/mm. Two discs from two other animals (I4 and I6) were loaded with the 15 mm indenter, under a 9 N load. This produced peak stresses between 0.12 and 0.13 MPa. Quite different pressure gradients were measured under these discs. Disc I6 had an average pressure gradient of 0.023 MPa/mm. In contrast, disc I4 had a very high pressure gradient of about 0.045 MPa/mm. The lower pressure gradient found under disc I6 appears to be at odds with the previous results (Figure 3.14). A 15 mm indentor was used to load the disc, yet the kurtosis was less than the kurtosis measured for discs H1 and H6, which had been loaded with the 62 mm indentor. In this particular case, the cross-section of the disc was such that there was remarkable congruity between the shape of the disc and the indentor. The result was a larger loading area and slower change in pressure with respect to distance. Peak stresses, however, remained the same between the discs. The most likely explanation for this is that disc I6 was thinner and the displacement of the indenter into disc I6 was approximately 25% of its unloaded thickness. Disc I4 was thicker, and loading of disc I4 produced a displacement of only 12% of the unloaded thickness.

The plot seen in Figure 3.16 shows the relationship between the pressure gradient of the stress concentration, and the consequent changes in the pressure distribution of the disc for a light load. Disc I6, which had the lowest pressure gradient, showed the least changes in the pressure distribution of a light load. The steepest pressure gradient of 0.046 MPa/mm was imposed on disc I4. This disc showed the largest percentage change in pressure distribution. All the discs improved in ability to distribute loads after an episode of stress concentration. This improvement in load distribution was due to the redistribution of water in the disc, which increased the area of contact between the disc and the indentor.

A more dramatic demonstration of the effect of water redistribution effects on pressure distribution is shown in Figure 3.17. In these experiments, two discs from two different animals were initially loaded using a 62 mm indenter under a 3 N load. This produced a series of stress distribution curves for light loads which were used as a baseline of comparison. All but one of the curves demonstrated a bell-shaped distribution of stress. The unusual stress distribution curve of Figure 3.17a, trial #3 was caused by a slight change in the mediolateral placement of the disc under the 62 mm indentor. This resulted in loading of the medial attachment of the disc, which created the higher stresses measured by transducers #8 and #9.

What was different in these experiments compared to previous experiments was that all episodes of high stress were produced using a 15 mm indentor and a 9 N load. The peak pressures of the stress concentration were between 0.13 and 0.19 MPa. The pressure gradients were between 0.039 and 0.047 MPa/mm. The result of these stress concentrations was a change in the shape of the pressure distribution by the disc. The change was from a bell-shaped pressure distribution curve to a bimodal distribution curve. The disc appeared to have expanded radially to encompass more loading area, with abnormalities showing up within the distribution curve. These abnormalities appear in the form of localized reductions of pressure in the middle of the disc and higher pressures medially and laterally. The magnitude of the reductions of local pressures appears to be by a factor of 10:1 to 20:1 with respect to the base line data. The two discs used in these experiments were of quite different thicknesses. This shows up as a difference in the peak pressures between the two discs.

3.6 **Discussion**

3.6.1 The role of the TMJ disc in stress distribution

In chapter 2, theoretical argument showed that significant local stresses may well occur due to incongruity of the joint surfaces of the condyle and articular eminence. A common assumption, however, is that the disc may act to smooth out these local stresses. Thus, conditions which might otherwise compromise lubrication and unduly fatigue the articular linings of the condyle and eminence are avoided. The results of this chapter show that the ability of the disc to prevent these high stresses is dependent on its thickness. The thinner the disc the more dramatic the increase in peak stresses with decreasing congruity of the loading surfaces and increasing load. The manner in which the TMJ disc thins is discussed in section 3.6.2. The discussion in this section will focus on the role of the disc in stress distribution and its relationship to the normal growth of the condyle.

The susceptibility of the growth cartilage of the condyle to mechanical stimuli has been reported by Copray et al. (1983; 1985a,b,c,d). It is doubtful that Copray and colleagues were able accurately to measure the magnitudes of loads, as claimed in their reports. The forces applied to the condylar explants were critically dependent on the bulk modulus of the explant. It was shown by Copray et al. (1985b) that for a 2.0 mm explant, it was possible to have a range of forces from less than 1 gram (0.0098N) to approximately 6 grams (0.0588 N). However, in the absence of any other data, the estimates of forces and areas of loading, as described by Copray and co-workers can be used, cautiously, to provide a first approximation of the pressures which facilitate and inhibit growth of the condyle. According to Copray, low intermittent stresses maximized the synthesis of glycosaminoglycans and initiated ossification in condylar explants. Copray estimated an average growth pressure of the cartilage at 0.025 MPa. From the published Figures (Copray, 1985b) and cited force levels of 0.004 to 0.015 N, the range of stresses which maximized matrix formation is between 0.012 and 0.035 MPa, with an average of 0.025 MPa.

In chapter 2, it was argued that the average stress during isometric biting in an adolescent was about 1.5 MPa. Clearly this is not the usual magnitude of stress during normal function. It is probable that the stresses which occur more frequently are more influential in the growth of the condyle. Therefore, the stresses occurring during mastication are probably more important. Evidence in support of this hypothesis has been reported by Copray et al. (1985b). Copray and co-workers showed that continuous loads and heavy intermittent loads were not as effective as light intermittent loads in facilitating the production of glycosaminoglycans and osteoid in condylar explants. In other articular tissues, shorter loading periods and lighter physiologic loads enhanced cartilage matrix synthesis and the aggregation capabilities of the proteoglycans (van Kempen et al.,1985).

A reasonable estimate of the masticatory forces, relative to isometric bite forces, suggests that they are 10% or less (Graf et al., 1974) of isometric maximum bite forces. Therefore, the likely average stress during normal mastication in an adolescent is about 0.15 MPa, one-tenth of the stress during isometric biting. An average stress of 0.15 MPa is still 4 to 10 times above the estimated range of stresses described by Copray, for the normal growth of the condyle.

It is possible to estimate the potential effect of the disc on the average stresses by assuming a worst-case situation that the average stresses without the disc are about the same as the thinnest of discs tested in this study. If the relationship of Figure 3.13 is correct, an average disc when compared to the thinnest disc will reduce the stresses by one-half for a given incongruity and load. This interpretation is based on the evidence that the peak stresses of the thinnest discs (Figure 3.13) were about two times that of the average. The result is an average stress of about 0.08 MPa (0.15 MPa/ 2). This magnitude of stress is close to the range of stresses (0.012 - 0.035 MPa) required for an increase in the synthesis of proteoglycans and ossification of the condyle. Note that this is the average stress, and a worst-case situation where it was assumed that the thinnest disc was not able to decrease the stresses on the condyle. Even in this scenario, large portions of the loaded condyle would have stresses less than 0.07 MPa, and well within the range of stresses for normal growth of the condyle. Thus, the average TMJ disc would facilitate growth of the condyle by reducing the average stresses to a level compatible with the ability of the chondroblasts to produce condylar growth.

The disc might also be responsible for the preferential growth of local areas of the condylar surface, which produces osseous changes in the condyle morphology. As was shown in Figure 3.17, areas of reduced stress are produced in areas where water has been redistributed because of stress concentration. The presence of these localized areas of reduced stress might provide some explanation for the development of abnormal condylar morphology, as described by Solberg et al. (1985). Take for example the adolescent case where peak stresses were shown to be upwards of 6.0 MPa during isometric biting. During mastication, the peak stresses are likely to be ten percent of this, or 0.6 MPa. For the two discs of Figure 3.17, transducer #6 showed a decrease in local stress by a factor of 10 to 20 times. The stress reduction was due to a previous loading between incongruent surfaces. If such a condition is capable of reducing peak stresses by this amount, then peak stress in the region would drop from 0.6 MPa to a range of 0.03 to 0.06 MPa (by a factor of 10 to 20). This range of stress is comparable to range of stresses (0.012 - 0.035 MPa) which produce the maximal amounts of glycosaminoglycans and accelerated alkaline phosphatase activity (Copray et al., 1985c).

Solberg et al. (1985) stated that the contour of the condyle can produce a hole in the disc. The results of this study suggest that the condyle shapes described by Solberg et al (1985) were caused by stress concentration on the disc. This results in water redistribution in the disc which lowers the local stresses enough to promote osteoid synthesis and growth into the region of reduced normal stress. Eccentric bruxism is a potential source of damaging stress concentration. Minor incongruities on the crest of the eminence, as shown in Figure 2.12 of chapter 2, in conjunction with high loads that occur during bruxism (Rugh and Ohrbach, 1988), could produce a pressure gradient adequate to move water out of the area, and create an area of reduced normal stress.

It is unclear how long it will take for water to move from the surrounding regions back into the dehydrated area. At issue, as well, is how much the fibrous matrix has been damaged as a result of these stress concentration, and whether the damage is enough to create a permanent change in the pressure distribution properties of the disc. These issues remain for future investigations.

3.6.2 Thinning of the TMJ disc and early joint disease

The most telling differences between natural discs were the differences in peak stresses generated under similar loading conditions, and the relationship between peak stresses and the thickness of the disc. As the results of Figure 3.13 show, with increasing normal displacement, there is an increase in peak stress under the disc. This may be interpreted as a stiffening of the disc with increasing compression. This results in greater peak stresses for increases in normal displacement. This strain dependent phenomenon has been reported by Mow et al. (1984) and Grodzinsky et al. (1981). The mechanism which accounts for increases in the stiffness is still a matter of debate. It is proposed that either the ion concentration effects of the proteoglycan, or an increase in the number of taut collagen fibrils, are responsible for the increase in tissue stiffness with increased compression. The ion concentration effects are produced by the electronegative groups of the proteoglycans, which bind the water of the connective tissue. The ability of the proteoglycans to bind the water is enhanced in conditions of compression in which the distances between negatively charged sulphate groups are reduced. This results in decreased water movement under compression, and is generally described as a reduction in pore size of the cartilage matrix. The other proposed mechanism is the recruitment of collagen fibres with increased compression. Normally, under light microscopy, the collagen fibres are loosely arranged and have a wavy appearance. As the tissue is compressed and the Poisson's phenomenon occurs, the fibres straighten out and become taut. Theoretically (Aspden, 1985), this produces the increase in tissue stiffness with increased compression.

Kopp (1976) and Solberg et al. (1985) have suggested that the thinning of the disc is a first sign of degenerative joint disease. The mechanism of thinning is unclear. It might be due to decreased glycosaminoglycan concentrations, which reduces the osmotic effect and increases the porosity of the tissue. In conditions such as this, the fluid is moved out easily, and there is a reduced osmotic pressure, which would slow the recovery of the tissue. Added to this is the possibility of localized failure of the disc fibres due to trauma or stress concentration. Local failure of the collagen matrix would reduce the effectiveness of the collagen net to trap the proteoglycan molecules. The area would not recover hydration due to the redistribution of the proteoglycans to positions peripheral to the compromised fibrous matrix. The redistribution of proteoglycans may reduce the osmotic pressure which otherwise helps in the rehydration of the more central regions of the dense intermediate zone of the disc.

The findings presented in this chapter may offer new insight into how thinning of the TMJ disc may affect the expression of degenerative joint disease in the TMJ. Thinning of the disc may occur generally or locally. Both types of thinning have been described by several authors (Westesson and Rohlin, 1984; Solberg et al., 1985; de Bont, 1985d; Hansson and Oberg, 1977; Hansson et al., 1977) as a sign of an early degenerative process. Irby and Zetz (1983) have stated that with respect to osteoarthritis, the state of health of the disc has a profound influence on the health and contour of the condyle. From the present study, it was shown that generalized thinning of the disc produced a general increase in peak and average normal stresses under the loaded disc. In the in vivo situation, a general increase in stresses is likely to produce fibrillation and general wear of the articular surfaces. As well, it might be expected that there would be a general sclerosing of the subchondral bone of the condyle and eminence.

In contradistinction, localized thinning of the disc, produced by events such as eccentric bruxing loads applied to areas of joint surface incongruity, would result in a general condition of reduced peak stresses. It might be expected that there would be a change from a bell shaped pressure distribution curve to a bimodal distribution, such as that seen in Figure 3.17. This would result in small areas in the middle of the disc where local stresses are reduced, and an increase in stresses in the medial and lateral portions of the disc. The reduction in stress in some areas may produce proliferative activity in the undifferentiated mesenchyme of the fibrous connective tissue of the condyle. The chondroblastic, and subsequent osteoid conversion of the matrix would occur in the localized regions of reduced stress. Proliferation would continue until a bell shaped stress distribution profile was reinstated. However, quiescence of the chondroblastic layer may not occur if there is a continuation of the episodic high stresses in the same area of stress concentration.

3.6.3 Stress distribution by the TMJ disc and disc analogues

The results show that although the disc is better at distributing loads over incongruent surfaces than the disc analogue Proplast, it is only marginally better than silicone rubber. The results of the pressure distribution experiments match the reported material stiffnesses found in the literature.

The results for the Proplast are of interest, given the current reports which suggest that Proplast should not be used as a disc replacement implant. Recently, Proplast has been reported to cause giant cell inflammatory reactions when used as a disc replacement (Merrill et al., 1990; Valentine et al., 1989; Berman and Bronstein, 1990). Pathology reports indicate that the teflon surface wears off the porous backing. Slivers of the graft are imbedded in the fibrous connective tissue of the condyle, which results in the inflammatory reaction. In some cases, a considerable portion of the condyle is lost due to the inflammatory response which destroys the osseous architecture. The results of the present study show that there are steep pressure gradients associated with loads applied to the Proplast allograft.

3.7 Summary

In chapter 2, it was shown that site specific areas of stress concentration occur in the TMJ. The objective in chapter 3 was to address the issue of whether the TMJ disc can be considered a peak stress reducing mechanism, by controlling the increase in stress concentration for conditions of increasing load and decreasing congruity between loading surfaces.

The results show that the ability of the disc to distribute load is not significantly better than silicone rubber, and that pressures under the disc are strongly dependent on the thickness of the disc. There is a rapid increase in peak stresses as the disc thins. The natural disc is substantially better in stress distribution compared to Proplast, which has been used, until recently, as a disc substitute. The nature of early damage to the TMJ disc may explain the different manifestations of condylar morphologies associated with degenerative joint disease. Stress concentrations were shown to create abnormal reductions in local stresses during light loading of the disc. These reductions of local stresses were probably due to water redistribution within the disc. These local areas of reduced stress could serve as a focal point for increased chondroblastic and osteoblastic activity, which would result in alterations in the normal morphology of the condyle.

Table 3.1 **Techniques in measuring synovial joint stress**

TECHNIQUE	AUTHORS	AUTHORS' COMMENTS
Thin films (static, whole joint) -thin pressure sensitive films which release a dye when exposed to specific pressures	Frisna and Lehneis (1970) Fukubayashi and Kurosawa (1980) Nelson et al. (1988) Werner et al.(1989) Newman et al.(1989) Ahmed et al (1977)	-static measurements with difficulty in obtaining spatial resolution. Films tend to disturb lubrication of the surfaces, and interfere with normal tissue mechanics.
Mechanically sensitive pads -indentation of the pad depends on the applied pressure	Ahmed and Burke (1983) Brehnan et al.(1981)	-static measurement with a poor degree of resolution for local stress measurement. Interferes with lubrication. In the Brehnan studies, the transducer measured load, but not stress.
Dye exclusion or casting techniques -India ink or polymethyl-methacrylate used to identify unloaded areas	Greenwald and O'Connor (1971) Greenwald and Haynes (1972) Walker and Hajek (1972) Seedhom and Hargreaves (1979) Walker and Erkman (1975)	-static global measurement. Defines the limits of the contact area.

Instrumented endoprosthesis -pressure sensitive areas, machined into the articulating surface of a prosthesis	Rushfeldt et al. (1979, 1981) Hodge et al (1986)	-extremely sensitive to fit of the endoprosthesis. Costly, and not feasible for small joints requiring good spatial resolution of local stresses.
Radiography/ Arthrography -dye exclusion on radiographs identifies unloaded areas	Brinckman et al. (1981) Kettlekamp and Jacobs (1972)	-static global measurement. The degree of invasiveness is prohibitive, but useful for conditions when radiographs are planned in the course of treatment.
Successive cartilage removal -identifies the loaded and unloaded regions of the joint based on the amount of compression during loading.	Day et al. (1975)	-static global measurement. Removal of cartilage alters boundary conditions and changes the fluid flow in the cartilage matrix. Roughly approximates the boundaries of the contact area.
Retrograde subchondral transducer -natural surface of the subchondral bone is machined to receive pressure transducers	Adams et al. (1978) Mizrahi et al. (1980) Christel et al. (1976)	-prohibitive because of poor spatial resolution of local stresses in smaller joints. Alters the material properties of the subchondral bone, which affects contact area of the articular tissues.

Intra-articular pressure -synovial fluid pressure measured by catheter inserted in the joint space	Walker and Erkman (1975) Ward et al. (1990) Roth et al., (1984) Findlay (1964)	-poor reliability in calibration and reproducibility. For global analysis only.
Surface miniature transducers -surface of the joint is machined to receive pressure transducers	Brown and Shaw (1982,1983) Inglemark and Blomgren (1947) Ahmed et al (1977, conductive paint sandwich) Piotrowski (1975) Brehnan et al. (1981)	-poor resolution of local stresses in smaller joints. Altered tissue mechanics due to presence of instrumentations on the surface, and machining of the cartilage which alters fluid flow path.

Table 3.2 Stress concentration data

Disc #	Disc Thickness (mm)	Indentor Radius (mm)	Load (N)	Peak Stress (MPa)	Pressure Gradient MPa/mm
H1 Trial 1 Trial 2	2.10	62	12	0.13 0.13	0.036 0.035
H6 Trial 1 Trial 2	1.55	62	12	0.19 0.19	0.037 0.032
I6 Trial 1 Trial 2	1.10	15	9	0.12 0.13	0.022 0.023
I4 Trial 1 Trial 2	2.20	15	9	0.12 0.12	0.046 0.044

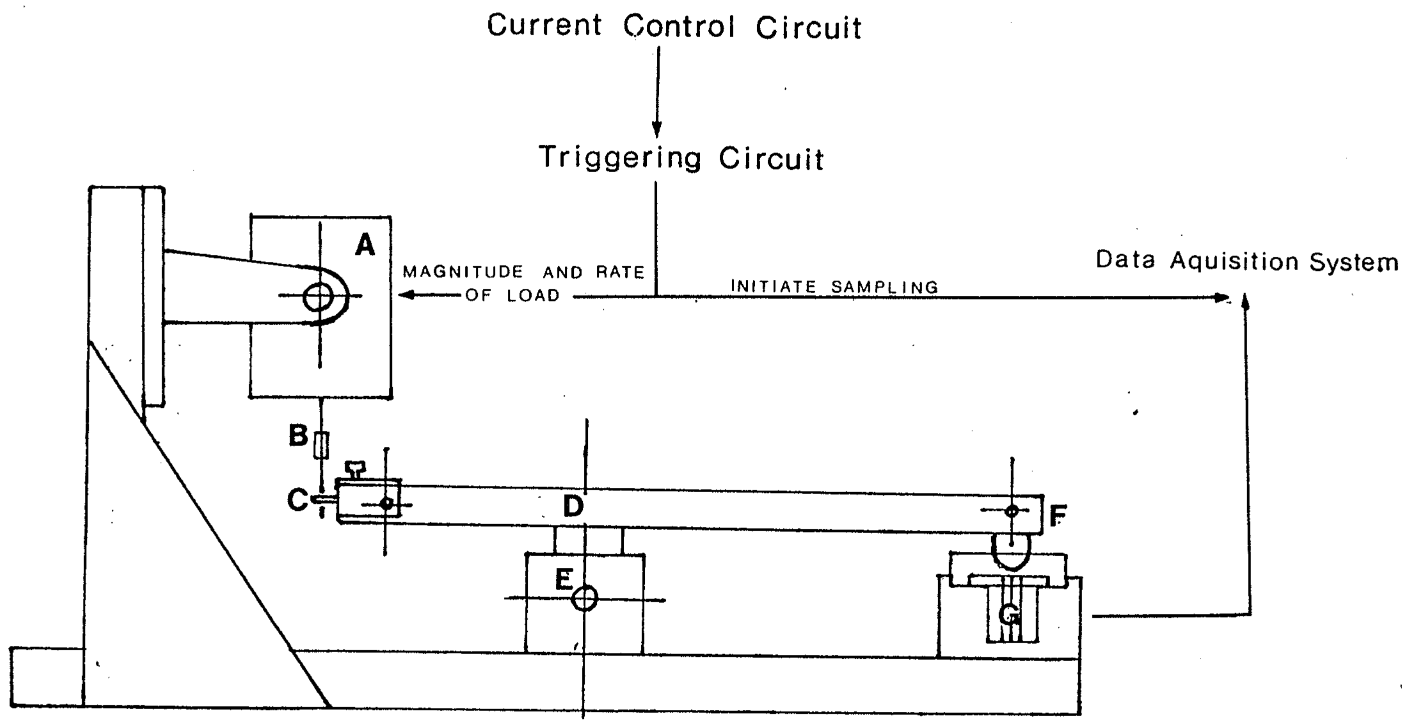

A. electromagnetic force generator
B. brass connector with load cell
C. adjustable pin coupling
D. aluminum beam
E. bearing
F. indentor attachment to the aluminum beam
G. pressure transducer array

Figure 3.1 Apparatus used to load the TMJ disc

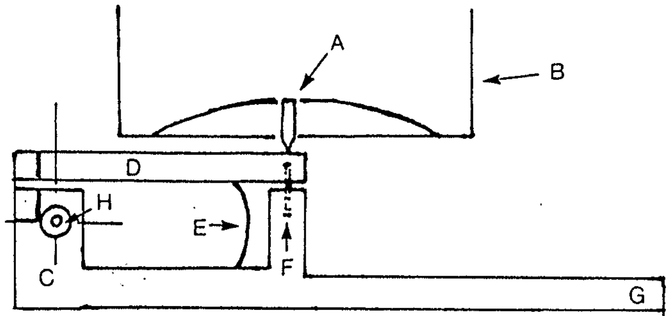

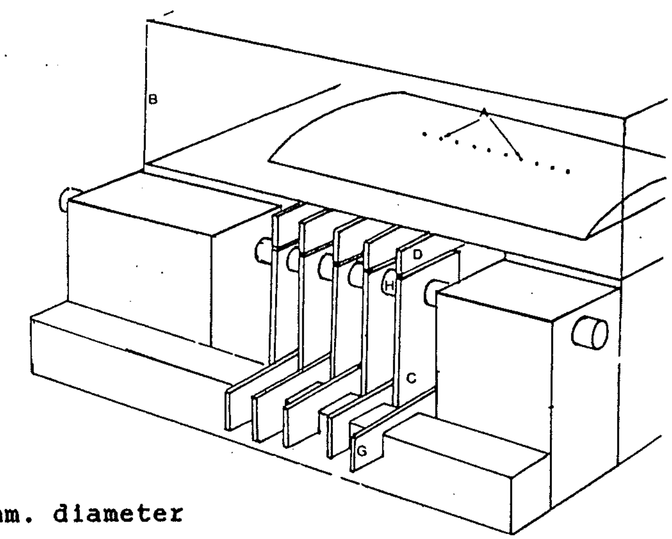

A. aluminum pin, 1.12 mm. diameter
B. acrylic tray (bath)
C. aluminum body of the transducer frame
D. hinged aluminum beam
E. 0.003 inch thick precurved brass strut
F. guide pin
G. tail of the transducer frame
H. brass bushing

Figure 3.2 Diagrams of a single transducer frame and one-half of the transducer assembly

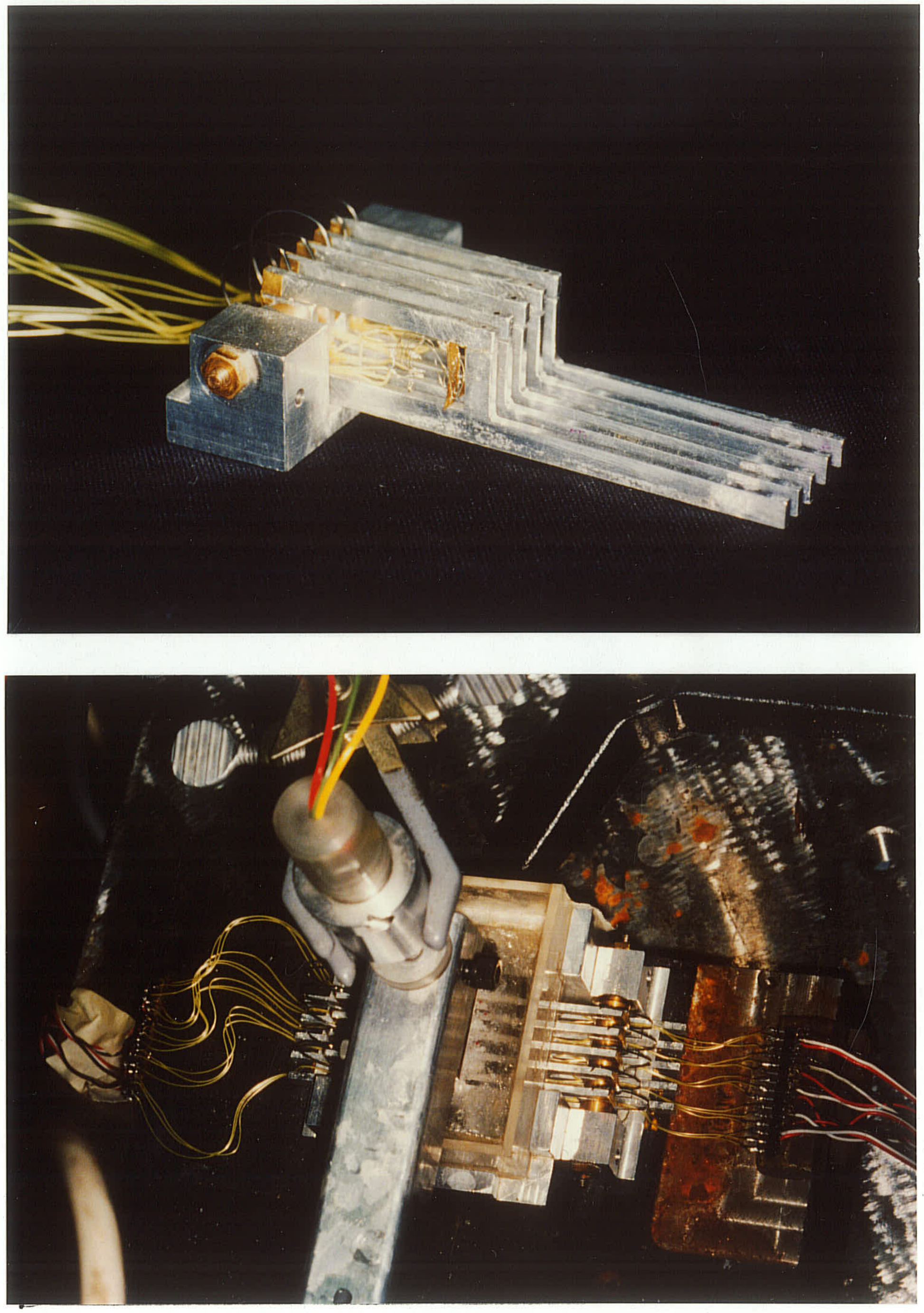

Figure 3.3 Photographs of segments of the assembled transducers and completely assembled apparatus

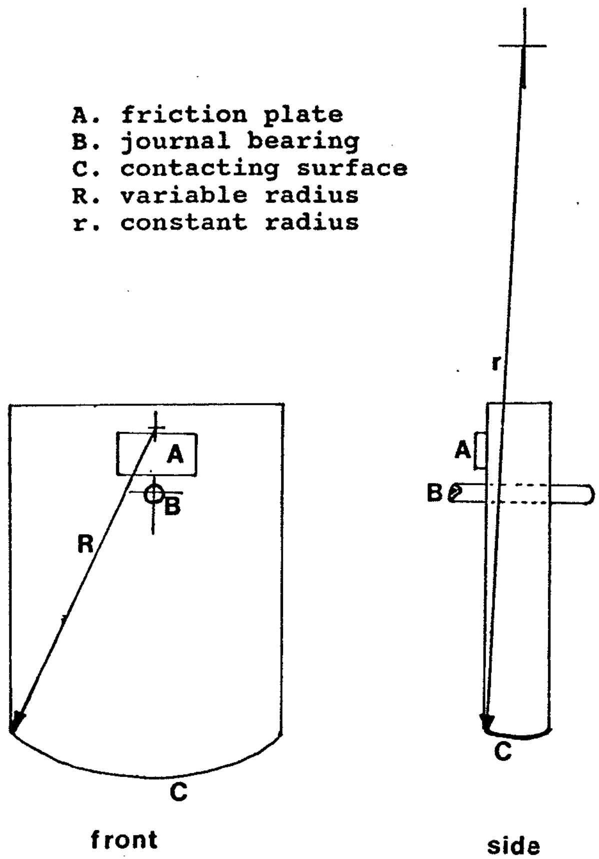

Figure 3.4 Indentors used to load discs

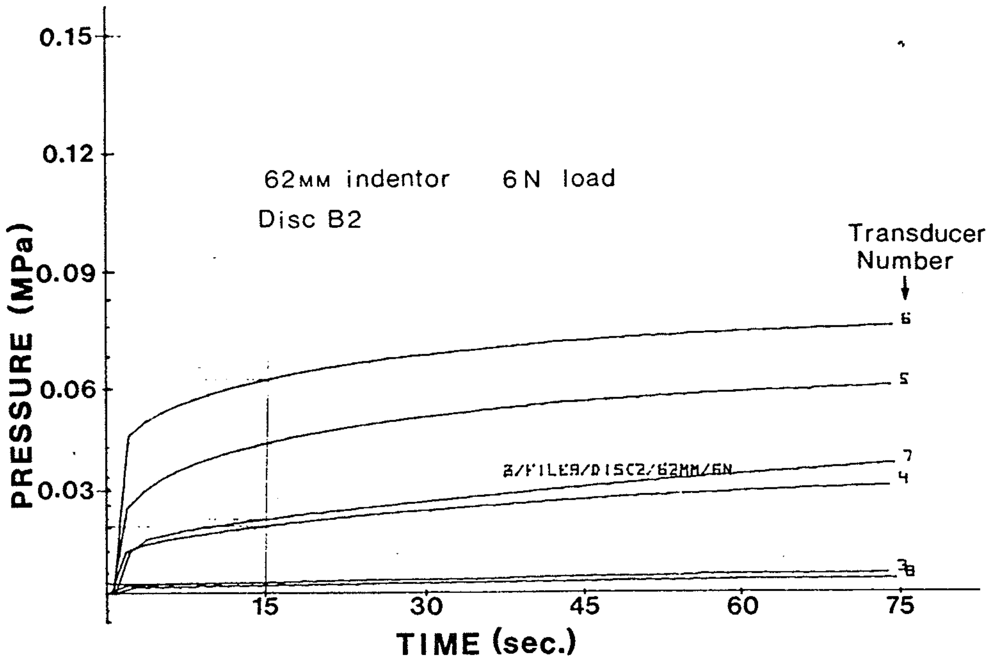

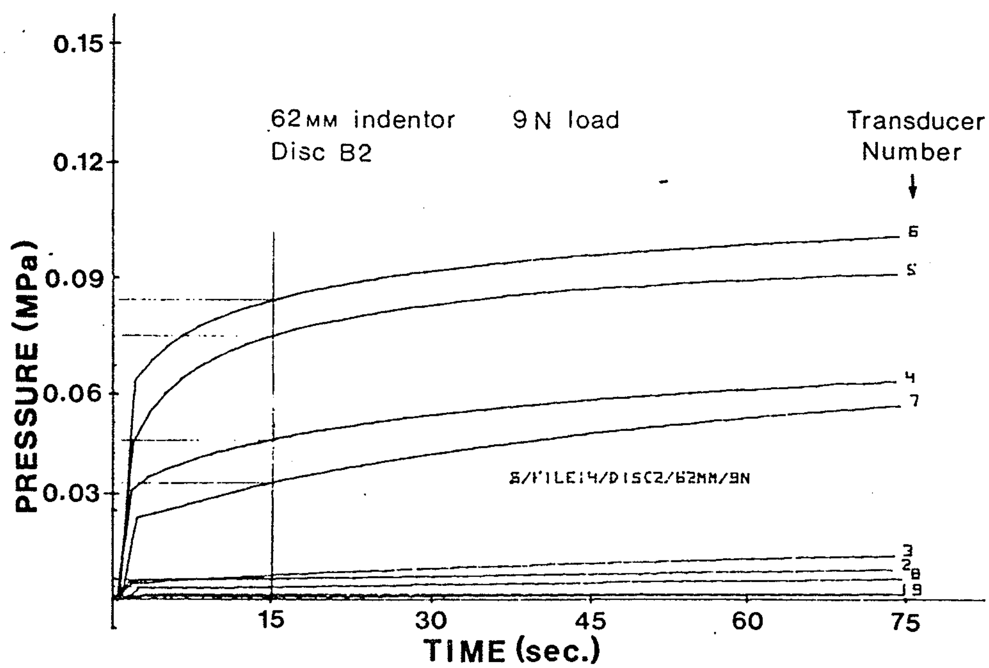

Figure 3.5 Pressure vs. time plot of individual transducer output

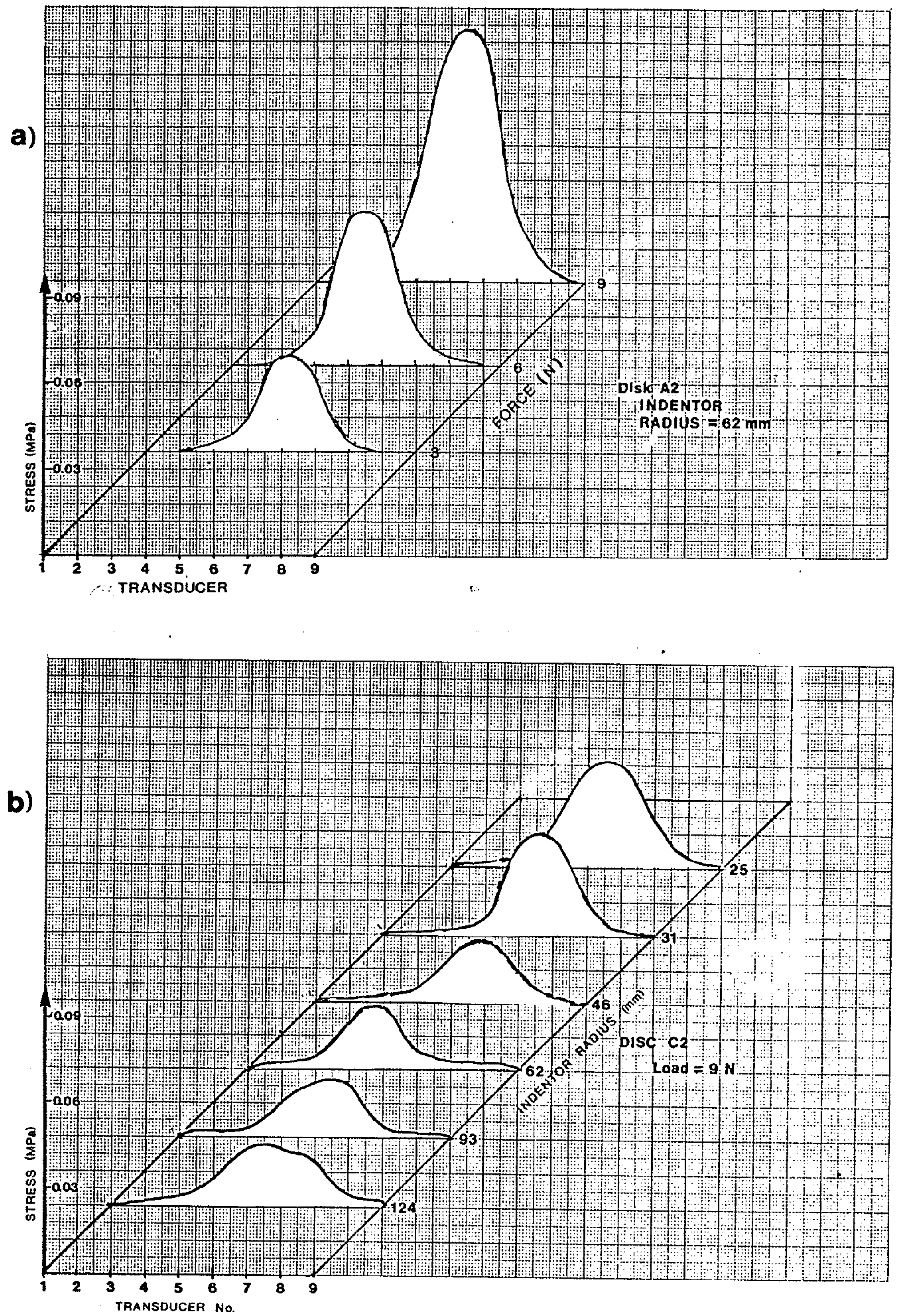

Figure 3.6 Quasi three-dimensional plots: a) varying load, b) varying indentor radius

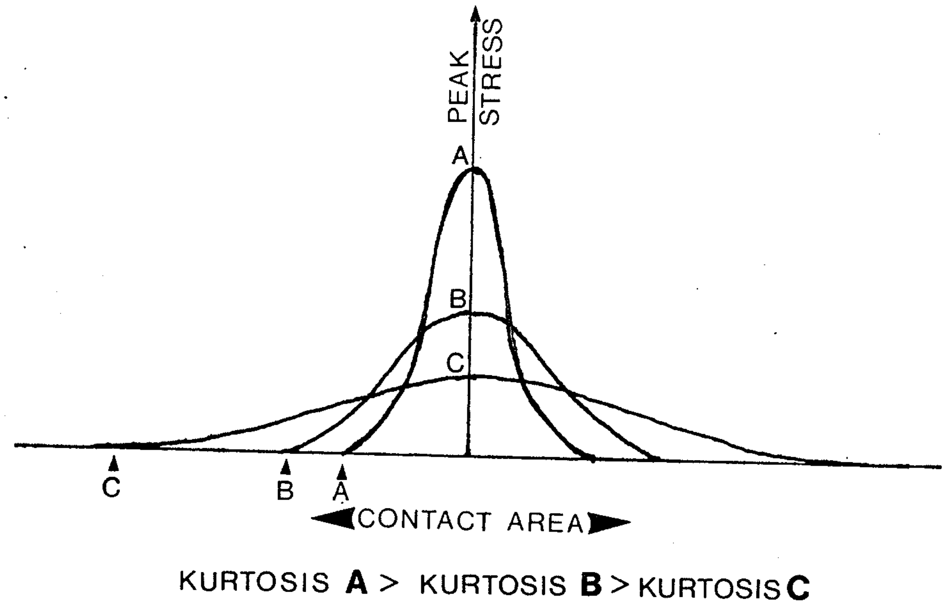

Figure 3.7 Pressure distribution curves with varying kurtosis

a)

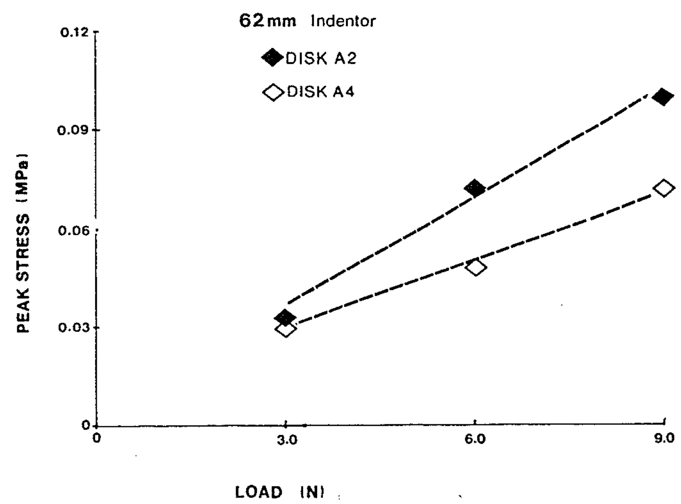

b)

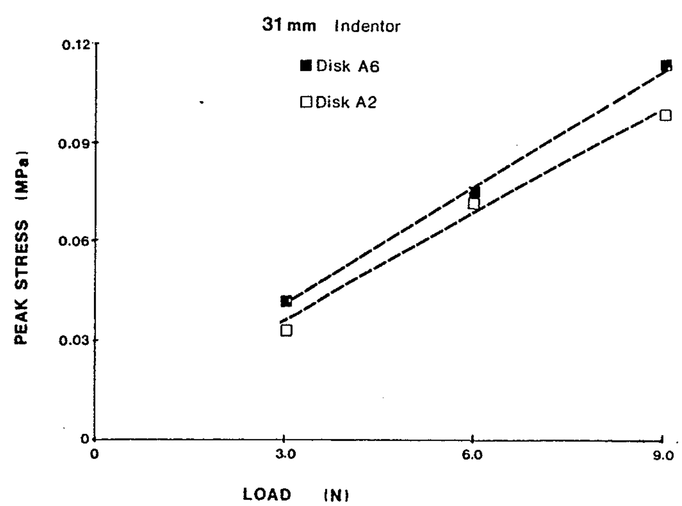

Figure 3.8 Peak stress vs. load: a) 62 mm indentor, b) 31 mm. indentor

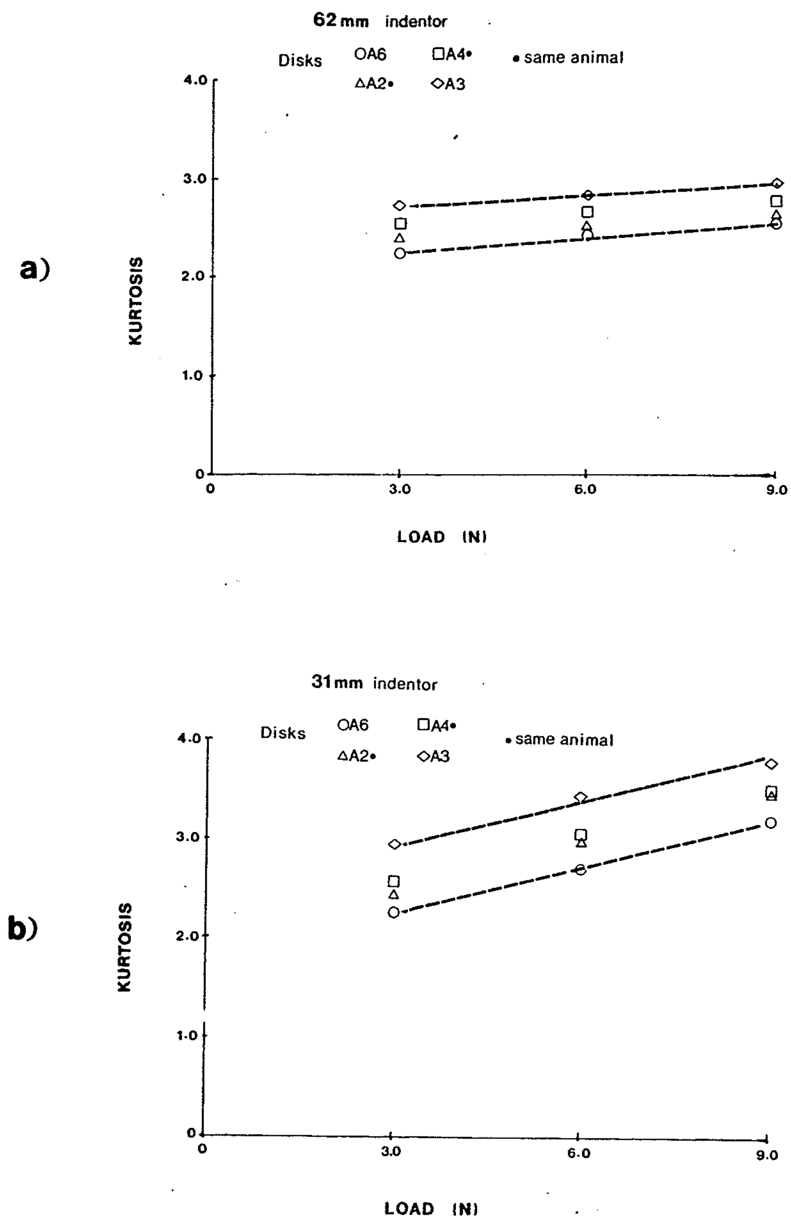

Figure 3.9 Kurtosis vs. load: a) 62 mm indentor, b) 31 mm. indentor

Figure 3.10 (following page)
Quasi three-dimensional plots of right-left symmetry within an animal:
a) thicker discs from a single animal (C2-Left, C4-Right)
b) thinner discs from a single animal (C3-Left, C1-Right)

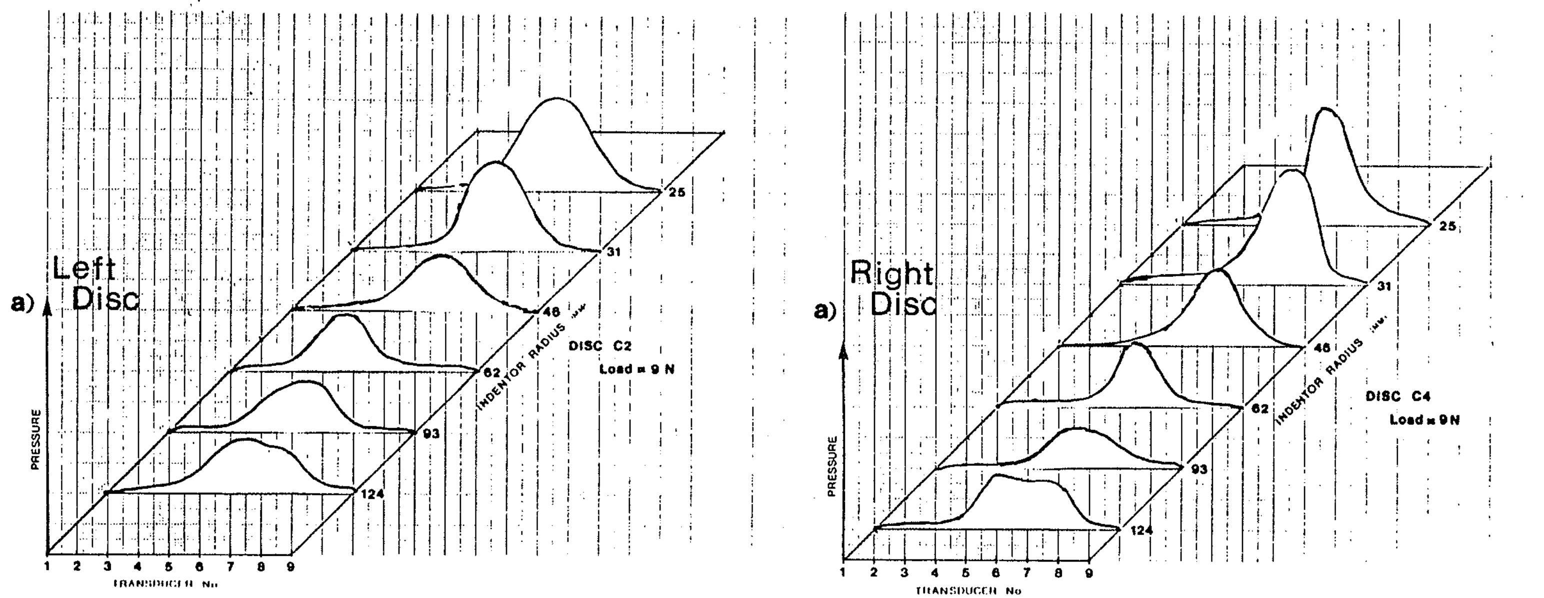
a)
Left Disc
PRESSURE
1 2 3 4 5 6 7 8 9
TRANSDUCER No
25
31
46
62
93
124
INDENTOR RADIUS (MM)
DISC C2
Load = 9 N
a)
Right Disc
PRESSURE
1 2 3 4 5 6 7 8 9
TRANSDUCER No
25
31
46
62
93
124
INDENTOR RADIUS (MM)
DISC C4
Load = 9 N

Figure 3.10

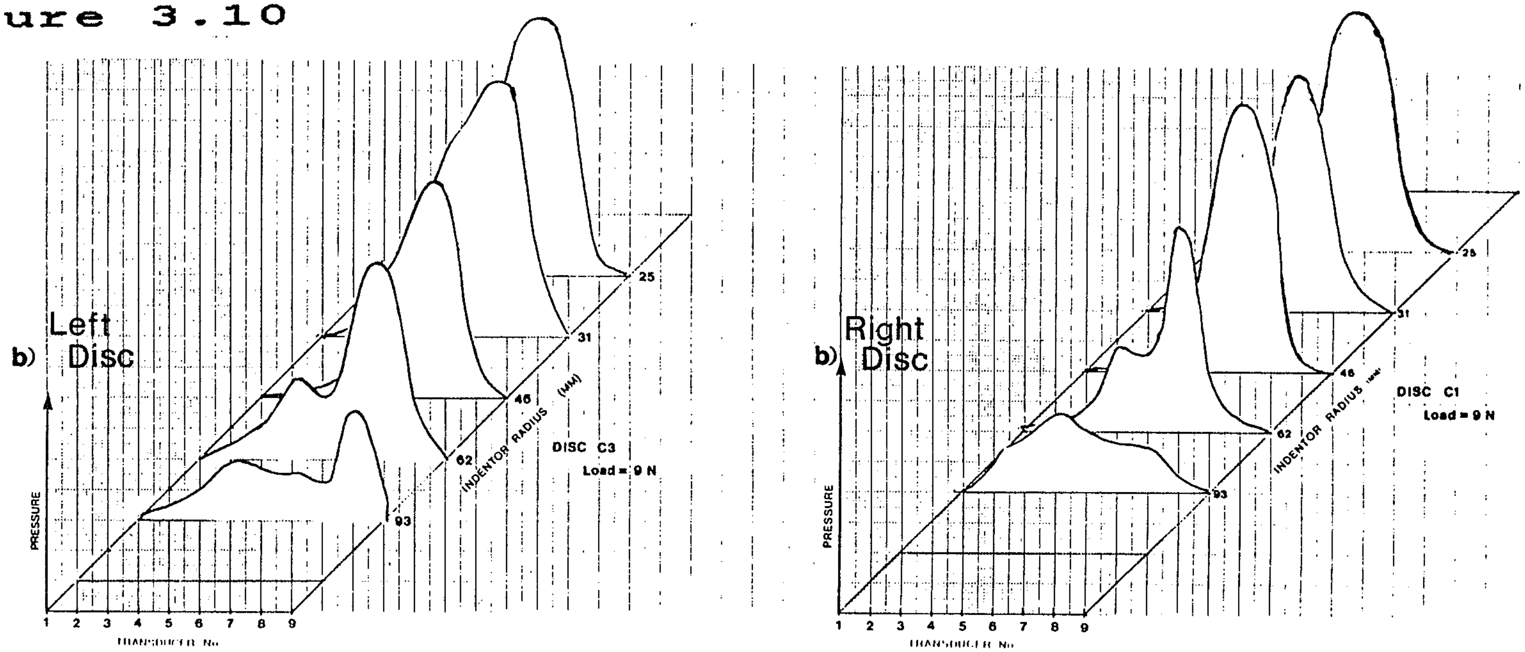
b)
Left Disc
PRESSURE
1 2 3 4 5 6 7 8 9
TRANSDUCER No
25
31
46
62
93
INDENTOR RADIUS (MM)
DISC C3
Load = 9 N
b)
Right Disc
PRESSURE
1 2 3 4 5 6 7 8 9
TRANSDUCER No
25
31
46
62
93
INDENTOR RADIUS (MM)
DISC C1
Load = 9 N

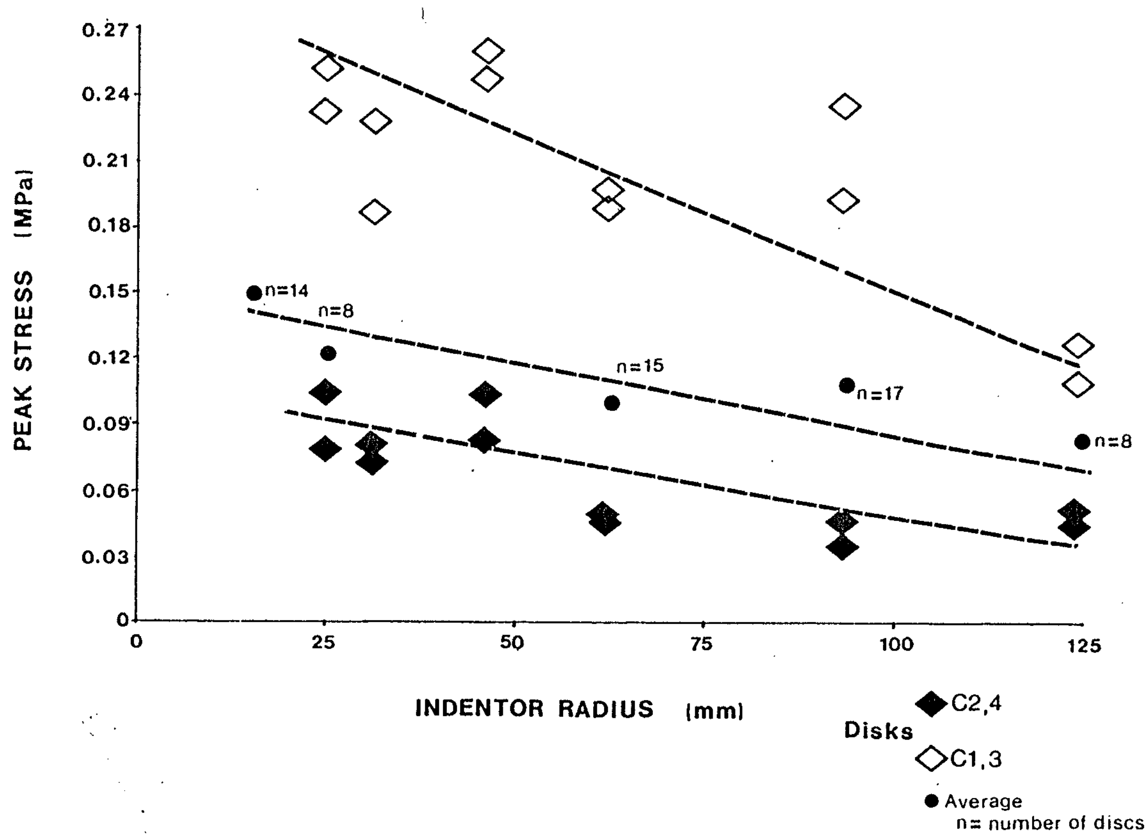

Figure 3.11 Effects of indentor radius on peak stress: Discs C2 and C4 = 0.9 mm thick, Discs C1 and C3 = 2.9 mm thick

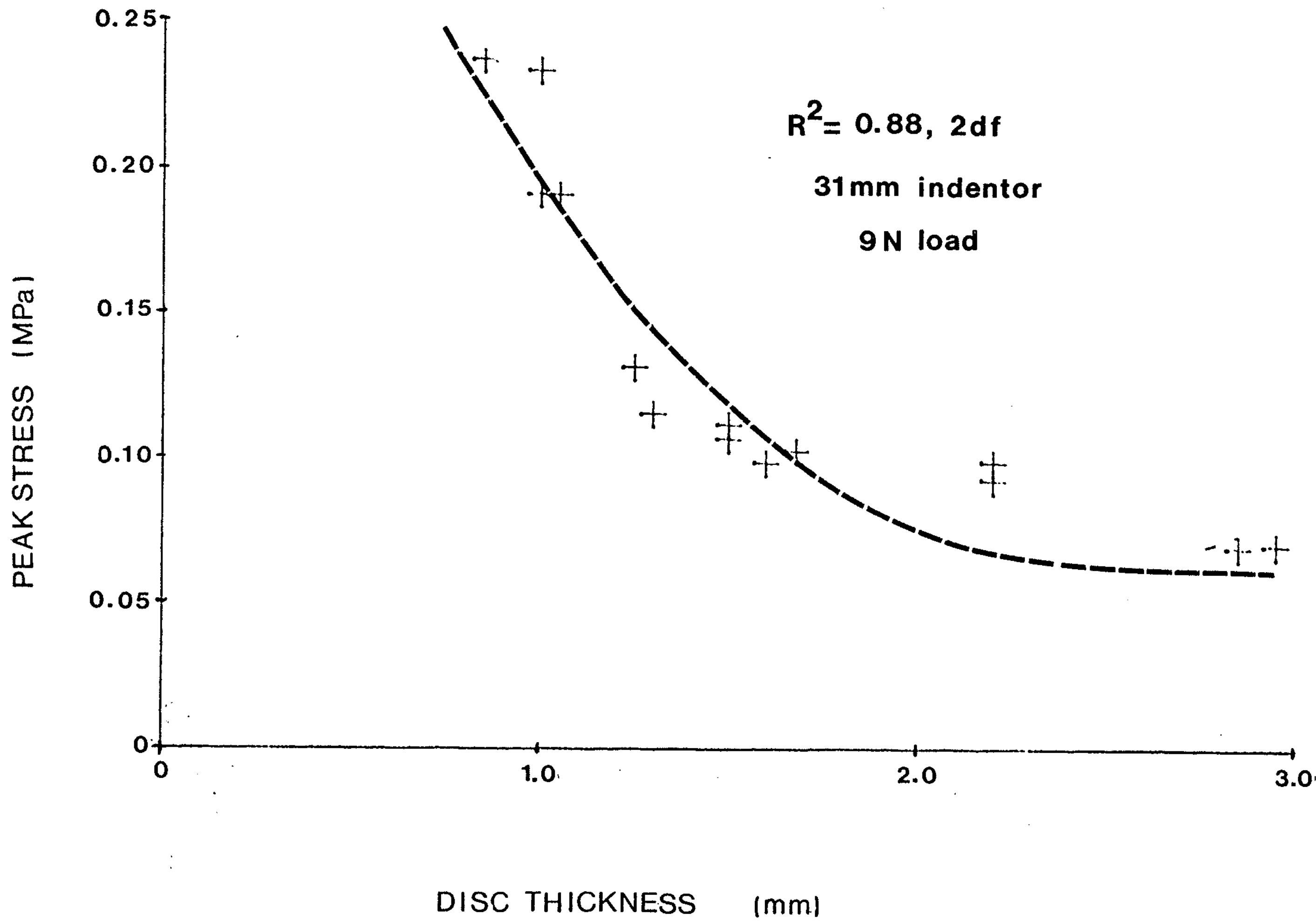

Figure 3.12 Peak stress vs. disc thickness

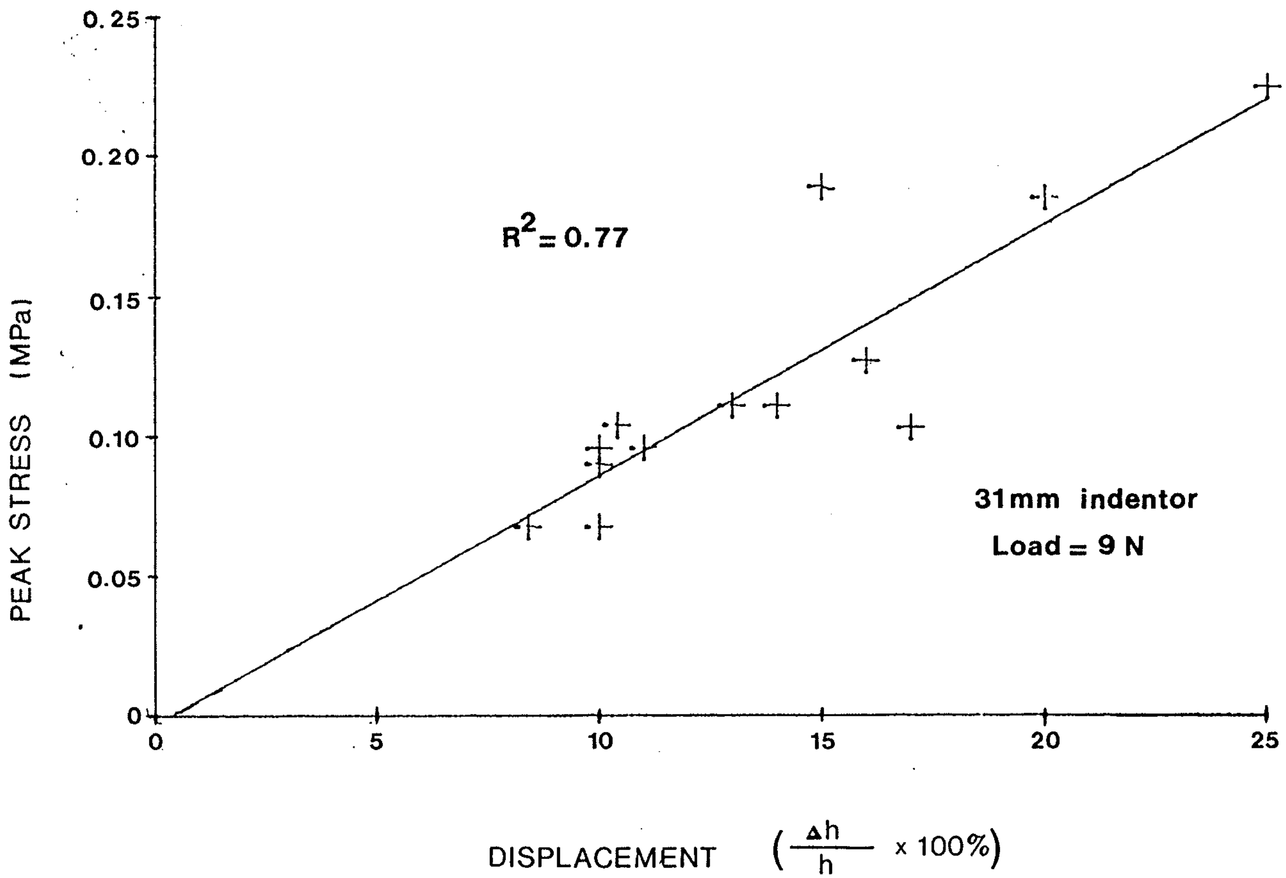

Figure 3.13 Peak stress vs. normalized displacement

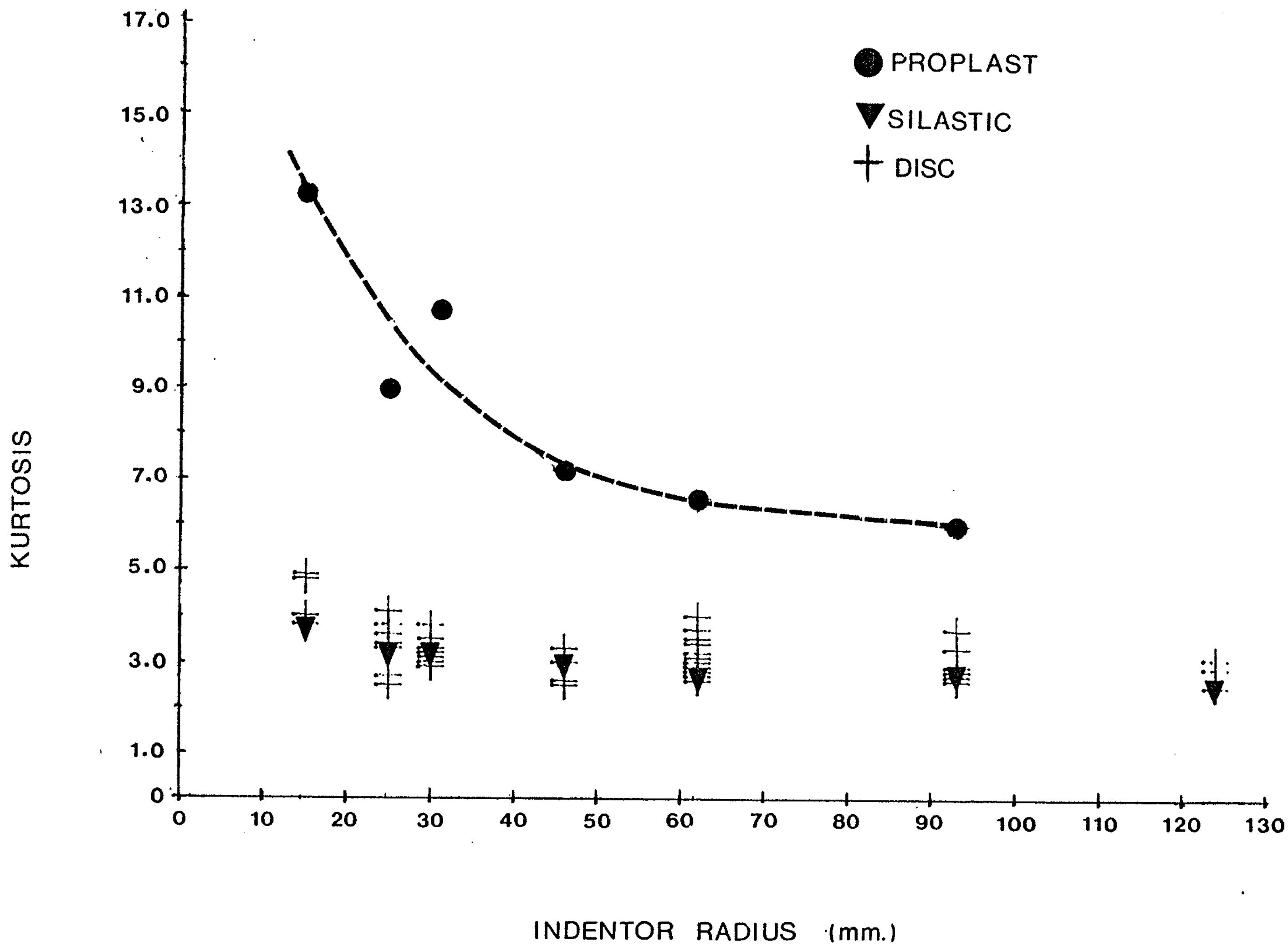

Figure 3.14 Kurtosis vs. indentor radius for Proplast, Silastic, and natural disc

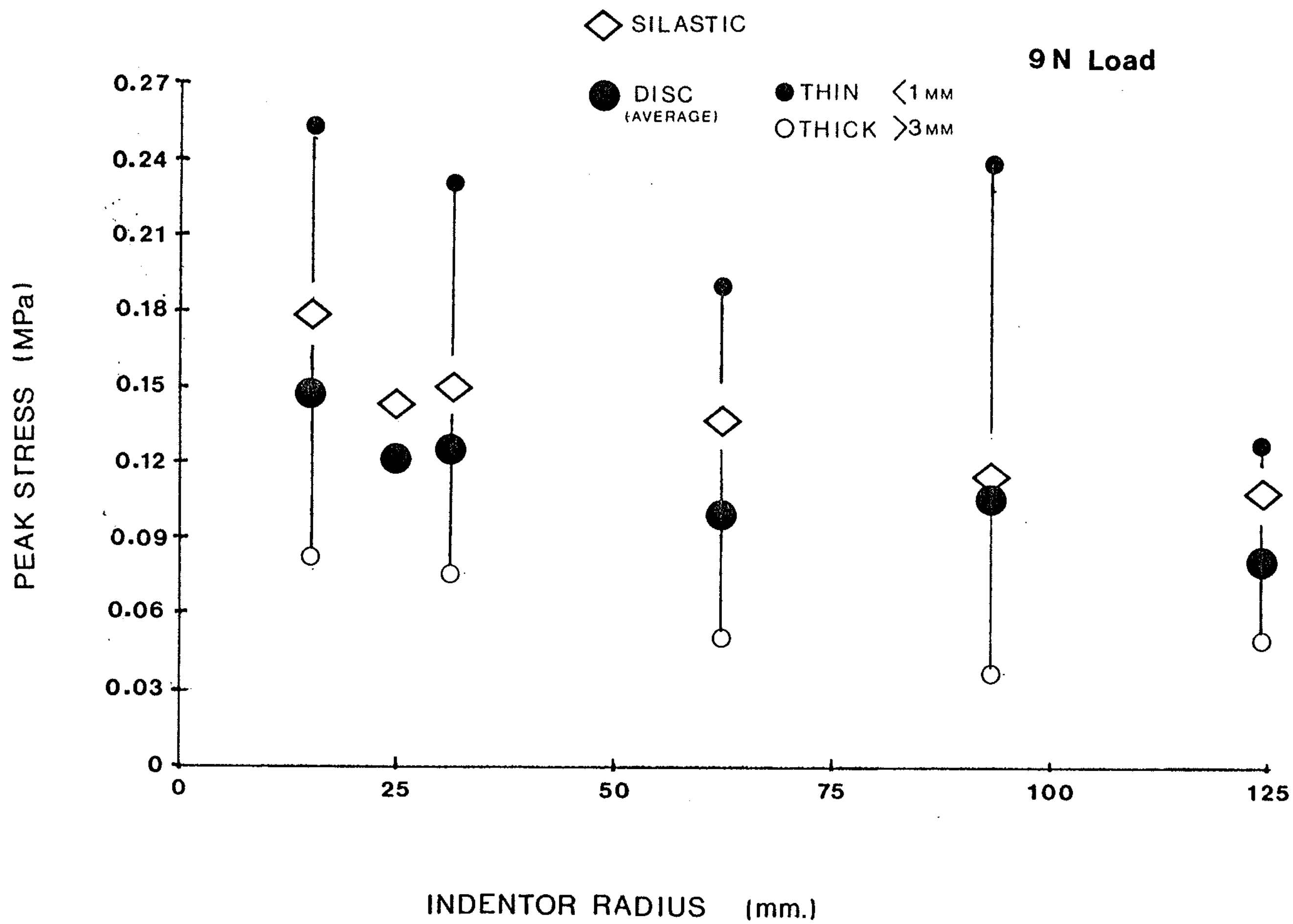

Figure 3.15 Peak stress vs. indentor radius for the range of normal discs and for silastic

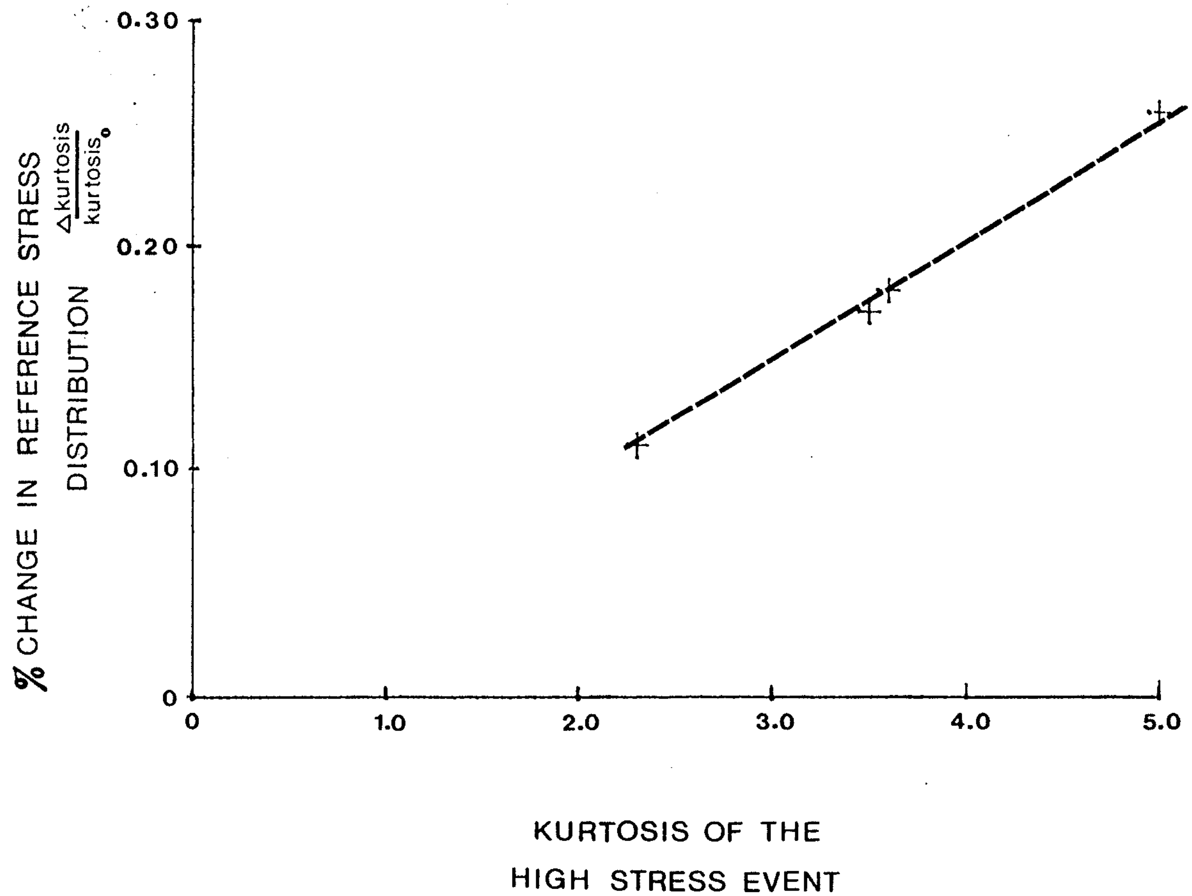

Figure 3.16 Percent change of a reference stress distribution due to stress concentrations of varying kurtosis

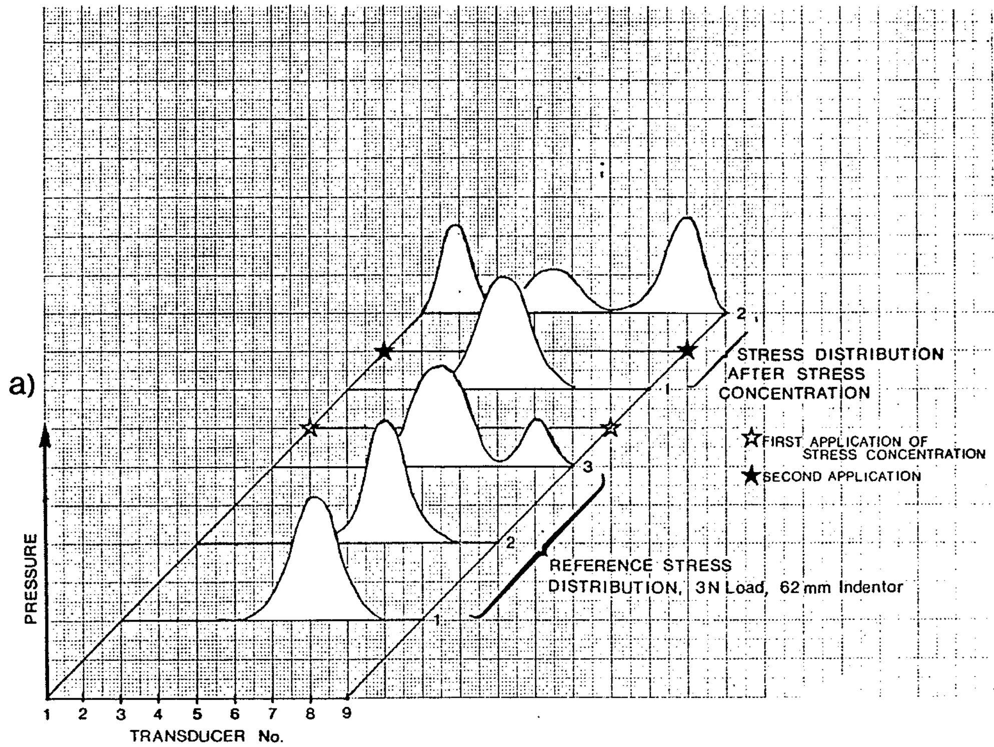

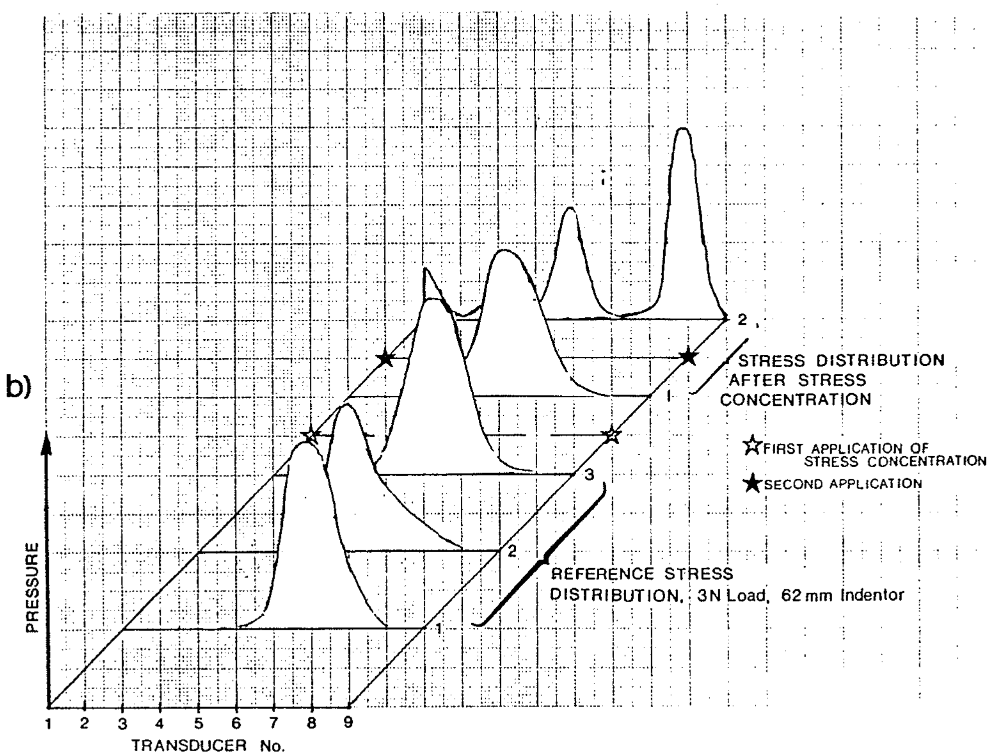

Figure 3.17 Change in stress distribution due to sequential episodes of stress concentration: a) thicker disc (2.97 mm), b) thinner disc (0.97 mm)

CHAPTER 4

Lubrication Properties of the Temporomandibular Joint Disc

4.1 Introduction

In chapter 1 it was noted that the control of stresses in the TMJ is important for the long term health of the articular tissues. For a given load on the TMJ condyle, there is normal (plane) stress in the articular tissues as well as tensile and shear stresses. The mitigation of normal stresses usually serves to reduce the magnitude of tensile and shear stresses that accompany loads which generate normal stress. But tensile and shear stresses can also be produced by other forces which act on the surface of articular cartilage, thus compounding the surface tensile and shear stresses that occur due to normal joint loading. One additional source of shear and tensile stress on the surface of articular joints is friction, due to disturbed lubrication of the surfaces, which occurs at the initiation of, and during movement of the joint. The other source of shear and tensile stress is due to deformational (ploughing) forces which occur at the initiation of, and during movement between compressed articular surfaces.

In the control of frictional forces on the surface of articular cartilage, the remarkable lubrication properties of cartilage gives synovial joints the ability to move with very low friction. This low friction (see Malcom, 1976; Swanson, 1979; and McCutchen, 1978, 1983 for reviews) is assumed to be the reason why joints may function for many years without perceptible wear (Clarke et al., 1975). However, the mechanism which produces this low friction is still a matter of debate. The pioneering work of McCutchen (1959, 1962, 1966), Linn and co-workers (1967, 1968), Maroudas (1969, 1975) and others (reviews by Malcom, 1976; McCutchen, 1978, 1983; and Swanson, 1979) continue to be the basis for current investigations concerning the mechanisms producing the unique tribology of articular cartilage. However, most of the studies of synovial joint lubrication have described the lubrication of hyaline cartilage of limb joints. There does not seem to be quantitative information describing the lubrication properties of articular fibrous connective tissue in general, and the fibrous connective tissue of the TMJ in particular.

In 1959, Charnley dismissed the possibility that the major source of lubrication of synovial joints was a hydrodynamic form of lubrication (Figure 4.1a). As pointed out by Charnley, hydrodynamic lubrication requires movement for its very low coefficient of friction. The mechanism fails at zero velocity. Charnley found that the lubrication of joints did not fail, even at zero velocity, and therefore concluded that hydrodynamic lubrication was not the principal means of lubrication in synovial joints. Charnley concluded that boundary lubrication must be the mechanism of lubrication in synovial joints.

McCutchen (1962) considered boundary lubrication (Figure 4.1b) to be an unlikely primary mechanism to explain the low friction characteristics of synovial joints. If this was the mechanism, the very low coefficients of friction were certainly lower than that produced by any known boundary lubricants. He felt that the synovial fluid would fail as a boundary lubricant at a stress level of about 1 MPa, a level frequently exceeded in joints. McCutchen proposed that the low friction of synovial joints, especially at the beginning of movement, was due to a combination of boundary lubrication and another mechanism, namely, self-pressurized hydrostatic lubrication. He described the mechanism as "weeping lubrication" (Figure 4.1c). In engineered hydrostatic bearings, a pressurized fluid prevents contact of the surfaces. In the natural bearing, it is assumed that irregularities between the loaded surfaces traps liquid between the surfaces. This helps to form an incomplete "squeeze film" form of lubrication. Synovial fluid is squeezed between loaded surfaces (Swanson, 1979), and as it is lost from between the surfaces, it is replaced by fluid movement from the matrix of the cartilage (McCutchen, 1962). At all times when there is fluid in the pockets, there is gentle contact between the boundary layers of lubricant which are deposited on the pocket walls of the weeping bearing. The boundary lubricant is able to remain effective during the early stages of loading because most of the load is carried by the synovial fluid in the pockets. This mechanism of lubrication is distinct from, but does not exclude, hydrodynamic lubrication because lubrication is present even at zero velocity. It is this mechanism which most likely produces the low friction in the TMJ, even after long periods of rest under load. Without this, as McCutchen noted, the joints would have high static friction every time they stop, and "....the treatment of joint disease would become a major paediatric problem..."(1983, p. 103). As the cartilage continues to lose fluid, the load is transferred to the boundary lubricant on the surfaces of the cartilage. But the boundary layer fails at very low magnitudes of stress. Consequently, the solid skeleton increases contact and carries a greater fraction of the load. Therefore, the sign of weeping lubrication alone, as described by McCutchen, is friction that is very low when load is first applied, and slowly rises to that of dry friction of the surfaces. For example, McCutchen used saline as a lubricating fluid when rubbing cartilage against sintered glass. He demonstrated that the weeping mechanism produced coefficients of static friction of approximately 0.003, which increased to a maximum value of around 0.3 when the weeping lubrication had completely failed (McCutchen, 1962, p. 16).

Although articular cartilage is able to lubricate with water or saline, it is a better bearing when lubricated with synovial fluid (Linn and Radin, 1968; Swanson, 1979; McCutchen, 1983; Malcom, 1976). McCutchen's explanation is that some component of the synovial fluid is a boundary lubricant. This boundary layer lubricates the gentle solid to solid contacts of the pocket walls of the bearing (Figure 4.1c). Several constituents of synovial fluid have been shown to have lubricating properties. Glycoproteins (Swann et al., 1981, 1985) have the potential to act as an active boundary lubricant. As well, the work of Hills (1984) and Hills and Butler (1989) on phospholipid surfactants have shown that multiple layers of these molecules are very effective boundary lubricants. McCutchen (1983) has noted that the oily properties of the cartilage do impart to it some slippery properties. Fat solvents seem to be the only way to remove these surface active agents. McCutchen has estimated that synovial fluid boundary lubrication does not support loading for stresses above 0.98 MPa (McCutchen, 1983, p. 95). Hills (1989) has shown that at low (non-zero) velocities, an oligolamellar boundary layer of phospholipid can support loads up to 13 Kg/cm^2 (1.3 MPa, p. 88) and maintain coefficients of friction of less than 0.005. The combination of weeping lubrication and boundary lubrication complement one another to produce a remarkably slippery surface.

The low wear rate experienced by cartilage surfaces and the long lasting quality of these bearing surfaces is believed to be due to the extremely low coefficient of friction. There is difficulty in confirming this, however, in that frictional forces can be measured in an instant, but wear must be measured over time (Swanson, 1979). Thus, statements about friction are based on experimental observations, whereas statements about wear rarely can be. In the few reports that are available (Radin and Paul, 1971; Simon, 1975), it has been shown that impact loading can result in increased friction which in turn produces wear.

Although lubrication of a traditional nature has received considerable attention, there is another form of energy loss which may account for fatigue or wear of the cartilage surfaces. This form of energy loss is known as deformational hysteresis or ploughing friction (Linn, 1967; McCutchen, 1983). Ploughing was first described by Bowden and Tabor (1950). In his early experiments, Linn (1967, 1968) showed that the ploughing associated with start up of motion involved the expenditure of energy to deform the cartilage compressively as the joint moves. In his experiments, the extent of ploughing energy loss was affected by the depth of compression of the cartilage. The consequences were that the initial frictional losses were greater than the later equilibrium values. The frictional losses due to ploughing start up from the beginning of motion. Linn showed that due to deformational losses, the start up friction is about 4 times the normal static friction. If the coefficient of friction is very low, "...the deformational losses can be the largest source of resistance..."(McCutchen, 1983, p. 441). The experimental results show that ploughing friction is a potential source of shear forces on the articular surface.

Chapters 2 and 3 of the present work have focussed on the factors which influence the magnitude of normal stresses on the TMJ surfaces. Chapter 4 presents some of the results of a study examining the frictional characteristics of the TMJ disc. Friction has been implicated in the destructive wear of the articular surfaces of other synovial joints (McCutchen, 1983). In the present chapter, the ability of the disc to prevent friction was tested and the results are presented. Factors such as the duration of loading, degree of hydration of the disc, and amount of injury to the disc were varied to determine the effect on friction.

4.2 Apparatus and Technique

4.2.1 Overview

In the literature, the historical progression in experimental design to test lubrication of articular cartilage reflected the need to control variables such as cartilage geometry and deformational (ploughing) losses which confounded attempts to measure true friction. The approaches used in previous experiments can be classified according to whether the experiment was performed on complete (intact) joints, or experiments on small cartilage specimens. A pendulum design

(Figure 4.2a) has been the most common method for testing the lubrication in intact joints (Linn, 1967; for review see McCutchen, 1978, 1983). This method of testing simulated, as near as practicable, the *in vivo* state of the joint during function. Variations of the pendulum design have been used in studies examining the wear properties of articular cartilage (Clarke *et al*., 1975). The results of pendulum experiments on intact joints were plagued by the lack of control of, or knowledge of cartilage thicknesses and loading areas. Deformation losses further confused measurements of pure frictional forces. In contrast, McCutchen (1959, 1962, 1966) and Malcom (1976) performed experiments on small cartilage specimens (Figure 4.2b). The difference between the experiments of McCutchen and Malcom was that McCutchen used a non-biological surface to test lubrication of cartilage, whereas Malcom machined a hyaline cartilage annulus, which then was loaded against periosteal connective tissue. In both cases, the small cartilage specimens allowed for simplified and controlled geometry of the cartilage, and provided for controlled unidirectional sliding of the articulating surfaces. This design eliminated most of the deformational (ploughing) losses which were known to exist in whole joint experiments. However, small cartilage specimens are produced by artificial cuts to the matrix of the connective tissue. These cut boundaries alter the characteristic fluid flow within the cartilage matrix, and will affect the rate of decay of the lubrication. Therefore, in testing the TMJ disc, it was preferable that the disc not be altered by dissection, and that the testing for friction be done on an intact disc.

As indicated by McCutchen (1983), the start up forces related to friction between the surfaces are probably the principal source of wear of the articular surfaces. Therefore, the most important time to measure lubrication by the TMJ disc is at the initiation of movement. The greater the force required to make the surfaces slip, the greater will be the tension and shear stresses along the surface of the cartilage. The measuring apparatus used in the current experiments was designed with the principal objective of testing the hypothesis of weeping lubrication by the TMJ disc. With this aim in mind, measurements were made of the time-dependent changes in the lubrication of the surface of the disc at the start of movement. The apparatus was built using a pendulum design, which was constructed in a fashion so as to make it possible to set a constant load on the TMJ disc and to maintain the load on the disc for any required period. The pendulum apparatus was capable of measuring the frictional forces on the cartilage surface during the entire period of loading.

4.2.2 Description of the pendulum

Figures 4.3a and 4.3b are sketches of the pendulum with the lever delivery system. The pendulum was made up of an aluminum cross beam with a weight attached to both ends. The force generated by the weights could be varied between 2 and 6 Newtons (N). Contact between the pendulum and the disc was made through an acrylic indentor attached to the pendulum (Figure 4.3c). The acrylic indentor was attached to the bottom surface of the cross beam. The indentor had a radius of 12 millimetres (mm) when viewed from the front, and a side view radius of 125 mm (Figure 4.3c). To control the position of the pendulum on the disc, a load delivery system was built. The system was comprised of a lever apparatus with a supporting fork which contacted the pendulum through aluminum wedges attached to the pendulum. The wedges were attached to the bottom surface of the cross beam and were equidistant from the centre of rotation of the pendulum. The supporting fork could be adjusted to various angles by rotating on a journal bearing and being fixed at any angle up to ± 5 degrees (Figure 4.3a,b). This in turn produced the various initial angular deflections to the pendulum to control the magnitude of the restoring force (Figure 4.4). The forks were connected to a trigger circuit which indicated when there was full contact between the pendulum and lever system. This simple electronic trigger circuit was used to indicate the instant at which the load was applied.

The experimental apparatus measured the frictional forces associated with the start-up of movement. The pendulum was used to load the TMJ disc. If there was no friction between the indentor and the disc, small deflections of the pendulum away from equilibrium would produce restoring forces that would return the pendulum to its original position (Figure 4.4). If, however, friction existed between the surface of the disc and the indentor, the deflected pendulum would only return towards its original equilibrium position if the restoring force was just greater than the frictional force. The objective in using the pendulum then was to find the point of maximum angular displacement without causing pendulum movement. This angular displacement was proportional to the frictional force just before the initiation of movement. It was this force which McCutchen (1983) suggested was the most damaging to the surface tissues.

The calculation of the magnitude of the frictional force between the indentor and disc depended on the assumption that because the friction measurements were made while the pendulum was in static equilibrium, the frictional forces on the surface of the disc produced a counter moment equal and opposite to the moment produced by the restoring force of the pendulum. Since the restoring force of the pendulum was proportional to the angular deflection, θ, of the pendulum, the frictional force was estimated from the following equation:

$$F_2 = \frac{x}{L}(\mathit{sine}\theta\ F_w)$$

The variables in the equation are as follows:

F_2 - frictional force
θ - angle of deflection
x - vertical distance from the centre of mass to the centre of rotation
L - radius of the indentor
F_w - weight of the pendulum

Before making this measurement, two criteria had to be met. Firstly, at the angular deflection, θ, the pendulum had to be in static equilibrium. Secondly, that the angular deflection, θ, was the maximum possible without violating static equilibrium. In this manner, for each measurement of the deflection of the pendulum, it was possible to calculate the restoring forces that occurred just "at the brink" of motion between the surfaces of the disc and indentor.

Once the frictional force (F_2) was determined, it was divided by the weight of the pendulum to give a coefficient called the coefficient of stiction ($\mu_{stiction}$).

$$\mu_{stiction} = \frac{F_2}{F_w}$$

This coefficient was calculated in exactly the same way as the more traditional coefficient of static friction. The term stiction was used, instead, as a reminder that the calculated restoring forces were a little less than needed to make the pendulum slip over the surface of the disc.

4.2.3 Measuring variables, storing data, and data analysis

The measurement of angular deflection of the pendulum was accomplished by using an optical transducer system, as seen in the diagram of Figure 4.3b. The transducer system consisted of a photoelectric transistor, focussing lenses, and a monofilament light source which produced a uniform, horizontal, linear beam. The system measured the horizontal displacement of the leading edge of a target flag, the leading edge of which interrupted part of the light beam. A lens system collected the light passing the flag, and focussed the light on the photoelectric transistor. Hence, a linear relationship between horizontal flag position and optical transducer was obtained. The flag was attached to the pendulum by means of a tower made of polystyrene foam. Calibration of the transducer system made it possible to measure the deflection of the flag and thereby calculate the angular displacement of the pendulum. The length of the tower was made as large as practicable so as to increase the horizontal deflection of the flag for a given angular displacement. This reduced errors in the measurements caused by small sideways movement of the centre of rotation of the pendulum. Thus, there was improvement in the signal to error ratio, and it was possible to measure smaller frictional forces. This system of measurement was also very insensitive to small vertical changes in the height of the pendulum.

Vertical displacement of the pendulum into the TMJ disc was monitored by a linear voltage differential transformer (LVDT). The LVDT measured the height of the lever system (Figure 4.3a,b). The LVDT was used to measure the height of the pendulum when the lifter had just broken contact with the pendulum. Over the course of loading of the TMJ disc, the LVDT gave a series of height measurements which were used to calculate the indentation of the pendulum into the TMJ disc.

Data was stored on a magnetic tape using a Hewlett Packard 3690 Instrument Recorder (registered trademark, Hewlett-Packard Company: Loveland, Colorado). The frequency modulated tape recorder had four channels, three of which were used to record the output of the LVDT, photoelectric transistor, and electronic trigger. Tape speed was set at 15/16 inches per second. A digital stop watch was also used to time the experiments. Monitoring the output of each channel was done using a storage oscilloscope. The electronic trigger, which indicated contact between the support forks and beam of the pendulum (Figure 4.3a,b), was used to trigger an oscilloscope trace. In this way, it was possible to determine when the weight of the pendulum was transferred to the TMJ disc, and coordinated the timing of the signals of the LVDT and the photoelectric resistor.

4.2.4 Loading of the disc

The loading of the TMJ disc by the pendulum involved removing the disc from a heated saline bath (37 degrees centigrade, $\pm$ 3 degrees), and placing the disc on the sandpaper surface of an aluminum platform. The sandpaper prevented slipping of the disc over the supporting aluminum platform. The pendulum was brought to a zero displacement (zero degrees deflection) position, and the timing clock and tape recorder were started. The lever system supporting the pendulum was lowered gently, which brought the pendulum to rest on the disc with the full weight of the pendulum supported by the disc. At this time, the zero displacement equilibrium position was centred on the oscilloscope.

Now that the pendulum was loaded on the disc, it was possible to begin measurements of the friction between the surfaces of the indentor and disc. To do this, the support fork was raised until the contacts were just closed, and then was carefully deflected to an angular deflection of greater than 0.5 degrees. This was done because the maximal measurable deflection using the described geometry of the pendulum was 0.5 degrees. From this position the pendulum was slowly lowered onto the disc. As the disc began to support the weight of the pendulum, the pendulum angle slowly reduced until it reached an angle at which static equilibrium occurred. Once static equilibrium was exhibited, the supporting fork was lowered away from the pendulum, and the full weight of the pendulum was supported by the TMJ disc. During these experiments, positive and negative angular deflections were imposed on the pendulum to ensure that there was symmetry in the measurements of friction. The loading continued until the pendulum reached static equilibrium with an angular deflection greater than 0.44 degrees, or the duration of loading exceeded 20 minutes. A deflection of 0.44 degrees was indicative of a stiction coefficient of greater than 0.020.

4.2.5 Sources of Error

The pendulum design used in the experiments has some drawbacks, but it did not have the problems of other pendulum designs as described in this chapter. The pendulum was unusual in that it was able to provide a means of measuring the friction during the start-up of movement. The measurements were made without interference due to the magnitude of deformational losses of other pendulum designs (Linn, 1967). The design was capable of measuring the very low coefficients which are typical of articular tissues. There are several other points which pertain to the design of the pendulum. These points are addressed below.

Effects of vibration: The behaviour of the pendulum and the ability to measure friction was critically dependent on the form of the release of the pendulum on the cartilage surface. To reiterate, the criteria of measurement were that the pendulum had to be at the maximum angular displacement possible, yet consistent with it remaining in static equilibrium. Energy in the form of vibration reduced the effect of the friction forces. This would result in an abnormally low value in the measurement of the friction. The effect of vibration is seen in some of the plots of $\mu_{stiction}$ vs. time (eg. Figure 4.7) as a drop of a datum point, which appears well below the regression line. The reduction of dynamic effects was achieved through practice with the equipment to reduce vibration inadvertently introduced by the operator. To reduce the effect of floor vibration, the entire apparatus was mounted on heavy concrete plinths.

Movement of the indentor over the surface of the disc: Theoretically, the design of the pendulum was such that the amount of surface movement of the indentor relative to the cartilage surface was very small. To validate that the pendulum was operating according to design, a travelling microscope was used to observe the interface between the disc and the indentor to ensure that the surface of the indentor was moving relative to the surface of the disc. As well, the microscope was also used to locate the centre of rotation of the indentor when the pendulum was placed in contact with the disc surface. Tattoos on the indentor aided in locating the centre of rotation. The results verified that movement of the indentor, relative to the surface of the disc, was occurring and that the centre of rotation was about the 12 mm centre of radius of the indentor (12 mm $\pm$ 0.25 mm).

Linear (sideways) translation of the centre of rotation: The lateral movement of the centre of rotation of the pendulum relative to the optical sensing system would be expected to cause considerable error in the deflection measurements. Lateral movement of the centre of rotation could occur if either the pendulum alone, or the disc and the pendulum moved in a horizontal manner perpendicular to the optical sensing system. As a precaution, the tower and flag of the pendulum were constructed as high as practicable to reduce the sensitivity of the apparatus to lateral translation relative to angular deflections, and thus increase the signal to error ratio. Direct observation using a travelling microscope confirmed that sideways movement of the centre of rotation was minimal and was within acceptable limits. Test trials with the pendulum showed that there was never any evidence of wandering of the initial "zero displacement" position on the oscilloscope.

Effect of variation of disc geometry: The varying thickness of the disc in the mediolateral direction had an effect on the contact area between the cartilage and the pendulum indentor. This introduced variation in the lubrication of the surfaces by varying factors such as the flow path of fluid escape and magnitude of the contact stress (Armstrong et al.,1984). In chapter 3, it was found that a smaller indentor had the least variation of all indentors in terms of differences in contact area, between discs, due to mediolateral changes in disc thickness. The right-left symmetry of discs from the same animals (Figure 4.6) gives encouragement that although not perfect, the 12 mm indentor was adequate to avoid serious errors due to contact area variation. However, differences in disc geometry relative to the indentor probably account for some of the scatter seen between discs of different animals (Figure 4.5).

<u>Dehydration of the disc</u>: Testing of the disc was done under very harsh conditions in order to demonstrate the mechanism of lubrication by the disc. By using an acrylic indentor, it was most likely that the disc rather than the indentor contributed the lubrication of the surfaces. However, under these harsh conditions, the rate of rise of the coefficient of stiction is likely to be faster than under natural conditions. In the intact joint there is a permanent reservoir of synovial fluid provided by the synovium of the joint. As well, the connective tissues of the condyle and eminence may "weep" fluid to lubricate the surfaces. Thus, in comparison to the results of this investigation, these additional sources of fluid in the intact joint would probably reduce the time-rate of increase in friction.

<u>Surface damage to the TMJ disc</u>: In a few cases, signs of early degeneration of the disc were evident. These cases had features such as brownish red staining over the lateral portion of the disc. Anteroposterior ridging, as opposed to a smooth matte surface, was also evident. The feature of

right-left symmetry of discs from the same animal provided a means of checking whether surface damage was affecting lubrication. In preliminary tests, surface damage was shown to result in an unusually high rate of rise of $\mu_{stiction}$ with time. This rate of increase was most notable when compared to the intact contralateral disc of the same animal. When conditions of surface damage were noted either by inspection or by asymmetry in the lubrication between the right and left discs, the results were not included in the study.

Errors in reading the oscilloscope and timing errors: The accuracy in reading the output of the photoelectric transistor on the oscilloscope was within ± 0.005 volts. This resulted in an error in the estimation of the coefficient of stiction of ± 0.0006. Timing errors were minimized by using a digital stopwatch as well as the tape counter. Errors in timing, from start to finish, were within ± 0.25 minutes.

4.3 Results

4.3.1 Friction vs. time

Figure 4.5 shows the characteristic increase in the coefficient of stiction with time that was found for discs tested under a 4 N load. The coefficient generally started at less than 0.007 and demonstrated a non-linear increase with time. Usually, a coefficient of 0.020 was achieved in under

15 minutes. The plot in Figure 4.5 was the result of loading on 5 discs which were considered representative of the average increase in $\mu_{stiction}$ with time. To demonstrate the full range of increase in the coefficient with time for all discs tested, Figure 4.6 shows the results of four discs (2 matched pairs from two animals) which represent the two extremes of $\mu_{stiction}$ vs. time. Discs 1A and 1B, which came from one pig, showed the slowest rate of increase in the coefficient of stiction. A best-fit straight line for the data during the first four minutes of loading had a slope of 0.0017 per minute. Conversely, discs 2A and 2B came from another pig, and showed the greatest increase in the coefficient during the first four minutes after load. A best-fit straight line of the data points for the first four minutes of loading had a slope of 0.0025 per minute. In both cases, the disc pairs demonstrated right-left symmetry.

4.3.2 Friction dependence on matrix hydration

According to McCutchen (1962), the sign of weeping lubrication is an initially low coefficient of friction which rises with time. The ability of the connective tissue to recharge the fluid between the surfaces will determine the rate of increase in frictional forces between the surfaces. To test if the degree of hydration had an effect on the rate of rise of friction, 5 discs of similar dimensions, free of apparent compromise in surface integrity, were used in a series of loadings with the pendulum. The course of the tests was as follows. In the first test, the loading of the disc was done using the 12 mm indenter under a 2 N load. The time dependent changes in the coefficient of stiction were measured for ten minutes or until the $\mu_{stiction}$ was approximately 0.020. Following completion of this first friction test, the disc was removed from the supporting block, and placed back in the saline bath for a period of two minutes. The pendulum was then placed back on exactly the same location of the disc as the previous load, and the friction test was repeated. Following the second test, the disc was removed from the supporting surface and placed back in the saline for a 15 minute period, after which the friction test was repeated.

The data from the tests performed on each disc were plotted in the form seen in Figure 4.7. The results showed that there was a direct relationship between imbibition time and the rate of increase in the coefficient of stiction. To demonstrate this, a best-fit straight line was drawn through the data points for the period between 1 minute and 4 minutes after loading. The slope of the line represented the rate of increase in the coefficient of stiction. The results showed (Figure 4.8) that trial 2, in which the disc was immersed in saline for only 2 minutes, had a greater rate of increase in the coefficient of stiction (steeper slope) than for either trial 1 or trial 3. Trial 3 gave an opportunity for the disc to take on a greater quantity of saline, which resulted in a slower rate of increase of the coefficient of stiction compared to trial 2. Trial 3 more closely approximated the rate of change of the coefficient of stiction found in trial 1.

4.3.3 Recovery of lubrication after surface drying

There has been debate (Swanson, 1979) as to whether or not articular cartilage lubricates by a squeeze film trapped between the opposing surfaces of cartilage. This type of lubrication is different from weeping lubrication, in which weeping of the fluid from the matrix of the disc replenishes the fluid lost from between the opposing cartilage surfaces. To test whether fluid from the matrix of the disc could replenish fluid removed from the surface of the disc, experiments were conducted in which the surface of the disc was dried and then monitored for changes in lubrication. Four pairs of discs from four pigs were exposed to drying. The steps used in these tests were as follows. There was an initial loading of each disc, using the pendulum, and measurements were made of the friction between the surface of the disc and the indentor of the pendulum. After these initial measurements, the pendulum was lifted off the surface of the disc and the surface of the disc was dried using nitrogen gas in time controlled bursts. For the first test, the drying time was 15 seconds. Following this, the pendulum was gently lowered back onto the disc and another set of friction measurements were made. After completing the test, the disc was placed back in saline solution for a period of one hour. After an hour, a second test was done in exactly the same manner except that the drying time was 5 seconds.

Figure 4.9 shows the results for two discs. In the first test, the drying time was 15 seconds. After drying and reloading the pendulum on the disc, there was an increase in the coefficient of stiction until such time that the magnitude of friction between the surfaces was too large to be measured by the apparatus. Eventually, lubrication by the disc began to reduce the friction to within the measurement range of the apparatus. The recovery of lubrication of the surface of the disc appeared to continue until the coefficient of stiction returned to a "normal" value. After recovery, the friction seemed to increase slowly, in a time-dependent fashion that was characteristic of the disc.

In the second set of tests on these discs, the duration of drying was 5 seconds. As seen in Figure 4.9, the increase in the coefficient of stiction after this brief period of drying was less than after 15 seconds of drying. As well, the rate of recovery of the coefficient was about 1.5 to 2.0 times faster for the shorter drying conditions. As a note of caution in interpreting the data, the peak coefficient of stiction measured may not represent the true peak friction between the surfaces of the pendulum and the disc. There was a 10 to 15 second delay between drying of the disc and the first friction measurements. During this period, the frictional forces may have been higher than those measured. Even so, the dramatic rise in the coefficient of stiction is clearly demonstrated. By modifying the method of placing the indentor on the disc, it may be possible to measure the friction within 5 to 10 seconds after drying. Time constraints prevented such a change being adopted in this work.

4.3.4 Impact loads and the coefficient of stiction

In 1971, Radin and Paul found that, in vitro, impact loads on hyaline cartilage resulted in an increase in friction during movement in intact joints. In their studies, they were able to demonstrate that the increased friction resulted in faster wear of the articular surfaces.

The TMJ disc separates the condyle and eminence, and therefore would receive impact loads due to blows to the mandible. It is unknown if impact loads have any effect on the stiction of the disc. In a series of tests, 3 pairs of discs were used to study the effect of 3 different magnitudes of impact load on the lubrication capability of the disc. In each disc pair, one disc was exposed to an impact load of known magnitude, while the other disc served as a control. Impact loads of known magnitude were delivered to the discs using a specially constructed apparatus. The apparatus was constructed in a manner so that a mass could be dropped from specified heights onto an acrylic indentor. The acrylic indentor rested on top of a TMJ disc. Strain gauges were luted to the indentor. These gauges made it possible to measure the shape and magnitude of the impulse delivered to the disc. The output from the gauges was connected to a storage oscilloscope for observation and measurement. From the oscilloscope screen, the impulse of each impact load was traced onto acetate. Analysis of the impulse involved determining the peak force and, by integration under the curve, the magnitude of the impulse in Newton-seconds.

The following steps were taken to expose the discs to impact loads and then measure for changes in $\mu_{stiction}$. Using the pendulum, an initial load was placed on each disc, and the time-dependent changes in stiction were measured. Each disc pair was checked for similar stiction characteristics. The discs were reimmersed in warmed saline for a period of one hour. Both discs were then removed from the saline bath, but only one disc was exposed to an impact load. The shape of the impulse due to the impact load was stored, and the discs were returned to the saline bath for a period of one hour. Each disc was then loaded with the pendulum, and the time-dependent changes in stiction were recorded.

The time-dependent changes in stiction by the experimental and control discs were plotted in the form seen in Figure 4.10a,b,c. As seen in this figure, the experimental discs which received impact gave greater stiction coefficients than the control discs. To help describe the relationship between lubrication and impact loads, two ratios were calculated. The first ratio, R_2, was the coefficient of stiction of the experimental disc at two minutes after loading, divided by the coefficient of stiction of the control disc at two minutes after loading.

$$R_2 = \frac{\mu_{stiction_{(impact)}}}{\mu_{stiction_{(control)}}}$$

This two minute stiction ratio was plotted with respect to magnitude of impact load. The results are presented in Figure 4.11a.

A second ratio was developed which was a measure of the increase of the coefficient of stiction of the experimental disc compared to the control disc. To calculate the ratio, the increase of the coefficient of stiction, $\Delta\mu_{stiction}$, was determined for both experimental and control disc for the time period between 1.5 minutes and 3 minutes after loading with the pendulum. The ratio, $R_{1.5}$, was then formed of $\Delta\mu_{stiction}$ (impact) and $\Delta\mu_{stiction}$ (control).

$$R_{1.5} = \frac{\Delta\mu_{stiction_{(impact)}}}{\Delta\mu_{stiction_{(control)}}}$$

The relationship between impact load and ratio of increase in stiction is seen in Figure 4.11b.

It was found that the larger the impulse of the impact load, the greater the increase of the two minute coefficient of stiction (Figure 4.11a). The rate of increase in stiction also reflected the energy delivered by the impact load (Figure 4.11b). The lowest impact load delivered to the discs was 0.64 Newton-seconds (N-sec.). Consequently, the exact nature of the effect of impact loads less than 0.64 N-Sec. is unknown. The data plotted in Figure 4.11a,b was presented in this form to help focus attention on the evidence that the point of inflection of both curves was between 0.40 and 0.60 N-Sec. This may indicate that there is a critical threshold of energy below which the disc remains unaffected by the impact load.

4.4. **Discussion**

4.4.1 Weeping lubrication by the TMJ disc

McCutchen's model of the weeping mechanism provided a means of developing simple experiments to test the mechanism of lubrication by the TMJ disc. The degree of hydration of the disc, and duration of surface drying resulted in changes in the lubrication by the disc. The results showed that in order for lubrication to occur, fluid had to move from of the deeper portions of the disc matrix to the articulating surface. Although the results of the experiments do not prove that weeping lubrication occurs on the surface of the TMJ disc, the results are consistent with the weeping lubrication hypothesis.

The amount of free fluid in the TMJ disc, like that of hyaline cartilage, is likely due to the concentration of proteoglycans in the disc. The suggestion that glycosaminoglycans are lost during thinning of the TMJ disc (Kopp, 1976) could possibly result in a reduction in lubrication properties of the disc. During the experiments it was noted that some of the pig discs displayed what was considered to be early signs of degeneration of the lateral portion of the disc. The signs included staining of the intermediate zone and anteroposterior ridging as opposed to the matte finish of the surface of a pristine disc. A less frequent finding was clefting between the intermediate zone of the disc and the posterior band. Discs which displayed these features of early degeneration showed a higher rate of rise in friction when compared to a healthy contralateral disc from the same animal. These observations should be followed up with a study of the histochemistry and ultrastructure to determine if these TMJ discs have characteristics typical of early degenerative disease. The pig may be a suitable model to study the natural development of degenerative changes of the disc and the effect on lubrication.

The experiments of this study did not attempt to determine to what degree the connective tissue of the eminence and condyle contribute fluid to the weeping mechanism. The fact that the tissues of the disc are thicker (Hansson _et al_., 1977) might indicate that the disc is the main fluid depot and source of weeping lubricant. Further study is required to examine the lubrication capacity of the connective tissue of the eminence and condyle. This is important, given the continued surgical practice of complete removal of the disc in cases of chronic anterior displacement. Remodelling of the displaced disc (Blaustein and Scapino, 1986) suggests that as long as some connective tissue remains between the condyle and eminence, the deformed disc may still perform a useful function.

4.4.2 Duration of loading and disc lubrication

The results of the friction experiments show the dramatic effect of duration of loading on the friction between the articulating surfaces. The longer the duration of loading, the greater the frictional forces between the sliding surfaces. It is not clear, however, if these experiments are representative of the time characteristics of lubrication _in vivo_. From chapter 2, the theoretical magnitudes of stress, _in vivo_, are higher than the experimental conditions using the pendulum to load the disc. The maximum load used in the friction experiments was 4 N, which was distributed over an estimated area of slightly less than 4 mm^2. This gives a plane stress of about 1 MPa, which is 2 to 3 times less than the general stresses calculated in adults (Figure 2.6). It is possible that the coefficient of stiction rises quicker, in vivo, due to the stress concentration. Experiments are required to examine the effect of a range of magnitudes of stress on the time-dependent changes in lubrication by the disc. It is likely that the most taxing of all condylar loads occurs during isometric function such as nocturnal asymmetric clenching and bruxing (Rugh and Ohrbach, 1988). During these periods of parafunction the contralateral condyle is protruded and loads against the crest of the eminence.

The results of increasing friction with duration of load is in keeping with Bell's (1982, p. 145) description of a phenomenon of sticking of the disc after a period of loading. However, this phenomenon is likely due to changes in the integrity of the disc and the ability to provide weeping lubricant rather than due to the nature of the lubrication properties of the synovial fluids. Linn and Radin (1968) have found that synovial fluids from osteoarthritic joints, in general, do not show a remarkable reduction in lubrication properties. Rather, as the present results show, the phenomenon is probably related to the integrity of the articular tissue. Damage to the fibrous component of the connective tissue will affect the rate of loss of fluid from the matrix. Proteoglycans may be moved away from areas where the damaged collagen is not able to form a stable net. The degree of hydration is compromised since there is no osmotic pressure to attract and hold water in the area. The consequence is a localized area which is not capable of supporting weeping lubrication.

4.4.3 Impact loads and TMJ disc lubrication

The structural integrity of the collagen fibres of the solid matrix of the disc appears to be essential for the operation of the weeping mechanism of lubrication. A gradation of matrix damage was produced by a series of impact loads of increasing energy. As demonstrated in Figure 4.11, there was a commensurate decrease in the ability of the disc to maintain a low coefficient of stiction as the energy of impact was increased. Trauma has often been implicated in the degeneration of the TMJ (Ogus, 79-80), although the mechanism by which trauma eventually leads to degenerative joint disease has never been determined. The immediate consequence of the trauma, that being increased frictional forces at the initiation of movement, would not be symptomatic. Usually there is recovery from the trauma with no apparent side effects. However, as noted by Weightman <u>et al</u>. (1973), fatigue failure due to increase in stress in the joint is a potent mechanism in producing degenerative changes in the articular tissues. In addition, the wear studies of Radin and Paul (1971) have shown that there is a relationship between an increase in sliding friction and wear of the articular surfaces. With respect to the TMJ disc, there is the possibility that increased friction on the surface of the disc may result in earlier development of fatigue of the articular surfaces. The finding that the discs, when tested under impact loading, displayed an immediate increase in coefficient of stiction and rate of increase in stiction was probably due to loss of integrity of the collagen fibres of the disc. It is unlikely that the disc had a sudden loss of proteoglycans which could account for the change in fluid available for lubrication. Lanir (1987) states that the resistance to fluid movement is due to the viscous interaction of the mobile fluid in the tissue with the collagen/proteoglycan portion of the cartilage matrix. The apparent viscosity is affected by the amount of fluid per unit volume of the disc. If the volume of fluid is greater, the fluid can move out of the tissue faster. By damaging the fibrous collagen net of the disc, more fluid is allowed into the disc. The amount of fluid that can enter the disc is normally limited by the balance of osmotic pressure with the swelling tension created in the fibres. Loss of fibre integrity allows for an increase in the amount of fluid per unit volume of the disc. In this manner, larger "pores" are created so that when compression of the disc occurs, the fluid is lost earlier and is not available to lubricate the surfaces. In this manner,the impact load might not create an obvious fracture of the disc, but does initiate the process leading to the eventual fatigue of the disc. The traumatic event that initiated the process is usually forgotten, but its legacy remains.

4.5 **Summary**

The longevity of the TMJ is dependent on the control of stresses in the joint. Normal or plane stresses occur due to functional loading. Tractional stresses are a result of friction and ploughing forces, which occur due to movement of surfaces over each other. In this chapter, it was shown that the TMJ disc is capable of controlling friction by lubricating the articulating surfaces. The efficacy of the lubrication was dependent on factors such as the duration of loading, degree of hydration of the disc, and the structural integrity of the disc. The evidence of increased friction due to reduced hydration is interesting because of reports that suggest that one of the signs of early degenerative joint disease is the loss of proteoglycans from the TMJ disc. The hydration of the disc is critically dependent on proteoglycan content. The loss of these macromolecules would result in a reduction in fluid content of the disc, and thus reduce the ability of the disc to lubricate. The effect of impact loads on the lubrication properties of the disc is also important. Impact loads to the mandible have been considered to be a likely cause of joint distress, but the evidence has not been clear because the onset of symptoms often follows many years after the traumatic event (Pullinger and Seligman, 1987). The loss of lubrication, without frank failure of the disc, indicates that a fatigue phenomenon may be responsible for the late onset of symptoms.

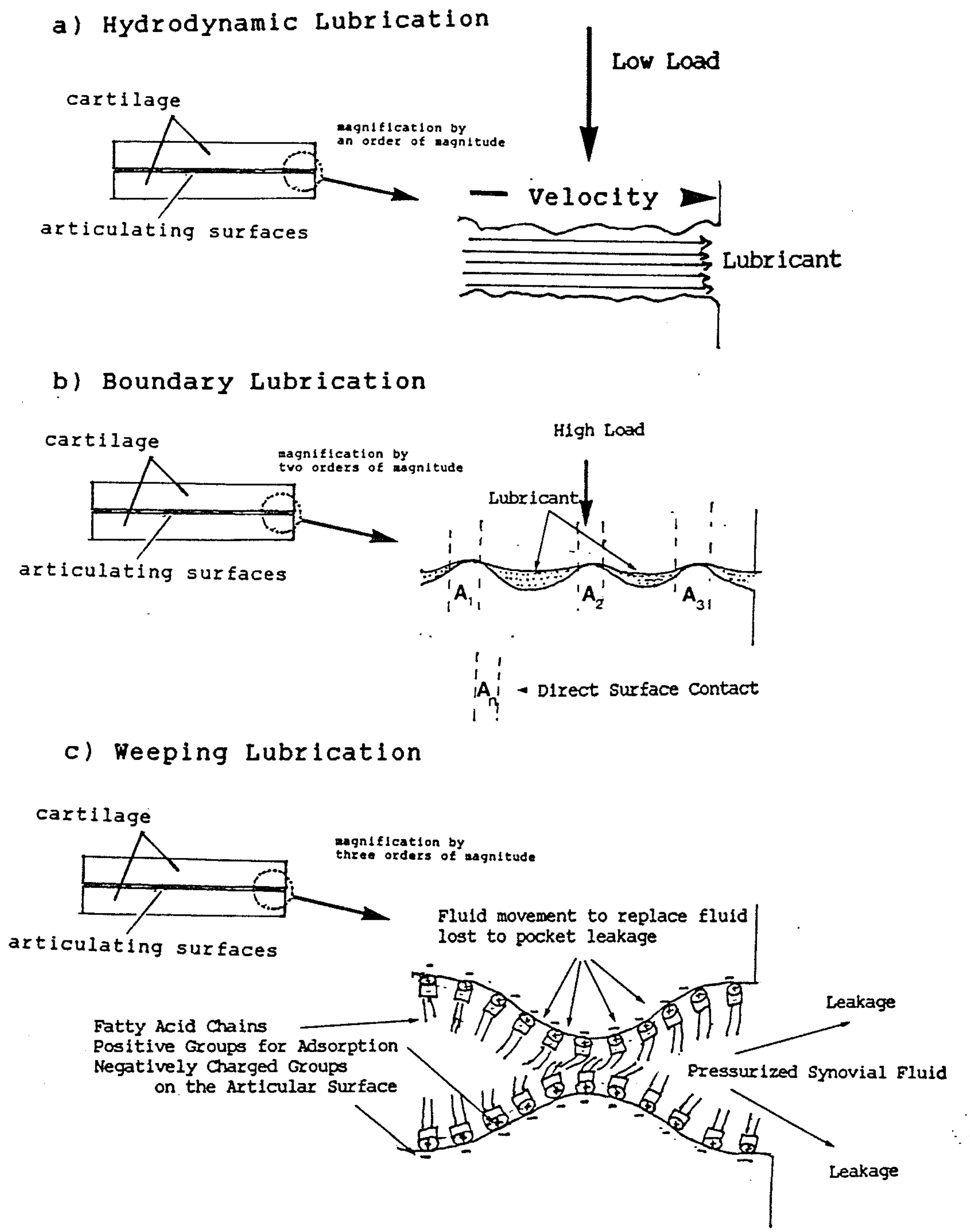

Figure 4.1 Various phenomena of lubrication: a) hydrodynamic lubrication, b) boundary lubrication, c) weeping lubrication

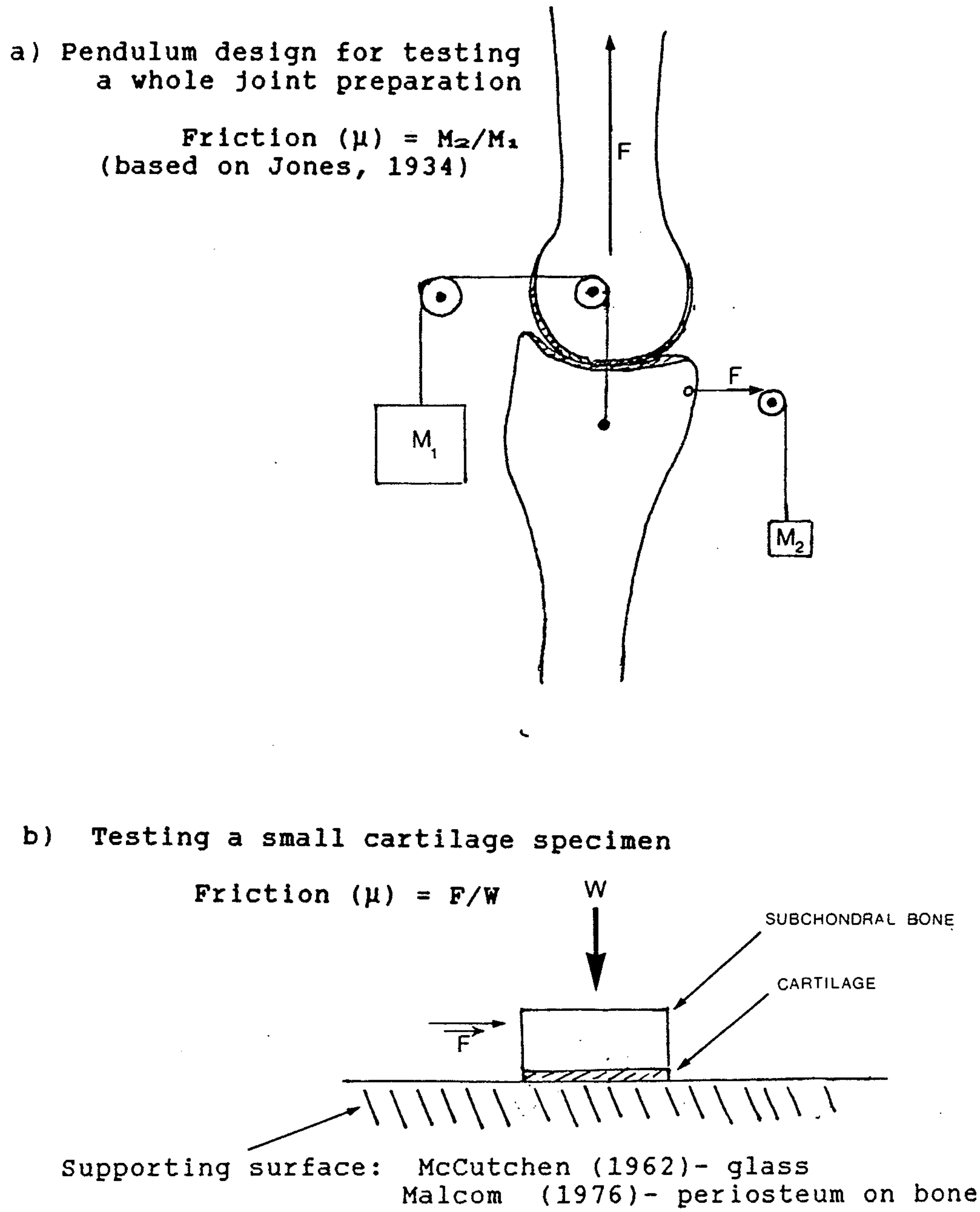

Figure 4.2 Common experimental designs for testing articular cartilage lubrication

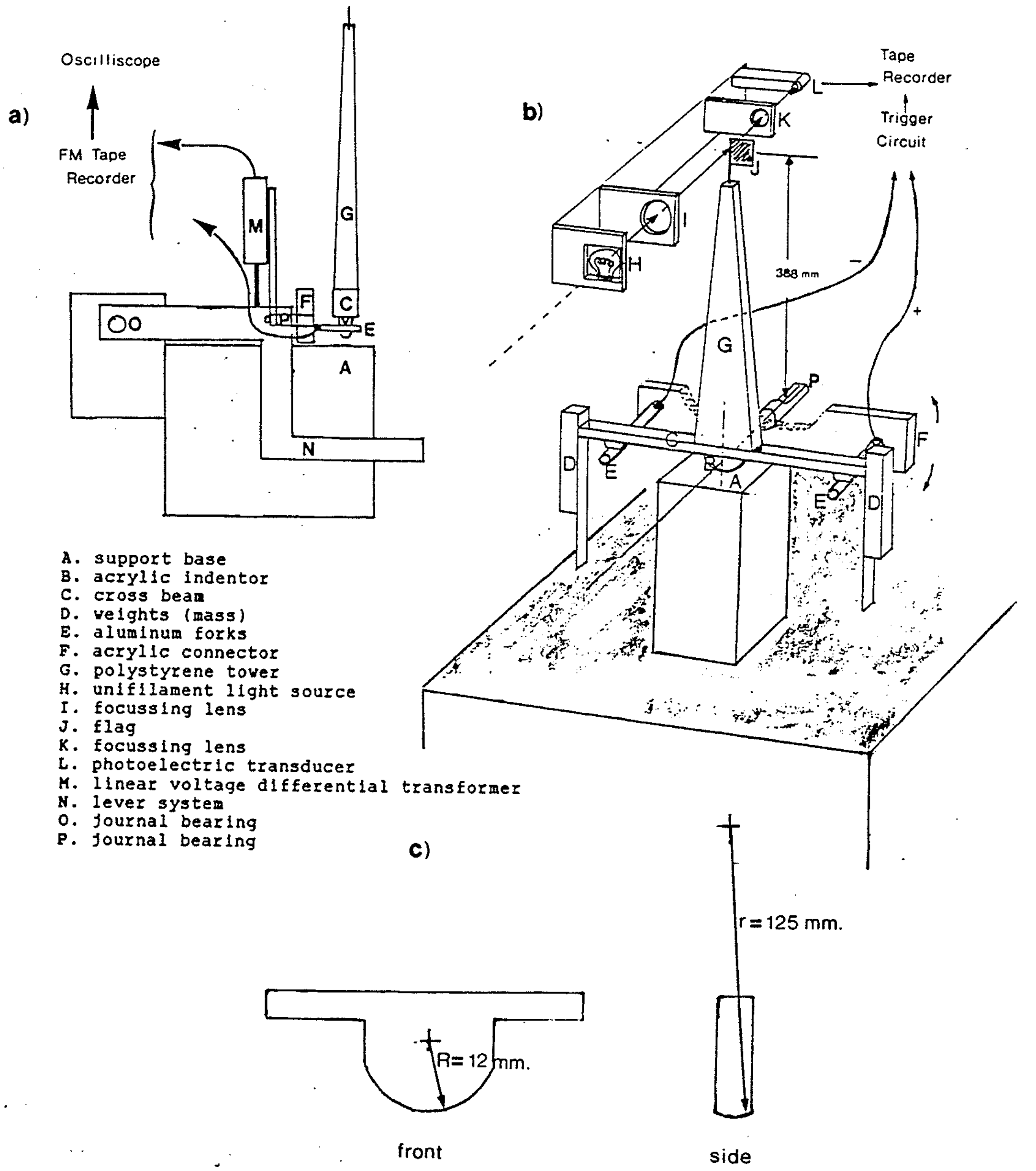

Figure 4.3 Sketches of the working components of the pendulum and optoelectric transducer: a) side view, b) oblique view without lever system, and c) indentor

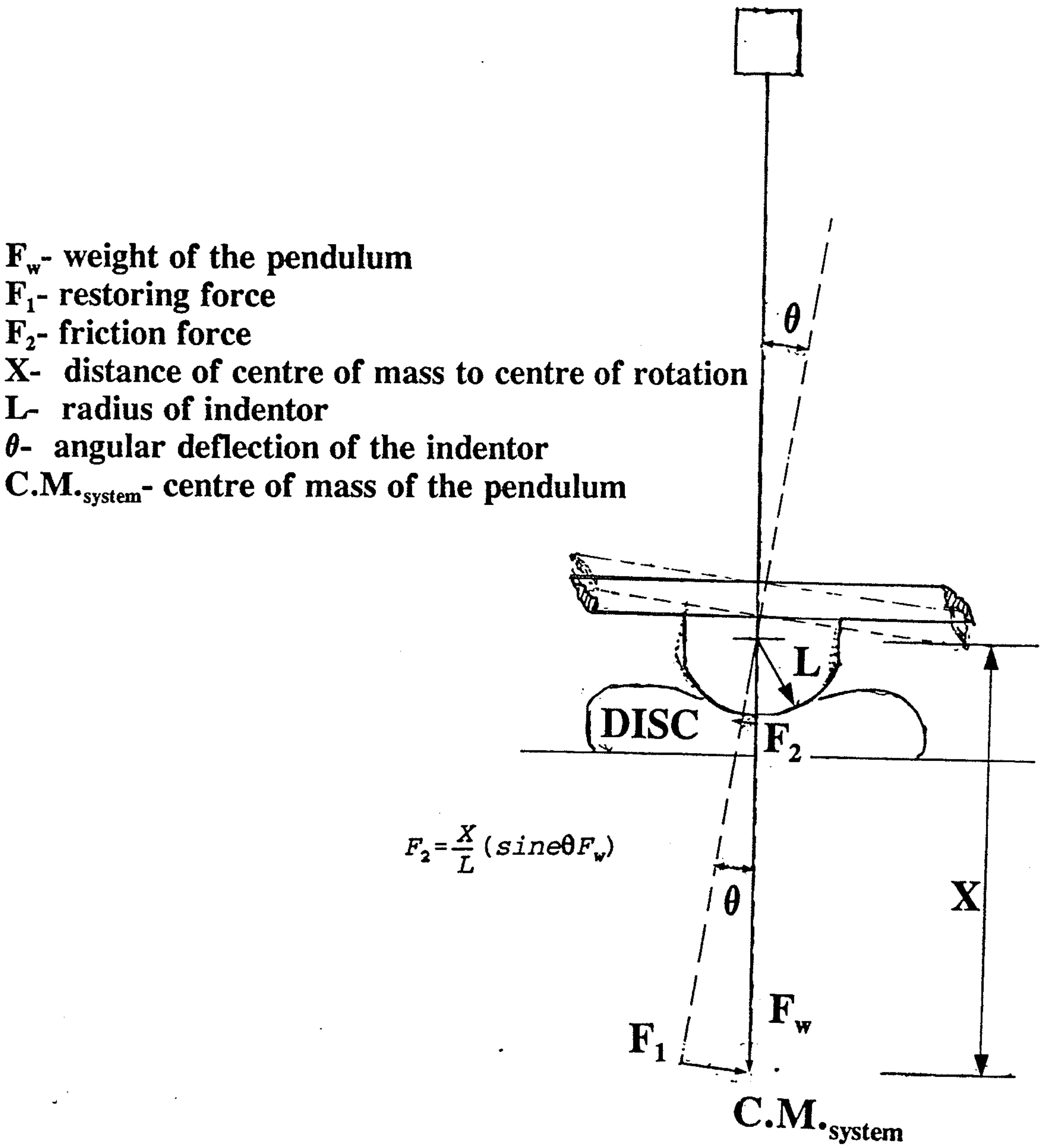

Figure 4.4 Geometry of the pendulum with an angular deflection

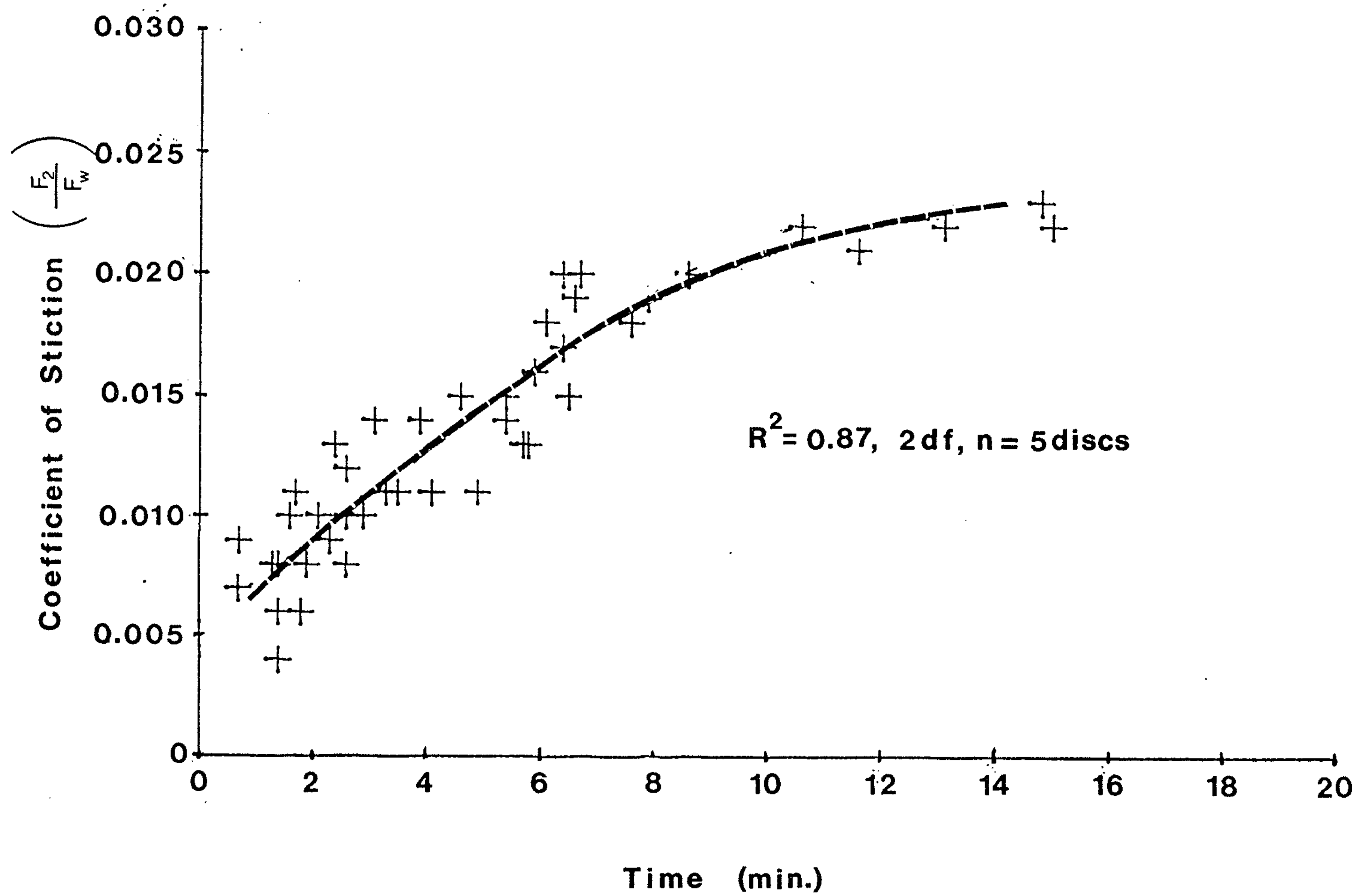

Figure 4.5 Coefficient of stiction vs. time: Five discs indicating the increase of stiction with respect to time

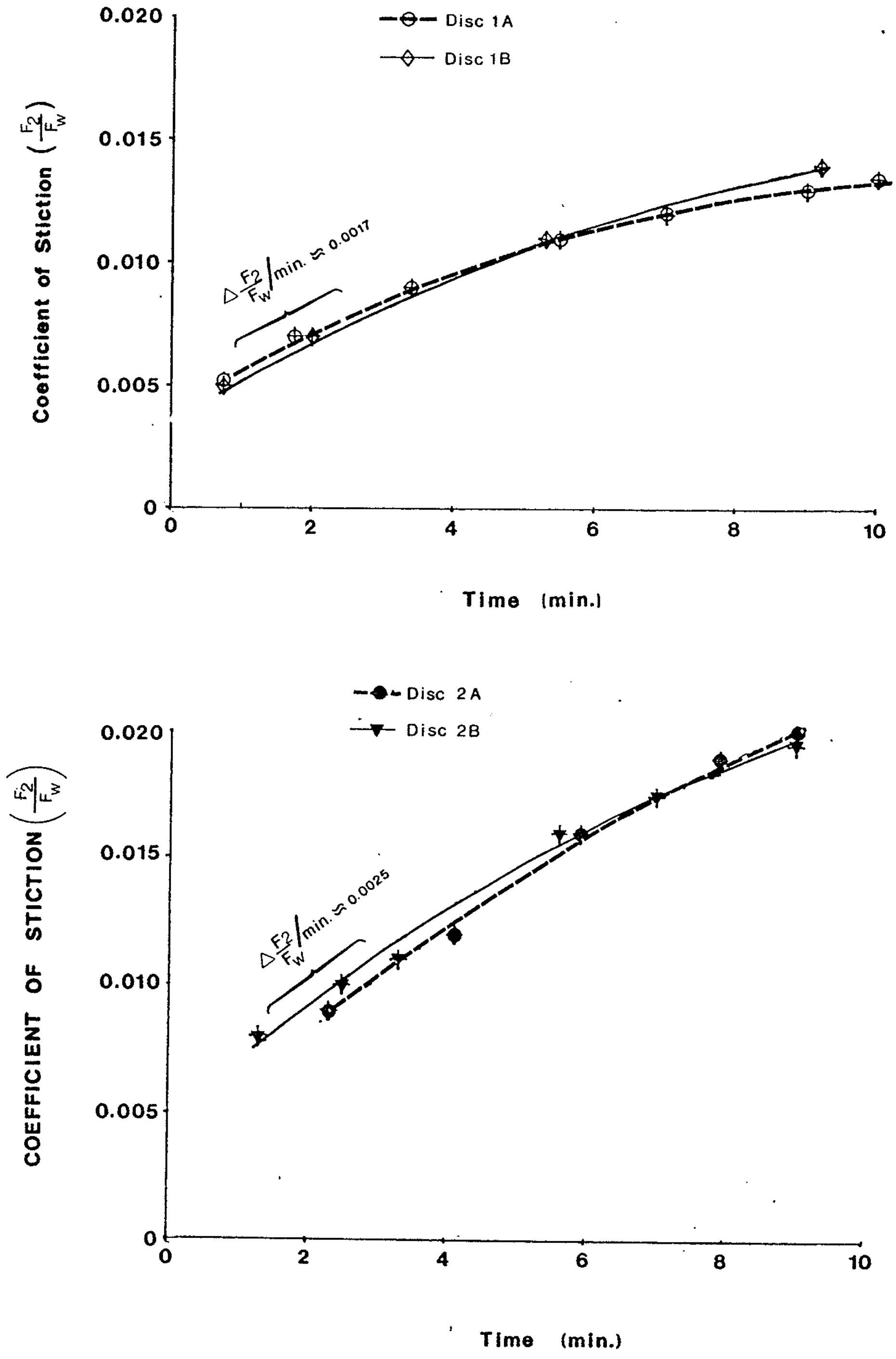

Figure 4.6 Coefficient of stiction vs. time: matched right/left discs which represent the extremes of the rate of increase of stiction per minute. Series 2, Discs 1A,B and 2A,B

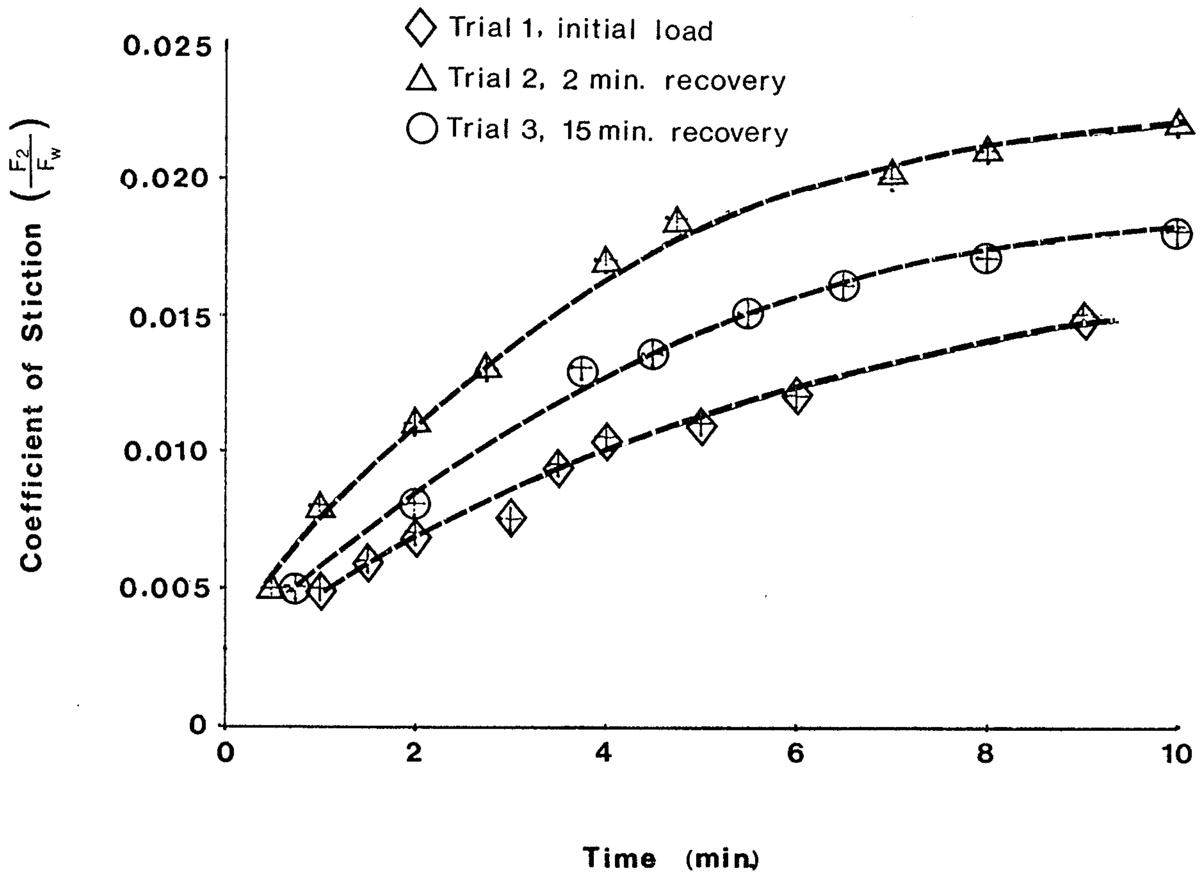

Figure 4.7 Coefficient of stiction vs. time: an example of the influence of hydration on stick-slip behaviour (Series 3, Disc 2B)

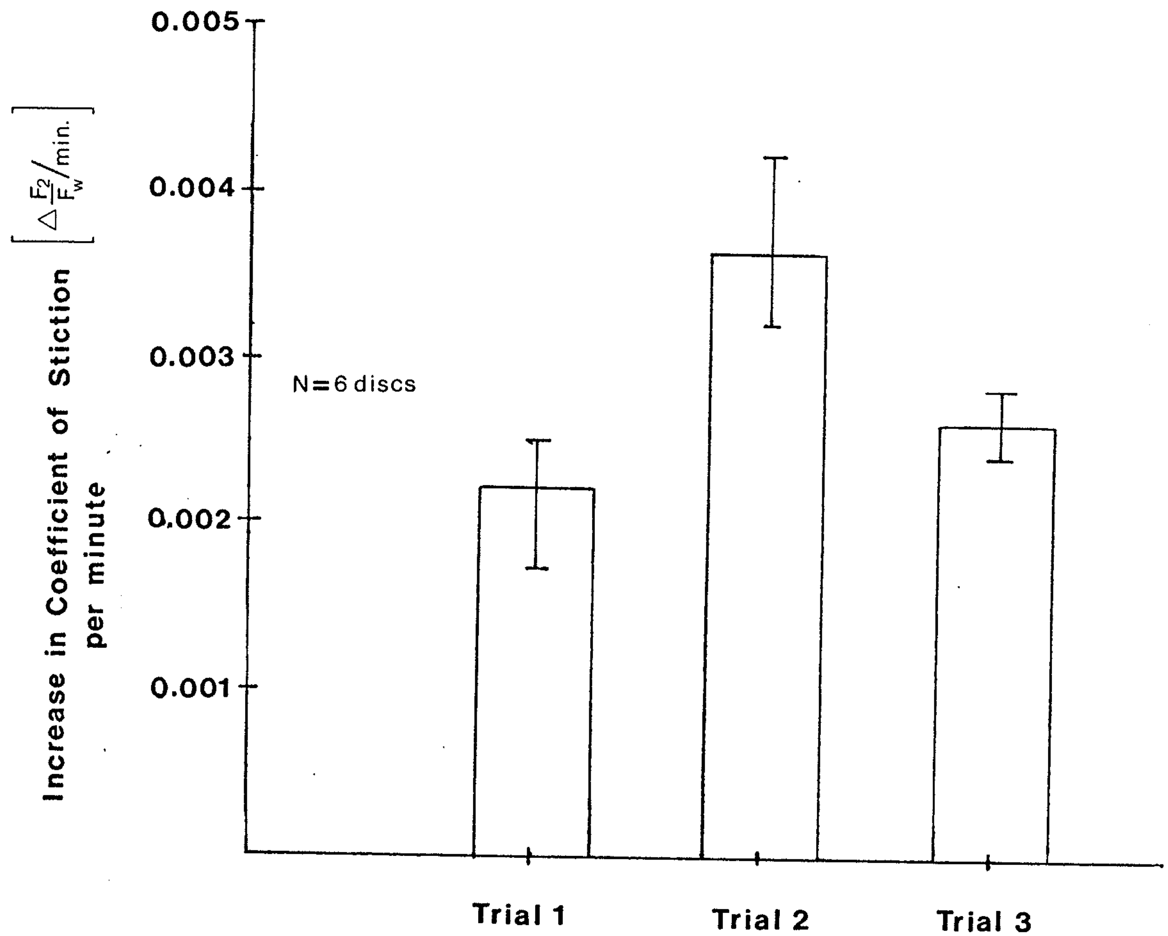

Figure 4.8 Rate of change of stiction vs. hydration time: Trial 1 (initial loading), Trial 2 (2 minute recovery time), Trial 3 (15 minute recovery time). Rate of change was determined for the period from 1 minute after loading to 4 minutes after loading.

a.)

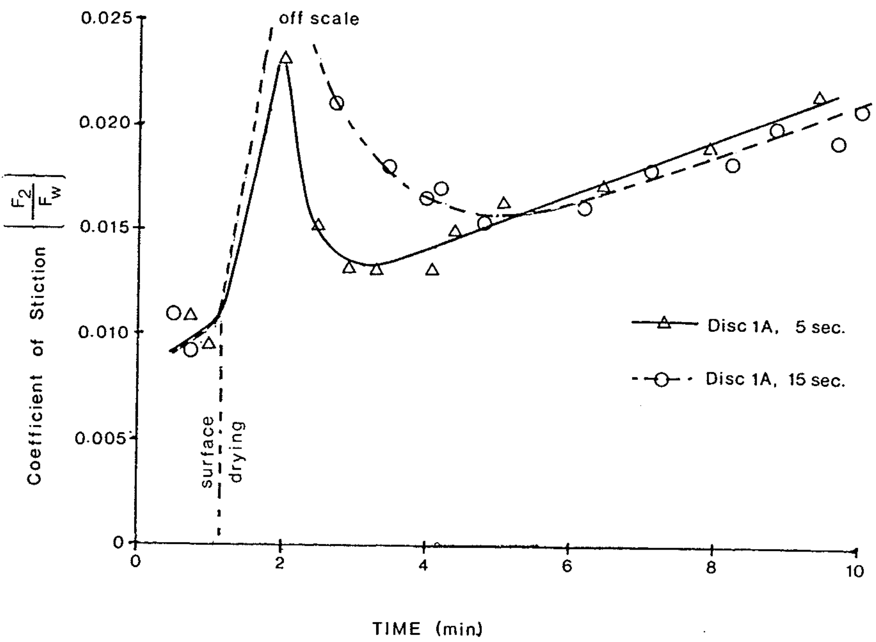

b.)

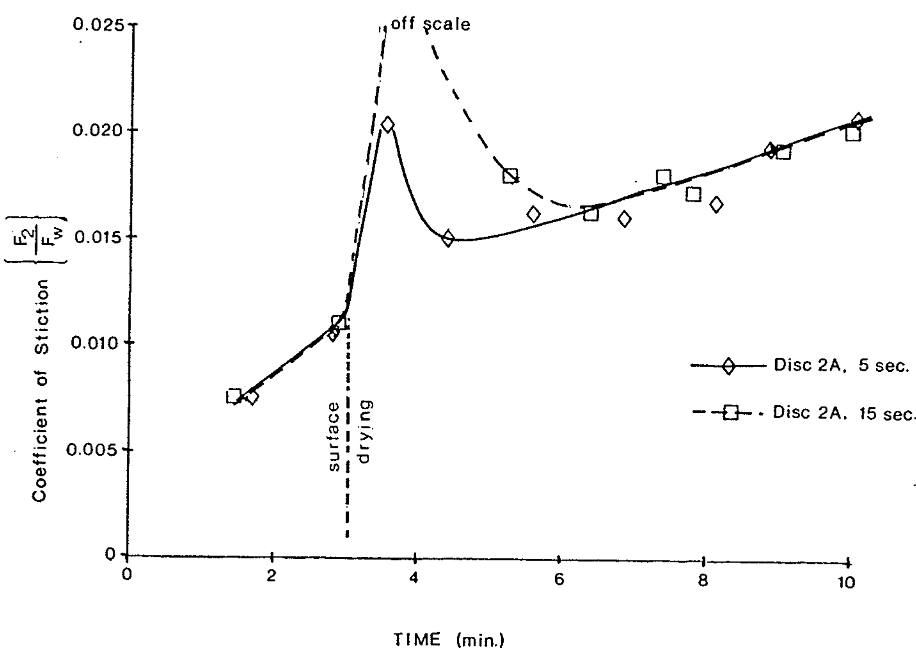

Figure 4.9 Coefficient of stiction vs. time: recovery of lubrication after surface drying (Series 4, Disc 1A and 2A)

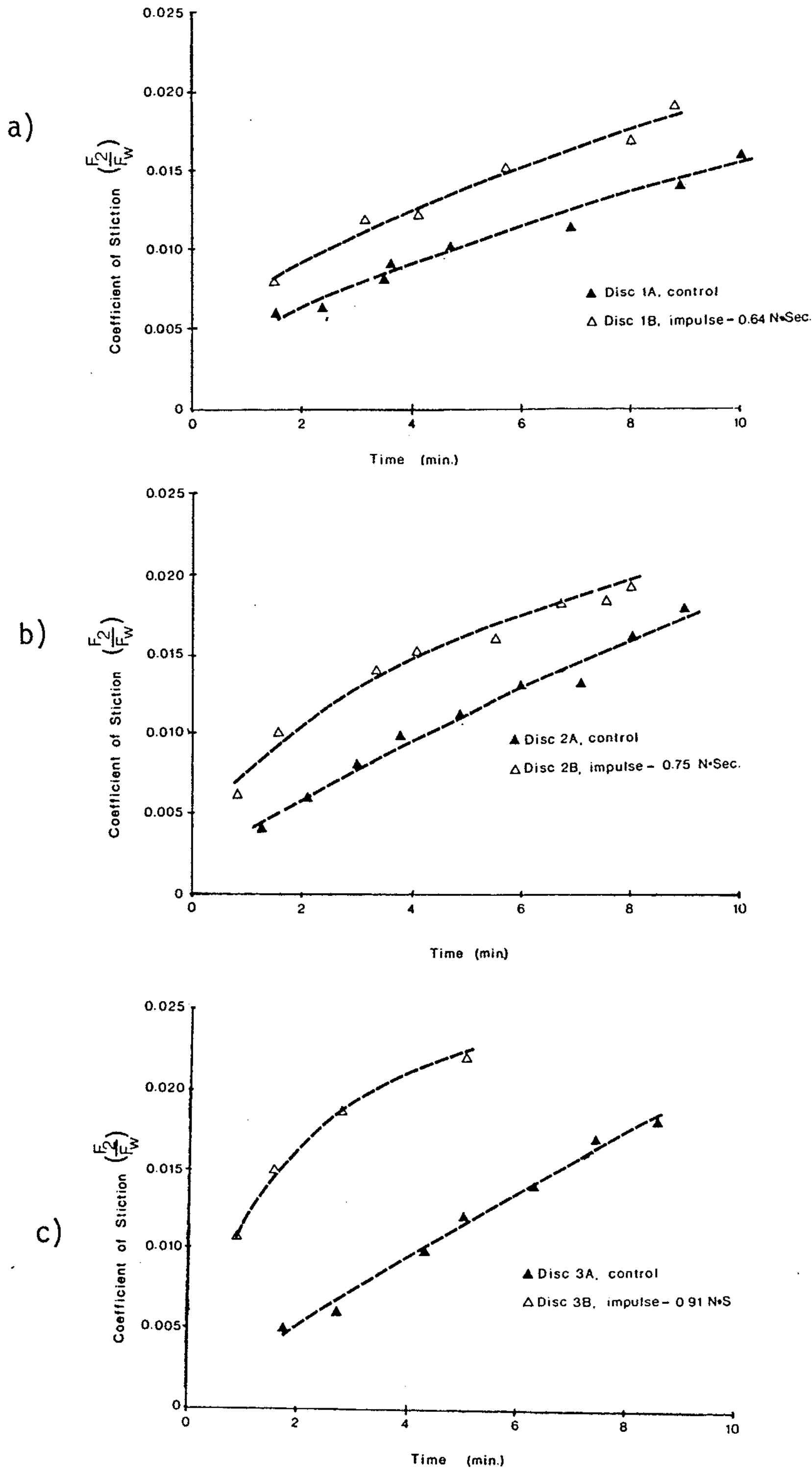

Figure 4.10 Coefficient of stiction vs. time: effect of three impulse loads- a) 0.64 N•Sec., b) 0.75 N•Sec., c) 0.91 N•Sec.

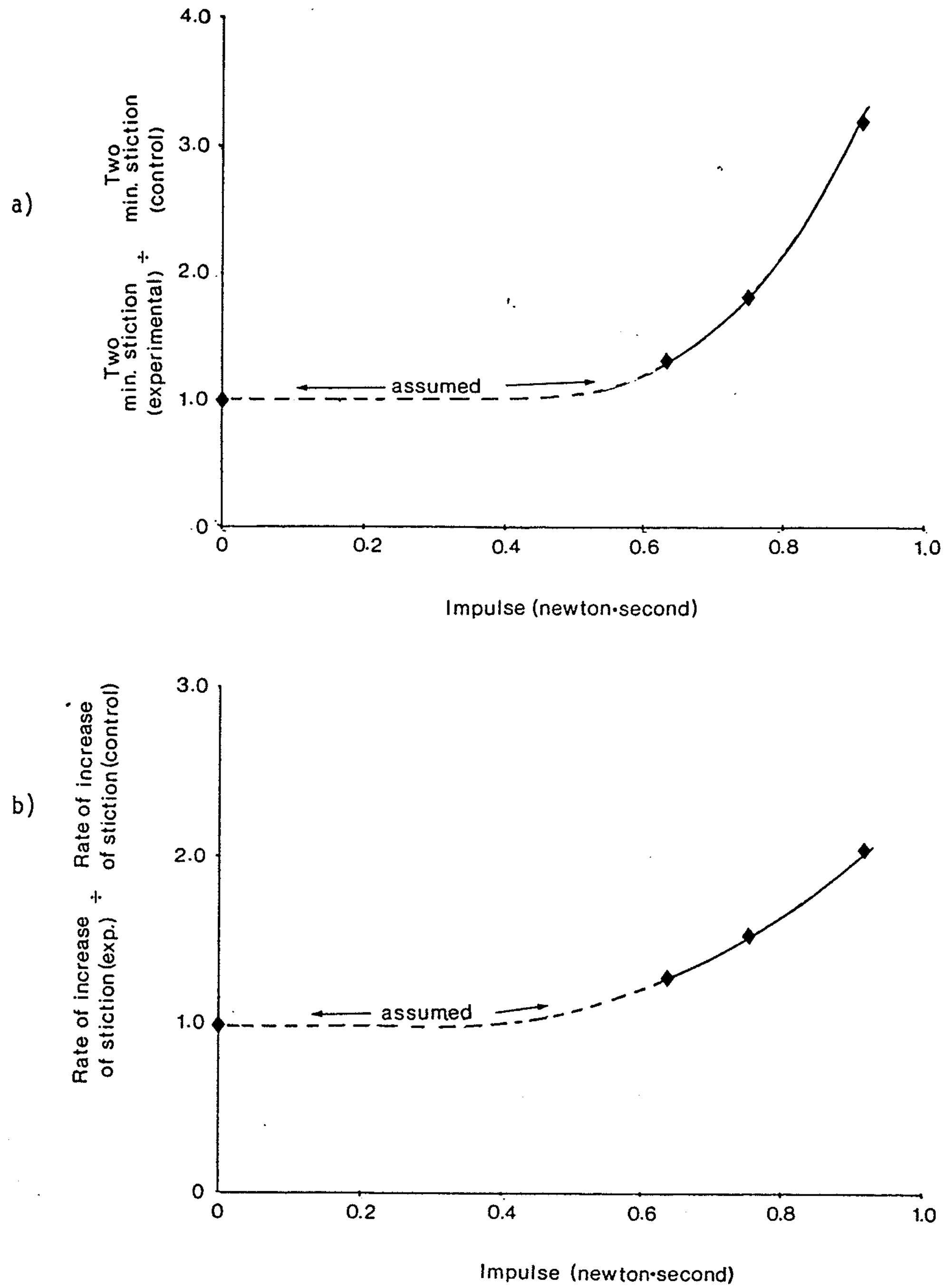

Figure 4.11 The relationship between impulse load and stiction: a) stiction ratio at two minutes, b) ratio of rates of increase of stiction between 1.5 and 3.0 minutes.

Chapter 5

Summary and Conclusions

A primary aim in studying stress in the TMJ was to identify various factors which influence the magnitudes of stresses in the TMJ. Mechanical stress has been considered to be a principal agent in the degeneration of articular cartilage. Extracapsular and intracapsular mechanisms are thought to prevent excessive stresses in the TMJ.

In the present study, several factors were examined to determine if their presence was influential in reducing plane, tensile and shear stresses in the TMJ. The factors included the general growth of the loading surface of the condyle and the degree of congruity of the hard surfaces of the condyle and articulating surface of the temporal bone. As well, the capacity of the disc to act as a load distributing mechanism and source of lubrication was explored.

In chapter 2, the results of a theoretical analysis showed that the general stresses in the TMJ are of the same magnitude as the general stresses in other synovial joints. It was shown that from birth, there was an age-dependent increase in general stress which was a consequence of increases in isometric bite force during the growing years of the child. However, the increase in the bite force was 6 to 8 times the increase in the general stresses in the joint.

Factors such as general growth of the size of the loading surface of the condyle, combined with minimization of condylar loads, prevented the stresses in the joint from increasing as quickly as the age-related increases in the bite force. However, evidence was presented in chapter 2 which suggested that the growth of the chondroid bone of the eminence produced incongruent loading surfaces in the protruded biting position. The growth mechanism of the eminence produces incongruity between the osseous surfaces of the condyle and eminence. This incongruity was shown to be most frequent at the crest of the eminence.

The evidence of surface incongruity in the joint meant that unless the TMJ disc was capable of distributing loads over incongruent surfaces, stress concentration would result. This would probably lead to early degeneration of the crest of the eminence. Experimental techniques were developed, as described in chapter 3, which measured the load distribution by the disc during loading between incongruent hard surfaces. The results showed that the disc was not remarkable in its stress distribution characteristics. Stress distribution by the disc was similar that of silicone rubber. The ability of the disc to distribute loads was dependent on the thickness of the disc. Thinner discs were not able to distribute loads nearly as well as thicker discs. The stresses measured under thinner discs were much larger than stresses measured under discs of average thickness. Although the disc does not prevent stress concentration on the surfaces of the condyle and eminence, the disc is much better than hard tissue contact and better than current alloplastic materials

In addition to information on the effects of general thinning of the disc, the results of chapter 3 also showed a mechanism which may produce aberrant condylar morphologies. It was found that localized damage of the disc caused by stress concentration produces an alteration in the general stress distribution profile of the disc. Most notably, there were changes in localized areas where stress was significantly reduced. It is proposed that these local areas provide an environment suitable for chondroblastic proliferation of the surface of the condyle. This proliferation may eventually produce the unusual changes in condylar morphology as reported in the literature.

The evaluation of the stresses in the TMJ included a study of the frictional forces which occur due to sliding between articulating surfaces. In a series of experiments, it was established that the TMJ disc is a potent mechanism of attenuating friction forces during the start up of movement. The major lubricating mechanism of the disc appears to be produced by a "weeping" of lubricating fluid to the surface of the disc from the deeper portions of the loaded disc. Two variables, namely hydration and trauma, were studied to determine the effect on friction by the lubrication provided by the disc. As shown in chapter 4, the degree of hydration of the TMJ disc affected the frictional characteristics of the surfaces. There was a faster rate of rise of the friction on the surface of the disc when there was less fluid available for lubrication. Traumatic injury of the disc was produced by using an impact loading device. It was shown that for an increase in the energy of an impact load, there was a commensurate increase in friction on the disc surface. The decreased ability of the disc to lubricate the articulating surfaces was probably due to damage to the collagen fibres of the disc.

Overall, the results support the premise that specific factors, such as growth of the joint and the presence of an intracapsular fibrous disc, favourably influence the load distribution in the joint. The presence of the TMJ disc also reduces the frictional forces produced during the initiation of movement between the articular surfaces. As well, the neuromuscular system of the growing child is able to minimize joint loads and thus prevent an accelerated increase in loads with age-related increases in bite force. However, conditions exist in which these mechanisms are compromised and there is a consequent increase in the stresses in the TMJ. The results of this theoretical and experimental study support the hypothesis that stress control in the TMJ is unstable because the aforementioned mechanisms are limited to indirectly influencing stress in the joint. There is a lack of neural receptors which could directly monitor magnitudes of stress in the articular tissues of the joint.

CONCLUSIONS

This study evaluated several factors which were thought to influence the magnitude of mechanical stresses in the TMJ. It is concluded that:

1. During isometric biting, the general stresses in the TMJ are of the same magnitude as reported for limb joints.

2. Incongruity between osseous surfaces in the TMJ creates local stresses which are approximately 2 to 3 times the magnitude of the general stresses.

3. Incongruities between joint surfaces occurred more frequently at the crest of the eminence of the TMJ.

4. Although the TMJ disc does distribute loads, for the conditions tested, it is not substantially better than silicone rubber.

5. Load distribution by the TMJ disc is dependent on the thickness of the disc.

6. Stress concentration on the disc results in changes in the average load distribution properties of the disc.

7. The TMJ disc has very low surface friction at the start of loading, but as the duration of loading continues, the friction increases.

8. The very low surface friction of the disc appears to be due to a weeping mechanism of lubrication which is sensitive to the degree of hydration of the disc.

9. Trauma to the surface of the TMJ disc results in an increase in the surface friction.

BIBLIOGRAPHY

Adams, D.; Kempson, G.E.; and Swanson, S.A.V. (1978) Direct measurement of local pressures in the cadaveric human hip joint, Med Biol Eng Compt 16: 113-115.

Ahmed, A.M.; Burke, D.L.; Tencer, A.; and Miller, J. (1977) In vitro measurement of pressure distribution at articular interfaces of synovial joints, In: Proceedings of the Society for Biomaterials, 3rd annual meeting, volume 1, Society for Biomaterials, p. 74.

Ahmed, A.M.; and Burke, D.L. (1983) In-vitro measurement of static pressure distribution in synovial joints- Part 1: Tibial surface of the knee, J Biomech Eng 105: 216-225.

Appenteng, K.; Conyers, L.; and Moore, J.A. (1989) The monosynaptic excitatory connections of single trigeminal interneurons to the V motor nucleus of the rat, J Physiol (London) 417: 91-104.

Appenteng, K.; Conyers, L.; Curtis, J.; and Moore, J. (1990) Monosynaptic connexions of single V interneurones to the contralateral V motor nucleus in anaesthetized rats, Brain Res 514: 128-130.

Armstrong, C.G; Lai, W.M.; and Mow, V.C. (1984) An analysis of the unconfined compression of articular cartilage, J Biomech Eng 106: 165-173.

Armstrong, C.G. (1986) An analysis of the stresses in a thin layer of articular cartilage in a synovial joint, Eng Med 15: 55-61.

Aspden, R.M. (1985) A model for the function and failure of the meniscus, Eng Med 14: 119-122.

Aspden, R.M. (1986) Relation between structure and mechanical behaviour of fibre-reinforced composite materials at large strains, Proc R Soc Lond A. 404: 287-298.

Bell, W.E. (1982) Clinical Management of Temporomandibular Disorders, Chicago: Year Book Medical Publishers, Inc.

Berman, D.N.; and Bronstein, S.L. (1990) Osteophytic reaction to a polytetrafluoroethylene temporomandibular joint implant: a report of a case, Oral Surg Oral Med Oral Pathol 69: 20-23.

Bhussry, B.R. (1976) Temporomandibular joint, In: Orban's Oral Histology and Embryology, 8th edition, S.N. Bhaskar, Ed., St. Louis: C.V. Mosby Company, pp. 395-404.

Blanksma, N.G.; and van Eijden, T.M.G.J. (1990) Electromyographic heterogeneity in the human temporalis muscle, J Dent Res 69: 1686-1690.

Blaustein, D.I. and Scapino, R.P. (1986) Remodelling of the temporomandibular joint disc and posterior attachment in disk displacement specimens in relation to glycosaminoglycan content, Plast Reconstr Surg 78: 756-764.

Bowden, F.P. and Tabor, D. (1950) The Friction and Lubrication of Solids, London: Oxford University Press, pp. 165-166.

Brehnan, K.; Boyd, R.L.; Laskin, J.; Gibbs, C.H.; and Mahan, P. (1981) Direct measurement of loads at the temporomandibular joint in Macaca actoides, J Dent Res 60: 1820-1824.

Brinckmann, P.; Frobin, W.; and Hierholzer, E. (1981) Stress on the articular surface of the hip joint in healthy adults and persons with idiopathic osteoarthrosis of the hip joint, J Biomech 14: 149-156.

Brown, T.D.; and Ferguson, A.B. (1980) The effects of hip contact abberations on stress patterns within the human femoral head, Ann Biomed Eng 8: 75-92.

Brown, T.D.; and Shaw, D.T. (1982) A technique for measuring instantaneous in vitro contact stress distributions in articular joints, J Biomech 15: 329-333.

Brown, T.D.; and Shaw, D.T. (1983) In vitro contact stress distributions in the natural human hip, J Biomech 16: 373-384.

Bullough, P.G.; Munuera, L.; Murphy, J.; and Weinstein, A.M. (1970) The strength of the menisci of the knee as it relates to their fine structure, J Bone Joint Surg 52-B: 564-570.

Carlson, D.S.; McNamara, J.A.; and Ribbens, K.A. (1985) Developmental Aspects of Temporomandibular Joint Disorders, Monograph #16, Craniofacial Growth Series, Centre for Human Growth and Development, University of Michigan, Ann Arbor, Michigan.

Carlsson, G.E.; and Oberg, T. (1974) Remodelling of the temporomandibular joints, Oral Sci Rev 6: 53-86.

Charnley, J. (1959) The lubrication of animal joints, In: Symposium on Biomechanics, London: Institute of Mechanical Engineers, pp. 12-22.

Christel, P.; Derethe, P.; and Sedel, L. (1976) Mesure par simulation de l'amortissement d'une haunche normale et prosthesee, Acta Orthop Belg 42 (suppl I): 183-193.

Christen, A. (1959) Die faserstruktur des discus temporomandibularis, Z Anat Entwickl Gesh 121: 322-336.

Clarke, I.C.; Contini, R.; and Kenedi, R.M. (1975) Friction and wear studies of articular cartilage: a scanning electron microscope study, J Lubr Tech 97: 358-368.

Copray, J.C.V.M.; Jansen, H.W.B.; and Duterloo, H.S. (1983) Growth of the mandibular condylar cartilage of the rat in serum-free organ culture, Arch Oral Biol 28: 967-974.

Copray, J.C.V.M.; Jansen, H.W.B.; and Duterloo, H.S. (1985a) Effects of compressive forces on proliferation and matrix synthesis in mandibular condylar cartilage of the rat in vitro, Arch Oral Biol 30: 299-304.

Copray, J.C.V.M.; Jansen, H.W.B.; and Duterloo, H.S. (1985b) The role of biomechanical factors in mandibular condylar cartilage growth and remodelling in vitro, In: Developmental Aspects of Temporomandibular Joint Disorders, D.S. Carlson, J.A. McNamara, and K.A. Ribbens, Eds., Monograph #16, Craniofacial Growth Series, Centre for Human Growth and Development, University of Michigan, Ann Arbor, Michigan, pp. 235-269.

Copray, J.C.V.M.; Jansen, H.W.B.; and Duterloo, H.S. (1985c) Effect of compressive forces on phosphatase activity in mandibular condylar cartilage of the rat in vitro, J Anat 140: 479-489.

Copray, J.C.V.M.; Jansen, H.W.B.; and Duterloo, H.S. (1985d) An in-vitro system for studying the effect of variable compressive forces on the mandibular condylar cartilage of the rat, Arch Oral Biol 30: 305-311.

Couly, G. and Vaillant, J.M. (1975) Les menisques temporo-mandibulaires, Rev Stomatol 76: 303-310.

Crompton, A.W. (1963) On the lower jaw of Diarthrognathus and the origin of the mammalian lower jaw, Proc Zool Soc Lond 140: 697-749.

Day, W.H.; Swanson, S.A.V.; and Freeman, M.A.R. (1975) Contact pressures in the loaded human cadaver hip, J Bone Joint Surg 57-B: 302-313.

de Bont, L.G.M. (1985a) Spatial arrangement of collagen fibrils in the articular cartilage of the mandibular condyle: a light microscopic and scanning electron microscopic study, Chapter 3, Ph.D. Dissertation, University of Groningen, The Netherlands. pp. 9-16.

de Bont, L.G.M. (1985b) Osteoarthritis of the temporomandibular joint: a light microscopic and scanning electron microscopic study of the articular cartilage of the mandibular condyle, Chapter 5, Ph.D. Dissertation, University of Groningen, The Netherlands. pp. 23-30.

de Bont, L.G.M. (1985c) Ultrastructure of the articular cartilage of the mandibular condyle: ageing and degeneration, Chapter 6, Ph.D. Dissertation, University of Groningen, The Netherlands. pp. 31-42.

de Bont, L.G.M. (1985d) Osteoarthrosis and internal derangement of the temporomandibular joint: a light microscopic study, Chapter 7, Ph.D. Dissertation, University of Groningen, The Netherlands. pp. 43-54.

Dixon, D.C.; Kull, R.S.; and McCall, W.D. (1990) Effect of bite force and bite position on jaw muscle activity: tests of models, J Dent Res 68 (special issue): 319.

Findlay, I.A. (1964) Mandibular joint pressures, J Dent Res 43: 140-148.

Flinn, R.A.; and Trojan, P.K. (1981) Engineering Materials and Their Application, Boston: Houghton Mifflin Company.

Fontenot, M.G. (1985) Viscoelastic properties of human TMJ discs and disc replacement materials, J Dent Res 64 (special issue): 163.

Frisna, W.; and Lehneis, H.R. (1970) Pressure mapping: a preliminary report, J Biomech 3: 526.

Fukubayashi, T.; and Kurosawa, H. (1980) The contact area and pressure distribution pattern of the knee- a study of normal and osteoarthritic knee joints, Acta Orthop Scand 51: 871-879.

Gerber, A. and Steinhardt, G. (1990) Dental Occlusion and the Temporomandibular Joint, Chicago: Quintessence Publ. Co.

Gillbe, G.V. (1975) The function of the disc of the temporomandibular joint, J Prosthet Dent 33: 196-204.

Graf, H.; Grassl, H.; and Aeberhard, H-J. (1974) A method for measurement of occlusal forces in three directions, Helv Odontol Acta 18: 7-11.

Granstrom, G.; and Linde, A. (1973) Glycosaminoglycans of temporomandibular articular discs, Scand J Dent Res 81: 462-466.

Greenwald, A.S.; and Haynes, D.W. (1972) Weight-bearing areas in the human hip joint, J Bone Joint Surg 54-B: 157-163.

Greenwald, A.S.; and O'Connor, J.J. (1971) The transmission of load through the human hip joint, J Biomech 4: 507-528.

Grodzinsky, A.J.; Roth, V.; Myers, E.R.; Grossman, W.D.; and Mow, V.C. (1981) The significance of electromechanical and osmotic forces in the non-equilibrium swelling behaviour of articular cartilage in tension, J Biomech Eng 103: 221-231.

Hansson, T.; and Nordstrom, B. (1977) Thickness of the soft tissue layers and articular disk in temporomandibular joints with deviation in form, Acta Odontol Scand 35: 281-288.

Hansson, T. and Oberg, T. (1977) Arthosis and deviation in form in the temporomandibular joint: a macroscopic study on a human autopsy material, Acta Odontol Scand 35: 167-174.

Hansson, T; Oberg, T.; Carlsson, G.; and Kopp, S. (1977) Thickness of the soft tissue layers and the articular disk in the temporomandibular joint, Acta Odontol Scand 35: 77-83.

Harrigan, T.P.; and Mann, R.W. (1987) State variables for modelling physical aspects of articular cartilage, J Solids Struct 23: 1205-1218.

Hasty, K.A.; Smith, G.N.; and Kang, A.H. (1983) Histochemical identification of sulfation position in chondroitin sulfate in various cartilages, J Histochem Cytochem 31: 1367-1374.

Hayes, W.C.; Keer, L.M.; Herrmann, G.; and Mockros, L.F. (1972) A mathematical analysis for indentation tests of articular cartilage, J Biomech 5: 541-551.

Herring, S.W. (1976) The dynamics of mastication in pigs, Arch Oral Biol 21: 473-480.

Hills, B.A. **(1989)** Oligolamellar lubrication of joints by surface active phospholipid, J Rheumatol 16: 82-91.

Hills, B.A. and Butler, B.D. **(1984)** Surfactants identified in synovial fluid and their ability to act as boundary lubricants, Ann Rheum Dis 43: 641-648.

Hirschmann, P.N.; and Shuttleworth, C.A. **(1976)** The collagen composition of the mandibular joint of the foetal calf, Arch Oral Biol 21: 771-773.

Hodge, W.A.; Fijan, R.S.; Carlson, K.L.; Burgess, R.G.; Harris, W.H.; and Mann, R.W. **(1986)** Contact pressures in the human hip measured in vivo, Proc Natl Acad Sci (U.S.A.) 83: 2879-2883.

Howell, A.H.; and Manly, R.S. **(1948)** An electronic strain gauge for measuring oral forces, J Dent Res 27: 705-712.

Ingelmark, B.E.; and Blomgren, E. **(1947)** An apparatus for the measurement of pressures, especially in human joints, Upsala Lakar Forhandl 53: 75-94.

Irby, W.B.; and Zetz, M.R. **(1983)** Osteoarthritis and rheumatoid arthritis affecting the temporomandibular joint, In: The President's Conference on the Examination, Diagnosis and Management of Temporomandibular Disorders, D. Laskin, Ed., Chicago: American Dental Association, pp. 106-111.

Isacsson, G.; and Isberg, A.M. **(1985)** Tissue identification of the TMJ disk and disk attachments and related vascularization, J Craniomandibular Pract 3: 374-379.

Jimenez, I.D. **(1985)** Electromyography of masticatory muscles during isometric contractions in three mandibular registration positions, M.Sc. Thesis, University of Manitoba, Winnipeg, Canada.

Jones, E.S. **(1934)** Joint lubrication, Lancet 1: 1426-1427.

Kettlekamp, D.B.; and Jacobs, A.W. **(1972)** Tibiofemoral contact areas- determination and complications, J Bone Joint Surg 54-A: 349-356.

Knox, J. **(1967)** Fibrillar arrangement in the articular disk of the human temporomandibular joint, Thesis, University of Illinois.

Kopp, S. **(1976)** Topographical distribution of sulphated glycosaminoglycans in human temporomandibular joint disks. A histochemical study of an autopsy material, J Oral Pathol 5: 265-276.

Kopp, S. (1978) Topographical distribution of sulfated glycosaminoglycans in the surface layers of the human temporomandibular joint. A histochemical study of an autopsy material, J Oral Pathol 7: 283-294.

Lanir, Y. (1987) Biorheology and fluid flux in swelling tissues- II. Analysis of unconfined compression response of transversely isotropic cartilage disc, Biorheology 24: 189-205.

Linn, F.C. (1967) Lubrication of animal joints. I. The anthrotripsometer, J Bone Joint Surg 49-A: 1079-1098.

Linn, F.C. and Radin, E.L. (1968) Lubrication of animal joints. III. The effect of certain chemical alterations of the cartilage and lubricant, Arthritis Rheum 11: 674-682.

Lund, J.P.; and Lamarre, Y. (1973) The importance of positive feedback from periodontal pressoreceptors during voluntary isometric contraction of the jaw closing muscles in man, J Biol Buccale 1: 345-351.

Lundgren, D.; and Laurell, L. (1986) Occlusal force pattern during chewing and biting in dentitions restored with fixed bridges of cross-arch extensions. I. Bilateral end abutments, J Oral Rehabil 13: 57-71.

Lunt, R.C.; and Law, D.B. (1974) A review of the chronology of the eruption of deciduous teeth, J Am Dent Assoc 89: 872-879.

Malcom, L.L. (1976) An experimental investigation of the frictional and deformational responses of articular cartilage interfaces to static and dynamic loading, Ph.D. Dissertation, University of California, San Diego, California, U.S.A..

Malemud, C.J.; and Shuckett, R. (1987) Impact loading and lower-extremity disease, In: Clinical Concepts in Regional Musculoskeletal Illness, M.M. Hadler, Ed., Grune and Stratton Inc., pp. 109-135.

Mansour, R.M.; and Reynik, R.J. (1975) In vivo occlusal forces and moments: I. Forces measured in terminal hinge position and associated moments, J Dent Res 54: 114-124.

Maroudas, A. (1969) Studies on the formation of hyaluronic acid films, In: Lubrication and Wear in Joints, V. Wright, Ed., London: Sector, pp. 124-133.

Maroudas, A. (1975) Fluid transport in cartilage, Ann Rheum Dis 34 (suppl 2): 77-81.

Maroudas, A. (1979) Physicochemical properties of articular cartilage, In: Adult Articular Cartilage, 2nd ed., M.A.R. Freeman, Ed., London: Pitman Medical, pp. 215-290.

McCutchen, C..W. (1959) Mechanism of animal joints. Sponge-hydrostatic and weeping bearings, Nature (London) 184: 1284-1285.

McCutchen, C.W. (1962) The frictional properties of animal joints, Wear 5: 1-17.

McCutchen, C.W. (1966) Boundary lubrication by synovial fluid: demonstration and possible osmotic explanation, Fed Proc Fed Am Soc Exp Biol 25: 1061-1068.

McCutchen, C.W. (1978) Lubrication of joints, In: The Joints and Synovial Fluid, vol. I, L. Sokoloff, Ed., New York: Academic Press, pp. 437-483.

McCutchen, C.W. (1983) Lubrication of and by articular cartilage, In: Cartilage: Biomedical Aspects, vol. III, B.K. Hall, Ed., New York: Academic Press, pp. 87-107.

Merrill, R.G.; Yih, W.Y.; Langan, M.J. (1990) A histologic evaluation of the accuracy of TMJ diagnostic arthroscopy, Oral Surg Oral Med Oral Pathol 70: 393-398.

Mills, D.K.; Daniel, J.C.; and Scapino, R. (1988) Histological features and in-vitro proteoglycan synthesis in the rabbit craniomandibular joint disc, Arch Oral Biol 33: 195-202.

Mizrahi, J.; Solomon, L.; and Kaufman, B. (1980) A method for direct measurement of local pressures in human cadaver hip joint, Phys Med Biol 25: 1181.

Moffett, B.C.; Johnson, L.C.; McCabe, J.B.; and Askew, H.C. (1964) Articular remodelling in the adult human temporomandibular joint, Am J Anat 115: 119-142.

Mohl, N.D. (1983) Functional anatomy of the temporomandibular joint, In: The President's Conference on the Examination, Diagnosis and Management of Temporomandibular Disorders, D. Laskin, et al., Eds., Chicago: American Dental Association, pp. 3-12.

Mow, V.C.; Holmes, M.H.; and Lai, W.M. (1984) Fluid transport and mechanical properties of articular cartilage: a review, J Biomech 17: 377-394.

Nelson, B.H.; Anderson, D.D.; Brand, R.A.; and Brown, T.D. (1988) Effect of osteochondral defects on articular cartilage: contact pressures studied in dog knees, Acta Orthop Scand 59: 574-579.

Newman, A.P.; Anderson, D.R.; Daniels, A.V.; and Jee, K.W. (1989) The effect of medial menisectomy and coronal plane angulation on in vivo load transmission in the canine stiffle joint, J Orthop Res 7: 281-291.

Nickel, J.C.; McLachlan, K.R.; and Smith, D.M. (1988a) Eminence development of the postnatal human temporomandibular joint, J Dent Res 67: 896-902.

Nickel, J.C.; McLachlan, K.R.; and Smith, D.M. (1988b) A theoretical model of loading and eminence development of the postnatal human temporomandibular joint, J Dent Res 67: 903-910.

Ogus, H. (1979-1980) Degenerative disease of the temporomandibular joint in young persons, Brit J Oral Surg 17: 17-26.

Okeson, J.P. (1985) Fundamentals of occlusion and temporomandibular disorders, St Louis: C.V. Mosby Company.

Parsons, J.R.; and Black, J. (1979) Mechanical behaviour of articular cartilage. Quantitative changes with alteration of ionic environment, J Biomech 12: 765-773.

Paul, J.P. (1980) Joint kinetics, In: The Joints and Synovial Fluid, vol. II, L. Sokoloff, Ed., New York: Academic Press, pp. 139-176.

Peiper, A. (1963) The neurology of food intake, In: Cerebral function in infancy and childhood, J. Wortis, Ed., International Behaviourial Sciences Series, New York: Consultants Bureau, pp. 396-491.

Piotrowski, G. (1975) Non-Newtonian lubrication of synovial joints, Ph.D. Dissertation, Case Western Reserve University, Cleveland.

Proctor, C.S.; Schmidt, M.B.; Whipple, R.R.; Kelly, M.A.; and Mow, V.C. (1989) Material properties of the normal medial bovine meniscus, J Orthop Res 7: 771-782.

Proffit, W.R.; and Fields, H.W. (1983) Occlusal forces in normal and long-face children, J Dent Res 62: 571-574.

Proffit, W.R.; Fields, H.W.; and Nixon, W.L. (1983) Occlusal forces in normal and long-face adults, J Dent Res 62: 566-570.

Pullinger, A.G.; and Seligman, D.A. (1987) TMJ osteoarthrosis: a differentiation of diagnostic subgroups by symptoms, history, and demographics, J Craniomandibular Disord 1: 251-256.

Pullinger, A.G.; Baldioceda, F.; and Bibb, C.A. (1990) Relationship of TMJ articular soft tissue to underlying bone in young adult condyles, J Dent Res 69: 1512-1518.

Radin, E.L. and Paul, I.L. (1971) Responses of joints to impact loading: I. in vitro wear, Arthritis Rheum 14: 356-362.

Roth, T.E.; Goldberg, J.S.; and Behrents, R.G. (1984) Synovial fluid pressure determination in the temporomandibular joint, Oral Surg Oral Med Oral Pathol 57: 583-588.

Rugh, J.D.; and Ohrbach, R. (1988) Occlusal parafunction, In: A Textbook of Occlusion, N.D. Mohl, G.A. Zarb, G.E. Carlsson, J.D. Rugh, Eds., Chicago: Quintessence Publishing Company Inc., pp. 249-257.

Rushfeldt, P.D.; Mann, R.W.; and Harris, W.H. (1979) Influence of cartilage geometry on the pressure distribution in human hip joint, Science 204: 413-415.

Rushfeldt, P.D.; Mann, R.W.; and Harris, W.H. (1981) Improved techniques for measuring in vitro the geometry and pressure distribution of the human acetabulum. II. Instrumented endoprosthesis measurement of articular surface pressure distribution, J Biomech 14: 315-323.

Saegesser, M. (1990) Disturbed joint mechanics, In: Dental Occlusion and the Temporomandibular Joint, A. Gerber and G. Steinhardt, Eds., Chicago: Quintessence Publ. Co., pp. 49-52.

Sasaki, K.; Hannam, A.G.; and Wood, W.W. (1989) Relationships between the size, position, and angulation of human jaw muscles and unilateral first molar bite force, J Dent Res 68: 499-503.

Scapino, R.P. (1983) Histopathology associated with malposition of the human temporomandibular joint disc, Oral Surg Oral Med Oral Pathol 55: 382-397.

Seedhom, B.B.; and Hargreaves, D.J. (1979) Transmission of the load in the knee joint with special reference to the role of the menisci. Part II: experimental results, discussion and conclusions, Eng Med 8: 220-228.

Sicher, H.; and DuBrul, E.L. (1975) Oral Anatomy, 6th edition, St. Louis: C.V. Mosby Company.

Simon, W.H. (1975) Wear properties of articular cartilage, Ann Rheum Dis 34 (suppl): 117-118.

Smith, D.M.; McLachlan, K.R.; and McCall, W.D. (1986) A numerical model of temporomandibular joint loading, J Dent Res 65: 1046-1052.

Sokoloff, L. (1969) The Biology of Degenerative Joint Disease, Chicago: The University of Chicago Press.

Solberg, W.K.; Hansson, T.L.; and Nordstrom, B. (1985) The temporomandibular joint in young adults at autopsy: a morphologic classification and evaluation, J Oral Rehabil 12: 303-321.

Spilker, R.L.; Suh, J-K.; and Mow, V.C. (1990) Effects of friction on the unconfined compression response of articular cartilage: a finite element analysis, J Biomech Eng 112: 138-146.

Spoor, C.W.; van Leeuwen, J.L.; de Windt, F.H.J.; and Huson, A. (1989) A model study of muscle forces and joint force direction in normal and dysplastic neonatal hips, J Biomech 22: 873-884.

Stockwell, R.A. (1979) Biology of Cartilage Cells, Cambridge: Cambridge University Press.

Strom, D.; Holm, S.; Clemensson, E.; Haraldson, T.; and Carlsson, G.E. (1986) Gross anatomy of the mandibular joint and masticatory muscles in the domestic pig (Sus scrofa), Arch Oral Biol 31: 763-768.

Swann, D.A.; Hendren, R.B.; Radin, E.L.; Sotman, S.L.; and Duda, E.A. (1981) The lubricating activity of synovial fluid glycoproteins, Arthritis Rheum 24: 22-30.

Swann, D.A.; Silver, F.H.; Slayter, H.S.; Stafford, W.; and Shore, E. (1985) The molecular structure and lubricating activity of lubricin isolated from bovine and human synovial fluids, Biochem J 225: 195-201.

Swanson, S.A.V. (1979) Friction, wear, and lubrication, In: Adult Articular Cartilage, 2nd edition, M.A.R. Freeman, Ed., London: Pitman Medical, pp. 415-460.

Taguchi, N.; Nakata, S.; Oka, T. (1980) Three-dimensional observation of the temporomandibular joint disk in the rhesus monkey, J Oral Surg 38: 11-15.

Tanne, K.; Tanaka, E.; and Sakuda, M. (1991) The elastic modulus of the temporomandibular joint disc from adult dogs, J Dent Res 70: 1545-1548.

Tanner, J.M. (1977) Human growth and constitution, In: Human Biology: an introduction to human evolution, variation, growth and ecology, G.A. Harrison, J.S. Weiner, J.M. Tanner, and N.A. Barnicott, Eds., Oxford: Oxford University Press, pp. 301-384.

Tepic, S.; Macirowski, T.; Mann, R.W. (1983) Mechanical properties of articular cartilage elucidated by osmotic loading and ultrasound, Proc Natl Acad Sci (U.S.A.) 80: 3331-3333.

Ter Horst, G.J.; Copray, J.C.V.M.; van Willigen, J.D.; and Liem, R.S.B. (1990) Contralateral projections of cells in the motor trigeminal nucleus of the rat, Neurosci Lett 113: 260-266.

Thilander, B. (1964) The structure of the collagen of the temporo-mandibular disc in man, Acta Odontol Scand 22: 135-149.

Toller, P.A. (1973) Osteoarthrosis of the mandibular condyle, Brit Dent J 6: 223-231.

Trainor, P.G.S.; and McLachlan, K.R. (1991) A numerical model to predict the force output of the jaw musculature, Eng Opt (in press).

Valentine, J.D.; Reiman, B.E.F.; Beuttenmuller, E.A.; and Donovan, M.G. (1989) Light and electron microscopic evaluation of Proplast II TMJ disc implants, J Oral Maxillofac Surg 47: 689-696.

van Kampen, G.P.J.; Veldhuijzen, J.P.; Kuijer, R.; van de Stadt, R.J.; and Schipper, C.A. (1985) Cartilage response to mechanical force in high-density chondrocyte cultures, Arthritis Rheum 28: 419-424.

Venn, M.; and Maroudas, A. (1977) Chemical composition and swelling of normal and osteoarthrotic femoral head cartilage. I. Chemical composition, Ann Rheum Dis 36: 121-129.

Walker, P.S.; and Hajek, J.V. (1972) The load-bearing areas in the knee joint, J Biomech 5: 581-592.

Walker, P.S.; and Erkman, M.J. (1975) The role of the menisci in force transmission across the knee, Clin Orthop 109: 184-192.

Ward, D.M.; Behrents, R.G.; and Goldberg, J.S. (1990) Temporomandibular synovial fluid pressure response to altered mandibular positions, Am J Orthod Dentofacial Orthop 98: 22-28.

Weightman, B.; Freeman, M.A.R.; and Swanson, S.A.V. (1973) Fatigue of articular cartilage, Nature 224: 303-304.

Werner, F.W.; Murphy, D.J.; Palmer, A.K. (1989) Pressures in the distal radioulnar joint: effect of surgical procedures used for Kienbock's disease, J Orthop Res 7: 445-450.

Westesson, P-L.; and Rohlin, M. (1984) Internal derangement related to osteoarthrosis in temporomandibular joint autopsy specimens, Oral Surg Oral Med Oral Pathol 57: 17-22.

Wood, W.W. (1986) A functional comparison of the deep and superficial parts of the human anterior temporal muscle, J Dent Res 65: 924-926.

Zarb, G.A.; and Carlsson, G.E. (1979) Temporomandibular Joint: Function and Dysfunction, St. Louis: C.V. Mosby.

APPENDIX A

Structure and Chemistry of the Fibrous Connective Tissue of the Temporomandibular Joint

1. Articular tissue of the mandibular condyle and temporal bone

The articular tissue which covers the mandibular condyle and temporal bone of the temporomandibular joint (TMJ) is a dense fibrous connective tissue (fibrocartilage), rather than a hyaline cartilage which is found in other synovial joints (Mohl, 1983). Moffett (1957) showed that the fibrous connective tissue was a consequence of embryonic development of the TMJ. Moffett suggested that the joint was loaded even though it did not have hyaline cartilage lining. The thicknesses of the soft tissues lining the condyle and temporal bone are considered to reflect the functional loads to which various areas of the joint are exposed (Hansson et al., 1977). In general, the tissues are thickest in the presumed areas of loading. On the condyle, the tissue was thickest on the anterior slope of the condyle. On the temporal bone, the tissue was thickest on the posterior slope of the eminence, and at the crest of the eminence.

The fibrous connective tissue of the TMJ is a mixture of collagen fibres and gel-like proteoglycans, which form the solid matrix of the tissue. Water, with dissolved electrolytes, forms a mobile fluid phase which is capable of moving through the solid matrix. Approximately 70% of the dry weight of the solid matrix is type I collagen (Landesberg et al., 1989; Fujita and Hoshino, 1989; Livne et al., 1985; Milam et al., 1989; Hirschmann and Shuttleworth, 1976). Small amounts of type III collagen have been reported in the *in vitro* development of the TMJ (Anderson et al., 1990; Yen et al, 1990). Type I collagen, as opposed to type III, forms large strong fibres which makes type I collagen useful in a joint that is under load.

The organization of fibres in the articulating layers of the condyle and temporal bone of the TMJ have been described using light microscopy (Thilander, 1964; Scapino, 1983; Isacsson and Isberg, 1985; de Bont, 1985a), or by a combined histological/ histochemical approach (Mills et al. , 1988, 1989). Scanning electron microscopic (SEM) descriptions have been reported by de Bont (1985a), Taguchi et al. (1980), and Toller (1973). With respect to the fibres of the connective tissue lining of the TMJ, several distinct microstructural zones are evident (Thilander, 1964; de Bont, 1985a; Taguchi et al., 1980). The articular surface is characterized by thinner collagen fibre bundles which are oriented parallel to the articular surface. The fibrils are closely packed, randomly oriented to form a tightly knit network. On occasions (Taguchi et al., 1980) a wavy pattern has been described, but Wilson and Gardner (1984) have expressed concern in interpreting surface characteristics of this type. The authors have shown that the techniques of fixation and critical drying for SEM significantly distorts the three-dimensional character of the fibrous matrix. In the deeper zones of fibrous connective tissue on the condyle, the collagen forms larger fibres (coarser), which appear to be anteroposteriorly oriented (de Bont, 1985a). In the deepest layers the fibres appear to arcade and insert perpendicular to the calcified tide zone of the supporting bone, then arch up and curve until parallel with the bone and articular surfaces (Ahing, 1984).

The three-dimensional character of the fibrous matrix is particularly relevant since the orientation of fibres has a significant effect on the stiffness and strength of a fibrous tissue (Aspden, 1985, 1986, 1988). For example, the typical collagen arrangement of a ligament or tendon is unidirectional, and is oriented so that fibre arrangement is parallel to the line of force that is usually placed on the tendon or ligament. Aspden considers collagen stiffness and strength to be the greatest when forces act along the long axis of the fibre.

The organization of the collagen in the superficial zone of fibrocartilage of the TMJ condyle and eminence is similar to that of hyaline cartilage found in other synovial joints. Aspden (1985) suggests that, theoretically, the random orientation of the collagen in fibrous connective tissue produces isotropy in strength of the superficial layer. In the deeper layers, which display a preferential collagen orientation, it might be expected that there would be anisotropy in material properties. This sort of relationship has been explored for the meniscus of the knee (Proctor et al., 1989), and the anisotropy in material properties of the meniscus have been elegantly demonstrated. Until X-ray diffraction is conducted on the connective tissues of the TMJ, electron and light microscopy are the only sources of information concerning collagen orientation in the matrix of the TMJ components. It has not been determined whether the different layers of the connective tissue have significantly different mechanical properties which reflect differences in fibre orientation.

The other major constituent of the solid matrix of the connective tissue of the condyle and eminence are the gel-like proteoglycans. Proteoglycans are large polyanionic molecules, composed of long chain glycosaminoglycans which are covalently linked to a protein backbone. Due to the polyanionic character and large molecular size, the molecules create a large osmotic gradient which causes fluid and free cation influx into the tissue. The result is a swelling of the solid matrix until such time that tension on the fibrous component of the matrix balances the pressure gradient created by the glycosaminoglycans (for review see Grodzinsky, 1983; Maroudas and Venn, 1977; Venn and Maroudas, 1977; Tepic et al., 1983; Harrigan and Mann, 1987).

The proteoglycan portion of the solid matrix is responsible for the unique fluid-filled character of the tissue. The ability of the tissue to absorb water accounts for the poroelastic (McCutchen, 1979, 1983) or viscoelastic (Mow et al., 1984) mechanical behaviour of the tissue. Compression of hydrated fibrous tissue such as hyaline cartilage and fibrocartilage (TMJ disc, intervertebral disc, meniscus of the knee) produces movement of the mobile water and unbound electrolytes. This mobile portion of the connective tissue matrix plays a fundamental role in several processes. The transport of nutrients (Ekholm and Norback, 1951; McKibben and Maroudas, 1979; Honner and Thompson, 1971; Salter et al., 1980) is augmented by the movement of water produced by tissue compression. Fluid movement also controls the rate of compression of the articular surfaces, and therefore influences the area of contact between articulating surfaces. This ultimately affects the contact stress between compressed surfaces. Finally, the movement of fluid through the cartilage and out to the surface, provides a weeping lubricant which gives the surfaces of synovial joints remarkably low coefficients of friction (for review see McCutchen, 1979, 1983; Swanson, 1979). The physicochemical basis of fluid flow in cartilage is dependent on the collagen-trapped proteoglycan molecules which, by the nature of their electronegativity and osmotic effect, affect the movement of the polar fluid (saline) through the solid matrix of the tissue (for review, see Mow et al., 1984).

The study by Kopp (1978) presented a topographical distribution of sulphated glycosaminoglycans in the lining of the condyle and temporal component of the TMJ. Keratin sulfate and chondroitin sulfate or dermatan sulfate were identified and found most prevalent in the assumed major loading areas of the condyle and temporal bone (Oberg 1964; Barbenel, 1974; Hansson and Oberg 1977). Kopp also determined that the degree of metachromasia, an indication of concentration of the pericellular and intercellular glycosaminoglycans, was higher in the lateral portions of the condyle and eminence than in the medial areas. Because of Kopp's report, it has been suggested that the loading of the condyle and eminence is predominantly on the lateral half of the joint structures.

The development of pathosis in other synovial joints has been shown to be related to the loss of proteoglycans (Venn and Maroudas, 1977). However, it is not known if the loss of proteoglycans is the crucial event that precedes the development of pathology of synovial joints in general, or the TMJ in particular. The earliest events which eventually result in degeneration of the tissues of the joint have not been identified.

2. <u>Chemistry and structure of the TMJ disc</u>

The disc of the TMJ, like the meniscus of the knee, is made up of fibrous connective tissue. Although gross features of the disc distinguish it from the meniscus of the knee, there are remarkable similarities in chemistry and fibrous matrix organization (Bullough et al., 1970; Taguchi et al., 1980; Proctor et al., 1989). Light and scanning electron microscopy has shown that the surface of the disc, like the surface of the condyle and eminence, is formed by a dense mass of finely woven fibrils with random orientation. In the intermediate portion of the disc, between the anterior and posterior bands, the deeper portions of the disc contain collagen which is coarser and wavy, and has a definite anteroposterior orientation (Taguchi et al., 1980; de Bont, 1985a,b,d; Thilander, 1964; Fujita and Hoshino, 1989; Scapino, 1983; Griffin et al., 1975; Christen, 1959; Knox, 1967; Isacsson and Isberg, 1985). In the anterior and posterior bands a three-dimensional latticework of collagen fibres is evident. Large, coarse, collagen fibres are oriented mediolaterally in the thickened anterior and posterior bands. This has been presumed to increase the strength of the bands in the mediolateral direction. The deeper collagen fibres of the intermediate zone of the disc (see figure 1.5 of chapter 1), which are oriented anteroposteriorly, flare into the anterior and posterior bands. In the bands, this collagen interlaces with the collagen running mediolaterally.

Like the fibrous connective tissue of the condyle and temporal bone, type I collagen fibres predominate in the solid matrix of the fibrocartilaginous disc (Hirschmann and Shuttleworth, 1976). There have been reports of very small amounts of type II collagen (Landesberg et al., 1989), but this may have been due to a dissection technique which included other tissues. Type III collagen has been reported in organ culture, although not in large amounts (Carvalho, 1990).

The proteoglycan component of the disc is dominated by chondroitin-6-sulphate and/or dermatan sulfate (Granstrom and Linde, 1973). Granstrom and Linde were unable to detect keratan sulfate, but they noted that it probably was present, and that the electrophoretic method of separating glycosaminoglycans did not separate out the keratan sulfate portion. Kopp (1976) found that dermatan sulfate was the major source of toluidine blue staining, although it was probably a mixture of chondroitin sulfate and dermatan sulfate. The author noted that dermatan sulfate hybridization occurs which results in chondroitin-6-sulfate and chondroitin-4-sulfate. This phenomenon been reported by Adams and Ho (1987) for other fibrous connective tissues. Kopp (1976) selectively stained for keratan sulfate, finding that the alcian blue stain was heaviest on the surfaces of the disc. He interpreted that to be the areas of concentration of the keratan sulfate. Stockwell (1970) had found similar results for the femoral condyles of the knee. Using an immunostaining technique, Mills et al. (1988) supported Kopp's description of the location of keratan sulfate. Mills and co-workers, using immunostaining, have identified chondroitin-6-sulfate. Concentrations were primarily pericellular in the anterior and posterior bands and at the junction of the bands and the intermediate zone of the disc. Kuc et al. (1989) used monoclonal antibodies to confirm Mill's reports of pericellular distribution of chondroitin-6-sulfate. They also reported surface localizations of prodermatan sulfate.

In summary, Kopp found that the highest concentrations of glycosaminoglycans were in the intermediate zone of the disc. This has been supported by Hasty et al. (1983), Granstrom and Linde (1973), and Mills et al. (1988, 1989). The glycosaminoglycan profiles described for the TMJ disc are similar to the profiles found in the highly ordered fibrocartilages of the intervertebral disc (Cole et al., 1985) and canine and human menisci (Adams and Ho, 1987). The mechanical behaviour of fibrous connective tissue under compressive loading depends mainly on the charge density of the proteoglycans and intermolecular constraints such as entanglements of the proteoglycans in the collagen fibrous net (Grodzinsky, 1983).

It was Kopp (1976, 1978) who suggested the relationship between thinning of the disc and scarcity of glycosaminoglycans. Kopp (1976) and Hansson et al. (1977) considered thinning of the disc as the early beginning of degenerative joint disease. It is not clear how thinning of the disc occurs, and whether there is frank loss of proteoglycans during the thinning process.

3. Structure and chemistry of degenerative disease in the TMJ

> "Optimal loading is thought to be necessary for the health of the joint, but overloading and underloading may involve the risk of injury to the joint tissues (Radin et al, 72; Lancet 9:519). According to this line of thought, analysis of stresses placed on the joints would be desirable, but this is a very difficult matter to investigate. No attempts have been made to measure such stresses in the TMJ *in vivo* though the methods for doing so have been developed for large joints (Nachemoson and Morris, 1964)." (from Carlsson and Oberg, Oral Sciences Rev 6:53-86, 1974, p. 79).

Perhaps Carlsson and Oberg were a bit optimistic in their expectations, for it was not until 1986 that Hodge *et al*. reported the first *in vivo* measurements of articular stress in the human hip. In fact, a theoretical analysis of stresses in the TMJ has not been possible until recently because the magnitudes of TMJ loads were not known (Smith *et al*., 1986).

It is generally agreed that osteoarthritis (degenerative joint disease) is a lesion brought about by either an increase in repetitive loading on a tissue so as to exceed the functional capacity of the tissue, or the functional capacity of the tissue is reduced to a point where it is unable to maintain integrity during normal loading (Ogus, 1979-80). Howell (1984) identified three major classes of degenerative joint disease based on aetiopathology. In the first class, mechanical forces result in biomechanical failure of the tissue, following which there is chemical degeneration of the cartilage. According to Howell's definition of the second classification, the mechanics of the cartilage is normal to begin with, but there is a failure of chondrocytes to repair and regenerate the normal ageing cartilage (Weiss and Mirow, 1972). Therefore, the tissue would eventually lose its ability to withstand routine stresses due to early chemical changes in the solid matrix of the tissue. Finally, the third class of degenerative joint disease is based on an aetiology of degeneration due to extracartilaginous factors such as synovial responses, microfracture of bones, and endocrine factors. This class is particularly interesting with respect to the TMJ since recent evidence of estrogen receptors in the TMJ (Aufdemorte et al., 1986) has renewed speculation as to why women seem to report having more problems associated with intracapsular derangement of the TMJ.

Ogus (1979-80) notes that degenerative changes of the TMJ in young patients is by no means a rarity. The earlier onset of degenerative joint disease in the TMJ, as opposed to other joints, suggests a special aetiology, such as increased stress on the joint surfaces (see also Solberg et al., 1985; van Willigan et al., 1986). For the TMJ, it may be possible to separate the degenerative process into a simple classification; that being primary and secondary processes (Mitchell and Cruess, 1977; Sokoloff, 1979). Primary degenerative disease is due to excessive stress on a normal matrix. Secondary degenerative disease is due to a compromised matrix and normal stresses. There is no evidence to suggest that the young TMJ is more likely to have an abnormal matrix than other joints in the body. Therefore, although the secondary mechanism can not be ruled out in specific cases of TMJ degenerative disease, the evidence of earlier development of TMJ degenerative disease suggests a predominance of a mechanism of excessive stress on a normal matrix.

There is debate concerning the differences between normal ageing of the articular tissues, and the earliest changes in the tissues that eventually lead to degenerative joint disease. Solberg et al.(1985) noted that it was not clear if the age changes such as localized thinning of the lateral component of the disc had an absolute, or merely contributory effect, on the development of degenerative joint disease. Solberg and co-workers reported that of all young adults (approximately 27 years of age) examined in their study, 87% showed intracapsular changes. Approximately 40% showed between mild and marked deviation in form of all three joint components. Milder forms occurred in younger individuals. The authors suggested that deviation in form was an adaptive phenomenon, and degenerative joint disease was not present. Rather, in these younger individuals, soft tissue changes were more prominent, which was in keeping with other studies

(Dolwick, 1983; Dolwick et al., 1983; Hansson and Oberg, 1977; Hansson and Nordstrom, 1977; Isberg-Holm and Westesson 1982). de Bont (1985b,c,d) concluded that several age related changes such as fibrillation and lipping are also histopathological characteristics of the degenerative joint disease. Structurally, these features are indistinguishable from normal ageing. However, the age factor must be considered, and if the disease occurs in a 20 year old, it is premature ageing, otherwise classified as primary degenerative joint disease. In contradistinction, a 60 year old individual with degenerative joint disease is likely to have developed the disease as a consequence of normal ageing, and hence it is a secondary joint disease.

Oberg et al. (1971) noted from observations, as did Blackwood (1963) and Moffett et al. (1964) that arthritis usually involved the disc first. It was noted that the discs in younger individuals were thicker in the periphery than was the case in discs from older individuals. The final arthrotic change in the disc was the development of a perforation. The articulating surface of the eminence was the next surface to show changes, and finally, the condyle surface was the last of all to show damage (Solberg et al., 1985).

In the studies of the TMJ, light microscopy (Steinhardt, 1934; Moffett et al., 1964; Blackwood, 1966; Hansson et al., 1977), and electron microscopy (Toller 1977; Toller and Wilcox, 1978; de Bont, 1985b,c,d; Taguchi et al., 1980) have enhanced the understanding of the histology associated with degenerative joint disease. The advancements made by scanning electron microscopy have been advantageous, for it gives the first opportunity to examine the surface of the cartilage for the minutest early changes. These early changes are particularly important, as noted by Byers (1975), who in conjunction with a working party of anatomists noted that the ordinary histologic descriptions of the disease are an oversimplification of the degenerative process, and do not take into account the very earliest changes in the articular cartilage.

The most notable change to the matrix of the fibrous connective tissue was the destruction and disarray of the collagen fibres. The fibres showed a looser disorderly arrangement, with individual fibre diameter being reduced and fibres showing signs of fragmentation. The degenerative features most frequently seen (de Bont, 1985b,c,d; 9 of 22 joints in a light microscopic study) was horizontal splitting of the fibrous connective tissue interface with the ossified cartilage. This type of splitting at the osseous tidemark has also been reported for the patella of the knee (Armstrong, 1986; Meachim and Bently, 1978; Meachim and Allibone, 1984). The feature was explained as a shear failure at the cartilage-bone interface. This horizontal splitting also occurred in the middle zones of the connective tissue lining the TMJ (de Bont, 1985b,c,d). Deeper zone splitting was usually accompanied by fibrosis of the adjacent bone marrow. The results are similar to the descriptions of Toller (1973, 1974) and Sokoloff (1979) for hyaline joints. Bean et al. (1977) noted that these degenerative changes can occur deep in cartilage, yet the cartilage has a macroscopically intact articular surface. The authors found that almost all degenerative lesions of the soft tissues were accompanied by destruction of the subarticular compact bone. It is not known what kinds of changes occurred in the mechanics of the tissue with these changes in the deeper layers of tissue.

There is debate whether glycosaminoglycan loss is the primary event leading to the fracture of the collagen matrix. Focal loss of glycosaminoglycans has been considered by many as the first event associated with onset of degenerative joint disease (reviewed by Ahing, 1984). There is an animal model, a strain of mice susceptible to degenerative joint disease, which supports this view (Livne et al, 1985). At maturation, the glycosaminoglycan profiles change, with smaller amounts produced. Only in a more advanced stage of the disease is there fibrillation and marked tissue changes. It must be pointed out that, in humans, there are age related changes in glycosaminoglycan synthesis (Roughley and White, 1980; Roughley 1987). According to definition, this type of degenerative joint disease is a secondary degenerative condition due to normal loading on a compromised matrix (Malemud and Shuckett, 1987; Mitchel and Cruess, 1977).

In the development of primary degenerative joint disease in hyaline cartilage, the loss of solid matrix integrity is due to excessive stress or frequency of loading. This can occur without early changes in the chemistry of the tissue. If, as concluded by de Bont (1985b,c,d), the process is the same for fibrous articular cartilage or hyaline cartilage, then the changes are in the fibrous component of the matrix without glycosaminoglycan loss. For example, Weightman et al. (1973), in a fatigue analysis of hyaline cartilage, produced surface fibrillation by repetitive loading. It was concluded that the fibrillation was caused by fatigue of the surface fibres. Chemical analysis conducted by the authors failed to demonstrate any changes in the fixed charge density (electronegativity), even though cartilage was fibrillated. Weightman and co-workers concluded that the surface damage was not due to the loss of glycosaminoglycans. Hukins et al. (1984), using numerical modelling, demonstrated that early failure of the matrix in the region of the middle and deep layers of bound connective tissue leads to increased compressibility of the cartilage. This results in an increase in tensile stress on the surface, which in turn increases the potential for surface fatigue.

These are interesting results since the surface of the cartilage is a potential porous filter (McCutchen, 1983) which excludes large volume macromolecules such as enzymes. Of particular interest, with respect to the surface barrier of articular cartilage, is the prevention of activation of latent metalloproteinases which would otherwise initiate catabolism of fibrous tissue proteoglycans (Campbell et al., 1986a,b; Tyler, 1985; Murphy et al., 1981; Pujol and Loyau, 1987). Although it has not been studied extensively in fibrocartilage, latent metalloproteinases of hyaline cartilage are secreted by the chondrocytes. Inhibition of these calcium dependent enzymes is by a macromolecule termed tissue inhibitor metalloproteinase (TIMP). Activation of the latent metalloproteinases is accomplished by factors such as plasmin, which remove the TIMP blocker from the enzyme, thus activating the enzyme to initiate proteoglycan degradation. Plasmin has been shown to activate the enzyme, and monocyte factor (MCF), which is released by macrophages in the synovial fluid, is capable of increasing the release of latent metalloproteinase from chondrocytes. Thus, not only are the concentrations of latent enzyme increased, but the rate of activation of the enzyme is also increased. MCF is released by macrophages which have been in contact with tissue debris and degradation products (Pujol and Loyau, 1987). MCF, once it is available to synovial cells, results in release of active plasmin from synovial cells. Thus, tissue debris has the double effect of causing the release of substances which increase the concentration of latent metalloproteinases, as well as the release of factors which activate the metalloproteinases in the cartilage. If the surface of the cartilage is compromised, these activator substances may gain access to the deeper portions of the matrix, and compromise the integrity of the tissue by causing degradation of proteoglycans. Although it has not been tested, this mechanism may account for the loss of glycosaminoglycans from tissues with fibrillated surfaces. With loss of glycosaminoglycans there is increased compressibility of the tissue for a given stress (Venn and Maroudas, 1977). As well, with loss of surface integrity, there is the potential for increase in surface roughness, and perhaps some reduction in the efficiency of lubrication between surfaces (Linn, 1967; Linn and Radin, 1968). The increased compressibility results in increased deformational losses (ploughing friction) during joint movement (Linn, 1967). A decreased efficacy in lubrication results in greater tractional stresses on the surfaces. All together, there are likely to be increased tensile and shear stresses on the surface which further compromise the integrity of the articulating layers.

4. The role of the disc in degenerative joint disease

Although Oberg et al. (1971) and others (Kopp, 1976; Solberg et al., 1985) have stated that the disc is often the first to display signs of degeneration, there is nothing in the literature to describe the earliest changes in disc microstructure. Oberg has noted that thinning, whether due to ageing or other processes, seems to be a common trait. Kopp

(1976) indicated that the earliest change detected was a thinning of the disc, and concomitant decrease in staining for glycosaminoglycans. This is what led him to conclude that thinning was the most important feature of early changes in the disc. It is not apparent how the thinning occurs, and whether it is preceded by loss of glycosaminoglycans.

A debate still continues concerning the displacement of the TMJ disc and the continued health of the condyle and eminence. de Bont (1985c) looked at disc position and degenerative changes in the condyle and eminence. de Bont noted that 11 of 14 patients with deviation in form or frank displacement of the disc showed degenerative changes such as horizontal splitting of the connective tissue surfaces on the condyles and eminence. It appeared that a displaced disc usually meant significant "ageing" of the condyle and eminence. However, similar degenerative changes were seen in 4 of 8 patients with so-called normal disc positions. Therefore, a disc in proper position did not always guarantee good health of the other components. However, for those cases in which he noted normal disc location, de Bont failed to detail whether significant thinning of the disc had occurred without frank displacement of the disc. Consequently, de Bont was unable to show that there was a causal relationship between disc thinning and/or disc position and degenerative joint disease. The results are similar to the results of Stockwell _et al_. (1983), Scapino (1983), and

Westesson and Rohlin (1984). There has been considerable interest in the relationship between disc displacement and degeneration of the condyle and eminence (Weinberg, 1980; Dolwick et al., 1983; Westesson and Rohlin, 1984; Blaustein and Scapino, 1986; Helmy et al., 1988; Kurita et al., 1989; Tolvanen et al., 1988). Perhaps future examination of the thickness of the disc, as well as position of the disc and congruity of the osseous surfaces, will resolve this issue.

BIBLIOGRAPHY TO APPENDIX A

Adams, M.E. and Ho, Y.A. (1987) Localization of glycosaminoglycans in human and canine menisci and their attachments, Connect Tissue Res 16: 269-279.

Ahing, S. (1984) A study of nerves and mast cells in osteoarthritis of the human temporomandibular joint, M.S. thesis, Indiana University School of Dentistry.

Anderson, A.N.; Whyte, W.A.; Yen, E.H.K.; and Suga, D.M. (1990) Effects of intermittent and continuous forces on collagen phenotype synthesis, J Dent Res 69 (special issue): 201.

Armstrong, C.G. (1986) An analysis of the stresses in a thin layer of articular cartilage in a synovial joint, Eng Med 15: 55-61.

Aspden, R.M. (1985) A model for the function and failure of the meniscus, Eng Med 14: 119-122.

Aspden, R.M. (1986) Relation between structure and mechanical behaviour of fibre-reinforced composite materials at large strains, Proc R Soc Lond A. 406: 287-298.

Aspden, R.M. (1988) The theory of fibre-reinforced composite materials applied to changes in the mechanical properties of the cervix during pregnancy, J Theor Biol 130: 213-221.

Aufdemorte, T.B.; van Sickels, J.E.; Dolwick, M.F.; Sheridan, P.J.; Holt, G.R.; Aragon, S.B.; and Gates, G.A. (1986) Estrogen receptors in the temporomandibular joint of the baboon (**Papio cynocephalus**): an autoradiographic study, Oral Surg Oral Med Oral Pathol 61: 307-314.

Barbenel, J.C. (1974) The mechanics of the temporomandibular joint: a theoretical and electromyographical study, J Oral Rehabil 1: 19-27.

Bean, L.R.; Omnell, K.-A.: and Oberg, T. (1977) Comparison between radiological observations and macroscopic tissue changes in temporomandibular joints, Dentomaxillofac Radiol 6:90-106.

Blackwood, H.J.J. (1963) Arthritis of the mandibular joint, Brit Dent J 115: 317-326.

Blackwood, H.J.J. (1966) Cellular remodelling in articular tissue, J Dent Res 45: 480-489.

Blaustein, D.I. and Scapino, R.P. (1986) Remodelling of the temporomandibular joint disc and posterior attachment in disk displacement specimens in relation to glycosaminoglycan content, Plast Reconstr Surg 78: 756-764.

Bullough, P.G.; Munuera, L.; Murphy, J.; and Weinstein, A.M. (1970) The strength of the menisci of the knee as it relates to their fine structure, J Bone Joint Surg 52-B: 564-570.

Byers, P.D. (1975) Conclusions of a working party of morbid anatomists, Ann Rheum Dis 34 (suppl): 147-148.

Campbell, I.K.; Golds, E.E.; Mort, J.S.; and Roughly, P.J. (1986a) Human articular cartilage secretes characteristic metal dependent proteinases upon stimulation by mononuclear cell factor, J Rheumatol 13: 20-27.

Campbell, I.K.; Roughley, P.J,; and Mort, J.S. (1986b) The action of human articular-cartilage metalloproteinase on proteoglycan and link protein. Similarities between products of degradation in situ and in vitro, Biochem J 237: 117-122.

Carlsson, G.E. and Oberg, T. (1974) Remodelling of the temporomandibular joints, Oral Sci Rev 6: 53-86.

Carvalho, R.S. (1990) The synthesis of collagen and glycosaminoglycans in vitro in rat and mouse temporomandibular disc, M.Sc. thesis, University of Manitoba, Winnipeg, Canada.

Christen, A. (1959) Die faserstruktur des discus temporomandibularis, Z Anat Entwickl Gesh 121: 322-336

Cole, T.C.; Burkhardt, D.; Frost, L; and Ghosh, P. (1985) The proteoglycans of the canine intervetebral disc, Biochim Biophys Acta 839: 127-138.

de Bont, L.G.M. (1985a) Spatial arrangement of collagen fibrils in the articular cartilage of the mandibular condyle: a light microscopic and scanning electron microscopic study, Chapter 3, Ph.D. Dissertation, University of Groningen, The Netherlands. pp. 9-16.

de Bont, L.G.M. (1985b) Osteoarthritis of the temporomandibular joint: a light microscopic and scanning electron microscopic study of the articular cartilage of the mandibular condyle, Chapter 5, Ph.D. Dissertation, University of Groningen, The Netherlands. pp. 23-30.

de Bont, L.G.M. (1985c) Osteoarthrosis and internal derangement of the temporomandibular joint: a light microscopic study, Chapter 7, Ph.D. Dissertation, University of Groningen, The Netherlands. pp. 43-54.

de Bont, L.G.M. (1985d) Ultrastructure of the articular cartilage of the mandibular condyle: ageing and degeneration, Chapter 6, Ph.D. Dissertation, University of Groningen, The Netherlands. pp. 31-42.

Dolwick, M.F. (1983) The temporomandibular joint: normal and abnormal anatomy, In: Internal Derangements of the Temporomandibular Joint, C.A. Helms et al., Eds., San Francisco: Radiology Research and Education Foundation, p. 1-14.

Dolwick, M.F.; Katzberg, R.W.; and Helms, C.A. (1983) Internal derangements of the temporomandibular joint: fact or fiction?, J Prosthet Dent 49: 415-418.

Ekholm, R. and Norback, B. (1951) On the relationship between cartilage change and function, Acta Orthop Scand 21: 81-89.

Fujita, S. and Hoshino, K. (1989) Histochemical and immunohistochemical studies on the articular disk of the temporomandibular joint in rats, Acta Anat 134: 26-30.

Gerber, A. and Steinhardt, G. (1990) Dental Occlusion and the Temporomandibular Joint, Chicago: Quintessence Publ Co.

Granstrom, G. and Linde, A. (1973) Glycosaminoglycans of temporomandibular articular discs, Scand J Dent Res 81: 462-466.

Griffin, C.J.; Hawthorn, R.; and Harris, R. (1975) Anatomy and histology of the human temporomandibular joint, In: The Temporomandibular Joint Syndrome, Monographs in Oral Science, vol. IV, Basel: S. Karger, 1-26.

Grodzinsky, A.J. (1983) Electromechanical and physicochemical properties of connective tissue, CRC Crit Rev Biomed Eng 9: 133-199.

Hansson, T. and Nordstrom, B. (1977) Thickness of the soft tissue layers and articular disk in temporomandibular joints with deviation in form, Acta Odontol Scand 35: 281-288.

Hansson, T. and Oberg, T. (1977) Arthrosis and deviation in form in the temporomandibular joint: a macroscopic study on a human autopsy material, Acta Odontol Scand 35: 167-174.

Hansson, T.; Oberg, T.; Carlsson, G.; and Kopp, S. (1977) Thickness of the soft tissue layers and the articular disk in the temporomandibular joint, Acta Odontol Scand 35: 77-83.

Harrigan, T.P. and Mann, R.W. (1987) State variables for modelling physical aspects of articular cartilage, J Solids Struct 23: 1205-1218.

Hasty, K.A.; Smith, G.N.; and Kang, A.H. (1983) Histochemical identification of sulfation position in chondroitin sulfate in various cartilages, J Histochem Cytochem 31: 1367-1374.

Helmy, E.; Bays, R.; and Sharawy, M. (1988) Osteoarthrosis of the temporomandibular joint following experimental disc perforation in **Macaca fascicularis**, J Oral Maxillofac Surg 46: 979-990.

Hirschmann, P.N. and Shuttleworth, C.A. (1976) The collagen composition of the mandibular joint of the foetal calf, Arch Oral Biol 21: 771-773.

Hodge, W.A.; Fijan, R.S.; Carlson, K.L.; Burgess, R.G.; Harris, W.H.; and Mann, R.W. (1986) Contact pressures in the human hip measured in vivo, Proc Natl Acad Sci (U.S.A.) 83: 2879-2883.

Honner, R. and Thompson, R.C. (1971) The nutritional pathways of articular cartilage, J Bone Joint Surg 53A: 742-748.

Howell, D.S. (1984) Etiopathogenesis of osteoarthritis, In: Osteoarthritis: diagnosis and management, R.W. Moskowitz et al., Eds., Philadelphia: W.B. Saunders Company, pp. 129-146.

Hukins, D.W.L.; Aspden, R.M.; and Yarker, Y.E. (1984) Fibre reinforcement and mechanical stability in articular cartilage, Eng Med 13: 153-156.

Isacsson, G. and Isberg, A.M. (1985) Tissue identification of the TMJ disk and disk attachments and related vascularization, J Craniomandibular Pract 3: 374-379.

Isberg-Holm, A.M. and Westesson, P-L. (1982) Movement of disc and condyle in temporomandibular joints with and without clicking. A high-speed cinematographic and dissection study on autopsy specimens, Acta Odontol Scand 40: 165-177.

Knox, J. (1967) Fibrillar arrangement in the articular disk of the human temporomandibular joint, Thesis, University of Illinois.

Kopp, S. (1978) Topographical distribution of sulfated glycosaminoglycans in the surface layers of the human temporomandibular joint. A histochemical study of an autopsy material, J Oral Pathol 7: 283-294.

Kopp, S. (1976) Topographical distribution of sulphated glycosaminoglycans in human temporomandibular joint disks. A histochemical study of an autopsy material, J Oral Pathol 5: 265-276.

Kuc, I.M.; Nakano, T.; and Scott, P.G. (1989) The extracellular matrix of bovine temporomandibular joint disc, J Dent Res 68 (special issue): 229.

Kurita, K.; Westesson, P-L.; Sternby, N.H.; Eriksson, L.; Carlsson, L-E.; Lundh, H.; and Toremalm, N.G. (1989) Histologic features of temporomandibular joint disk and posterior disk attachment: comparison of symptom-free persons with normally positioned disks and patients with internal derangement, Oral Surg Oral Med Oral Pathol 67: 635-43.

Landesberg, R.; Rosier, R.N.; and Puzas, J.E. (1989) Cellular and biochemical characterizations of the temporomandibular joint meniscus, J Dent Res (special issue) 68: 897.

Linn, F.C. (1967) Lubrication in animal joints- I. The anthrotripsometer, J Bone Joint Surg 49-A: 1079-1098.

Linn, F.C. and Radin, E.L. (1968) Lubrication of animal joints. III. The effect of certain chemical alterations of the cartilage and lubricant, Arthritis Rheum 11: 674-682.

Livne, E.; von der Mark, K.; and Silbermann, M. (1985) Morphologic and cytochemical changes in maturing and osteoarthritic articular cartilage in the temporomandibualr joint of mice, Arthritis Rheum 28: 1027-1038.

Malemud, C.J. and Shuckett, R. (1987) Impact loading and lower-extremity disease, In: Clinical Concepts in Regional Musculoskeletal Illness, M.M. Hadler, Ed., Grune and Stratton Inc, pp. 109-135.

Maroudas, A. and Venn, M. (1977) Chemical composition and swelling of normal and osteoarthrotic femoral head cartilage-II. Swelling, Ann Rheum Dis 36: 399-406.

McCutchen, C.W. (1979) Lubrication of joints, In: The Joints and Synovial Fluid, vol. I, L. Sokoloff, Ed., New York: Academic Press, pp. 437-483.

McCutchen, C.W. **(1983)** Lubrication of and by articular cartilage, In: Cartilage: Biomedical Aspects, vol. III, B.K. Hall, Ed., New York: Academic Press, pp. 87-107.

McKibben, B. and Maroudas, A. **(1979)** Nutrition and metabolism, In: Adult Articular Cartilage, 2nd ed., M.A.R. Freeman, Ed., London: Pitman Medical, pp. 461-486.

Meachim, G. and Bently, G. **(1978)** Horizontal splitting in patellar articular cartilage, Arthritis Rheum 21: 669-674.

Meachim, G. and Allibone, R. **(1984)** Topographical variation in the calcified zone of upper femoral articular cartilage, J Anat 139(2): 341-352.

Milam, S.B.; Klebe, R.J.; and Triplett, R.G. **(1989)** Distribution of fibronectin, collagen, and link protein in the TMJ, J Dent Res 68 (special issue) 229.

Mills, D.K.; Daniel, J.C.; and Scapino, R. **(1988)** Histological features and in-vitro proteoglycan synthesis in the rabbit craniomandibular joint disc, Arch Oral Biol 33: 195-202.

Mills, D.K.; Daniel, J.C.; and Herzog, S. **(1989)** Remodelling of the displaced TMJ disc in rabbit, J Dent Res (special issue) 68: 415.

Mitchell, N.S. and Cruess, R.L. **(1977)** Classification of degenerative arthritis, Can Med Assoc J 117: 763-765.

Moffett, B.C.; Johnston, L.C.; McCabe, J.B.; and Askew, H.C. **(1964)** Articular remodelling in the adult human temporomandibular joint, Am J Anat 115: 119-142.

Moffett, B.C. **(1957)** The prenatal development of the human temporomandibualr joint, In: Contributions to Embryology, publication no. 611, volume 36, Washington: Carnegie Institution of Washington, pp. 19-28.

Mohl, N.D. **(1983)** Functional anatomy of the temporomandibular joint, In: The President's Conference on the Examination, Diagnosis and Management of Temporomandibular Disorders, D. Laskin et al., Eds., Chicago: American Dental Association, pp. 3-12.

Mow, V.C.; Holmes, M.H.; and Lai, W.M. **(1984)** Fluid transport and mechanical properties of articular cartilage: a review, J Biomech 17: 377-394.

Murphy, G.; McGuire, M.B.; Russell, R.G.G.; and Reynolds, J.J. **(1981)** Characterization of collagenase, other metalloproteinases and an inhibitor (TIMP) produced by human synovium and cartilage in culture, Clin Sci 61: 711-716.

Oberg, T. (1964) Morphology, growth , and matrix formation in the mandibular joint of the guinea pig, Trans R Sch Dent Stockh Umea 10: 1-161.

Oberg, T; Carlsson, G.S.; and Fajers, C.M. (1971) The temporomandibular joint: a morphologic study on a human autopsy material, Acta Odontol Scand 29: 349-384.

Ogus, H. (1979-80) Degenerative disease of the temporomandibular joint in young persons, Brit J Oral Surg 17: 17-26.

Proctor, C.S.; Schmidt, M.B; Whipple, R.R.; Kelly, M.A.; and Mow, V.C. (1989) Material properties of the normal medial bovine meniscus, J Orthop Res 7:771-782.

Pujol, J-P. and Loyau G. (1987) Interleukin-1 and osteoarthritis, Life Sci 41: 1187-1198.

Roughley, P.J. (1987) Structural changes in the proteoglycans of human articular cartilage during aging, J Rheumatol 14 (special issue): 14-15.

Roughley, P.J. and White, R.J. (1980) Age-related changes in the structure of the proteoglycan subunits from human articular cartilage, J Biol Chem 255: 217-224.

Salter, R.B.; Simmonds, D.F.; Malcolm, B.W.; Rumble, E.J.; Macmichael, D.; and Clements, N. (1980) The biological effect of continuous passive motion on the healing of full-thickness defects in articular cartilage, J Bone Joint Surg 62-A: 1232-1251.

Scapino, R.P. (1983) Histopathology associated with malposition of the human temporomandibular joint disc, Oral Surg Oral Med Oral Pathol 55: 382-397.

Smith, D.M., McLachlan, K.R., and McCall, W.D. (1986) A numerical model of temporomandibular joint loading, J Dent Res 65: 1046-1052.

Sokoloff, L. (1979) Pathology and pathogenesis of osteoarthritis, In: Arthritis and Allied Conditions: a textbook of rheumatology, 9th ed., D.J. McCarty, Ed., Philadelphia: Lea and Febiger, pp. 1135-1153.

Solberg, W.K.; Hansson, T.L.; and Nordstrom, B. (1985) The temporomandibular joint in young adults at autopsy: a morphologic classification and evaluation, J Oral Rehabil 12: 303-321.

Steinhardt, G. (1934) Untersuchungen uber die beanspruchung der kiefergelenke und ihre geweblichen folgen, Dtsch Zahnheilkd 91: 1-78

Stockwell, R.A. (1970) Changes in the acid glycosaminoglycan content of the matrix of ageing human articular cartilage, Ann Rheum Dis 29: 509-515.

Stockwell, R.A. and Billingham, M.E.J.; and Muir, H. (1983) Ultrastructural changes in articular cartilage after experimental section of the anterior cruciate ligament of the dog knee, J Anat 136(2): 425-439.

Swanson, S.A.V. (1979) Friction, wear, and lubrication, In: Adult Articular Cartilage, 2nd ed., M.A.R. Freeman, Ed., London: Pitman Medical, pp. 415-460.

Taguchi, N.; Nakata, S.; and Oka, T. (1980) Three-dimensional observation of the temporomandibular joint disk in the rhesus monkey, J Oral Surg 38: 11-15.

Tepic, S.; Macirowski, T.; Mann, R.W. (1983) Mechanical properties of articular cartilage elucidated by osmotic loading and ultrasound, Proc Natl Acad Sci (U.S.A.) 80: 3331-3333.

Thilander, B. (1964) The structure of the collagen of the temporo-mandibular disc in man, Acta Odontol Scand 22: 135-149.

Toller, P.A. (1973) Osteoarthrosis of the mandibular condyle, Brit Dent J 134: 223-231.

Toller, P.A. (1974) Temporo-mandibular arthropathy, Proc R Soc Med 67: 153-159.

Toller, P.A. (1977) Ultrastructure of the condylar articular surface in severe mandibular pain-dysfunction syndrome, Int J Oral Surg 6: 297-312.

Toller, P.A. and Wilcox, J.H. (1978) Ultrastructure of the articular surface of the condyle in temporomandibular arthropathy, Oral Surg Oral Med Oral Pathol 45: 232-245.

Tolvanen, M.; Oikarinen, V.J.; and Wolf, J. (1988) A 30 year follow up study of temporomandibular joint menisectomies: a report on five patients, Brit J Oral Maxillofac Surg 26: 311-316.

Tyler, J.A. (1985) Chondrocyte mediated depletion of articular cartilage proteoglycans in vitro, Biochem J 225: 493-507.

van Willigen, J.D.; de Bont, L.G.M.; Broekhuijsen, M.L.; van der Kuijl, B. (1986) On the perception of jaw position and bite force by subjects with craniomandibular disorders, J Craniomandibular Pract 4: 127-133.

Venn, M. and Maroudas, A. (1977) Chemical composition and swelling of normal and osteoarthrotic femoral head cartilage. I. Chemical composition, Ann Rheum Dis 36: 121-129.

Weightman, B.; Freeman, M.A.R.; and Swanson, S.A.V. (1973) Fatigue of articular cartilage, Nature 224: 303-304.

Weinberg, L.A. (1980) The etiology, diagnosis and treatment of TMJ dysfunction syndrome: differential diagnosis, J Prosthet Dent 43: 58-70.

Weiss, C. and Mirow, S. (1972) An ultrastructural study of the osteoarthritic changes in the articular cartilage of human knees, J Bone Joint Surg 54-A: 954-972.

Westesson, P-L. and Rohlin, M. (1984) Internal derangement related to osteoarthrosis in temporomandibular joint autopsy specimens, Oral Surg Oral Med Oral Pathol 57: 17-22.

Wilson, N.H.F. and Gardner, D.L. (1984) The microscopic structure of fibrous articular surfaces: a review, Anat Rec 209: 143-152.

Yen, E.H.K.; Carvalho, R.S.; Suga, D.M. (1989) Collagen synthesis of temporomandibular disc tissues in vitro, J Dent Res 68 (special issue): 885.